2006

CARDIO-RESPIRATORY INTERACTION AND ITS CONTRIBUTION IN SYNCOPE

Xue Wang
University of Kentucky, xuewang2@gmail.com

ABSTRACT OF DISSERTATION

Xue Wang

The Graduate School
University of Kentucky
2005

CARDIO-RESPIRATORY INTERACTION AND ITS CONTRIBUTION IN SYNCOPE

ABSTRACT OF DISSERTATION

A dissertation submitted in partial fulfillment of
the requirements for the degree of Doctor of Philosophy in the
Graduate School
at the University of Kentucky

By
Xue Wang

Lexington, Kentucky

Director: Dr. Abhijit Patwardhan, Associate Professor of Biomedical Engineering
Lexington, Kentucky

2005

ABSTRACT OF DISSERTATION

CARDIO-RESPIRATORY INTERACTION AND ITS CONTRIBUTION IN SYNCOPE

A hypothetical causal link between ventilatory regulation of carbon dioxide and development of syncope during orthostatic challenges is reduction in arterial partial pressure of carbon dioxide and resultant reduction in cerebral blood flow. We performed two experiments to investigate the ventilatory sensitivity to carbon dioxide and factors affecting cerebral autoregulation (CA). We also studied the nonlinear phase coupling between cardio-respiratory parameters before syncope.

For experiment one, in 30 healthy adults, we stimulated chemo and baro reflexes by breathing either room-air or room-air with 5 percent carbon dioxide in a pseudo random binary sequence during supine and 70 degree head up tilt (HUT). Six subjects developed presyncope during tilt.

To determine whether changes in ventilatory control contribute to the observed decrease in $PaCO_2$ during HUT, we assessed ventilatory dynamic sensitivity to changes in $PaCO_2$ during supine and 70 degrees HUT. The sensitivity of the ventilatory control system to perturbations in end tidal carbon dioxide increased during tilt.

To investigate nonlinear phase coupling between cardio-respiratory parameters before syncope, bispectra were estimated and compared between presyncopal and non-presyncopal subjects. Our results indicate that preceding presyncope, nonlinear phase coupling is altered by perturbations to baro and chemo reflexes.

To investigate the effects of gender in CA, we selected 10 men and 10 age-matched women and used spectral analysis to compare differences in CA between men and women. Our results showed that gender-related differences in CA did exist and gender may need to be considered as a factor in investigating CA.

To investigate the influence of induced hypocapnia on CA in absence of ventilatory variability, we performed experiment two in which subjects were randomly assigned to a Control (under normocapnia) or Treatment (under hypocapnia) group. Both groups voluntarily controlled their breathing pattern yet two groups breathed in air with different levels of carbon dioxide. Our results show that changes in mean blood pressure at middle cerebral artery level were less transferred into mean cerebral blood flow in the Treatment group than in the Control group, suggesting better CA under hypocapnia relative to under normocapnia.

KEYWORDS: Autonomic Control; Bispectrum; Cerebral autoregulation; Gender differences; Hypocapnia.

Xue Wang

December 5th, 2005

CARDIO-RESPIRATORY INTERACTION AND ITS CONTRIBUTION IN SYNCOPE

By

Xue Wang

Dr. Abhijit Patwardhan
(Director of Dissertation)

Dr. Abhijit Patwardhan
(Director of Graduate Studies)

December 5th, 2005

RULES FOR THE USE OF DISSERTATIONS

Unpublished dissertations submitted for the Doctor's degree and deposited in the University of Kentucky Library are as a rule open for inspection, but are to be used only with due regard to the rights of the authors. Bibliographical references may be noted, but quotations or summaries of parts may be published only with the permission of the author, and with the usual scholarly acknowledgements.

Extensive copying or publication of the dissertation in whole or in part also requires the consent of the Dean of the Graduate School of the University of Kentucky.

A library that borrows this dissertation for use by its patrons is expected to secure the signature of each user.

DISSERTATION

Xue Wang

The Graduate School
University of Kentucky
2005

CARDIO-RESPIRATORY INTERACTION AND ITS CONTRIBUTION IN SYNCOPE

DISSERTATION

A dissertation submitted in partial fulfillment of
the requirements for the degree of Doctor of Philosophy in the
Graduate School
at the University of Kentucky

By
Xue Wang

Lexington, Kentucky

Director: Dr. Abhijit Patwardhan, Associate Professor of Biomedical Engineering
Lexington, Kentucky
2005

ACKNOWLEGEMENTS

The following dissertation benefited from the insights and direction of several people. First, my Dissertation Chair, Dr. Abhijit Patwardhan. Next, I wish to thank the complete Dissertation Committee, and outside reader, respectively: Dr. Eugene Bruce, Dr. Charles Knapp, Dr. David Randall and Dr. Dexter Speck. Each individual provided insights that guided and challenged my thinking, substantially improving the finished product.

I also want to thank Joyce Evans for her timely help at every stage of my study.
In addition to the technical and instrumental assistance above, I received equally important assistance from family and friends.

TABLE OF CONTENTS

LIST OF TABLES

LIST OF FIGURES

LIST OF FILES

Chapter 1 Introduction

Hemodynamic and respiratory parameters adjust in response to changes in posture from supine to an upright position. During orthostasis, fluid shifts toward the lower extremities because of gravitational effects. A slight increase in mean blood pressure, heart rate and peripheral resistance occurs to compensate for this shift (13). Decreases in end tidal (about 4mmHg) and arterial partial pressures of carbon dioxide (about 2 mmHg) are also observed during head up tilt (60, 71). Although decreases in end tidal carbon dioxide ($ETCO_2$) and arterial partial pressure of carbon dioxide ($PaCO_2$) are consistently observed during head up tilt, the mechanisms responsible for such decreases remain unclear (60).

Recent studies (36, 39, 52) have shown that alterations in the interaction between hemodynamic and respiratory regulation may contribute to posturally mediated orthostatic intolerance and unexplained syncope (7, 52). Hyperventilation, hypocapnia and increase in respiratory variability were observed in some syncopal subjects prior to syncope (39, 52). A hypothetical causal link between ventilatory regulation of CO_2 and development of syncope is reduction in $PaCO_2$ and the resultant reduction in cerebral blood flow. The above results suggest that it is important to investigate mechanisms via which CO_2 is decreased during tilt because it is possible that alterations in these same mechanisms may also be responsible for, or contribute to, initiation of events that ultimately culminate in unexplained syncope.

Our first objective in the present study was to determine if sensitivity of ventilatory regulation in response to perturbations in $PaCO_2$ is diminished during tilt. We hypothesized that diminished ventilatory sensitivity to $PaCO_2$ may accommodate

decreased levels of $PaCO_2$ resulting from a change in perfusion and other effects of change in posture. We assessed dynamic sensitivity of ventilatory regulation in response to changes in $PaCO_2$ during supine and 70 degree passive head up tilt. Our results showed that during tilt, instead of a decrease, ventilatory sensitivity to CO_2 was enhanced compared with that in supine. The observation that during tilt $ETCO_2$ decreased while minute ventilation increased, combined with increased sensitivity, suggests that with postural change there may be a change in the 'set point', i.e. change in the level of $PaCO_2$ that is regulated.

The widely used spectral and multi-variate analyses, such as transfer functions and coherencies (33, 72), are based on the assumption that the underlying system is linear. However, as is the case with many physiological systems, complex cardio-respiratory control systems may have nonlinear components as well. Previous studies provide evidence of nonlinear components in heart rate variability (8, 22, 29). Non-linear indexes reveal information regarding cardiovascular regulation and cardio-respiratory interactions that is different from information obtained using linear variability measures (10, 44, 64, 65, 70). Hoyer et. al. (25) suggested that one possible source of nonlinearity in these systems is coupled neuronal generators within the medulla that are related to cardiovascular and respiratory controls (74).

Our second objective was to explore the nonlinear dynamic changes in presyncopal subjects compared with non-presyncopal subjects using bispectral analysis. We used the bispectrum to estimate non-linear phase coupling. Bispectral analysis can be used to detect non-linear properties and quadratic phase coupling (QPC) (63). This method has been used to investigate a variety of physiological systems, such as analysis of EEG (23, 50, 51, 63), sympathetic nerve discharge (21) and ECG (40, 56). In the present study, auto and cross bispectrum were used to compute phase coupling among oscillations at different frequencies in and between RR intervals, systolic blood pressure (SBP), tidal

volume (V_t), $ETCO_2$ and mean cerebral blood flow velocity (CBFM) from groups of subjects who did and did not develop orthostatically mediated presyncopal symptoms.

Cerebral blood flow (CBF) is maintained at a relatively constant level despite changes in arterial blood pressure. This phenomenon, known as cerebral autoregulation (CA), occurs between blood pressure limits of approximately 50 and 170 mm Hg (2). The pressure-dependent activation of the smooth muscle in the arterioles of the cerebral vascular beds is the main regulator. A lack of blood flow for a few seconds leads to syncope and for a few minutes leads to permanent brain damage, therefore, it is very important to maintain the cerebral blood flow. Impaired CA is thought to contribute to the onset of syncope (33).

In one study, the incidence of presyncope in astronauts after spaceflight was higher in women (35%) than in men (5%) (20). Also orthostatic intolerance happened 3-4 times more frequently in young women than men (59). Gender-related differences in cerebral blood flow velocity (CBFV) (3, 45), cerebral vasomotor reactivity (30) and cerebrovascular CO_2 reactivity (31, 32) have been investigated in several recent studies. The results showed that women have higher CBFV (3, 45), higher CO_2 reactivity (31, 32) and higher vasomotor reactivity (30) than men. However, gender-related differences in CA are somewhat less explored. Our third objective was to compare the CA between women and men using spectral analysis methods (67).

The partial pressure of carbon dioxide in arterial blood also plays an important role in cerebral blood flow regulation. CO_2 is known as a vasodilator, therefore, increases in level of CO_2 lead to a decrease in the cerebral vascular resistance (CVR) and an increase in the CBF, and vice versa. A study by Aaslid R et. al.(2) used acute step decreases in blood pressure to investigate the response rate of CA (the response rate of full restoration of blood flow to the pretest level) under different CO_2 levels. The rate of regulation in hypocapnia, normocapnia, and hypercapnia was 0.38, 0.20, and 0.11/sec. In recent

studies (33, 34, 61, 72, 73) spectral analysis methods, such as transfer function and coherence, were used to investigate the dynamic relationship between blood pressure and cerebral blood flow. Zhang et. al.(72) found that CA can be modeled by a transfer function with the quality of a high-pass filter in the frequency range of 0.07-0.30 Hz. The gain relating mean blood pressure at middle cerebral artery level (BP_{MCA}) to CBFM increased during 5% CO_2 inhalation (72). In another study by Edwards et. al.(16), a two-input (BP_{MCA} and $ETCO_2$) and one-output (CBFM or CVR) autoregressive moving average (ARMA) model was used to investigate the relationship between CBF and two factors which will affect CBF simultaneously. The method was able to attribute the variations in CBFM to changes in BP_{MCA} and $ETCO_2$ separately and simultaneously.

Changes in respiration affect intra-thoracic pressure, cardiac output and heart rate (through the mechanism named respiratory arrhythmia sinus (RSA)). Control of breathing pattern will also affect CA (15, 17). In most of previous studies, respiratory pattern control was conducted by following auditory signal (16, 17). This auditory feedback method can only control the respiratory rate. In our current study, we used a visual feedback method, by which we can control both breathing rate and tidal volume, thus minute ventilation calculated as the ratio of tidal volume to breath duration was also controlled. The breathing pattern was controlled so that the CO_2 effects on cerebral regulation could be investigated without concomitant effects from changes in respiration. Our fourth objective was to investigate hypocapnia's effects on CA with minor changes in breathing pattern using spectral analysis methods. To accomplish our fourth objective, we asked our subjects to breathe room air with 2.5% CO2 during supine and then maintained their ventilation constant via voluntary control of respiratory rate and tidal volume. During HUT, we removed inspired CO_2 in one group of subjects (Treatment group) while the subjects' ventilation was maintained at previously adapted levels. For these subjects in the Treatment group, they were under hypocapnia with minor changes in their ventilation.

The outline of the dissertation is as follows. Chapter 1 describes the background of our study and gives the four specific objectives of our study. Chapter 2 gives a brief review of the involved physiology background. Chapter 3 presents the experimental protocols and setup for experiment one and two. Chapter 4 describes the data analysis methods used in this dissertation. Chapter 5 includes results from both experiments. Chapter 6 discussed the results. The first three objectives were accomplished by experiment one and the fourth objective by experiment two.

Chapter 2 Background

2.1 Syncope

In this section, the definition, symptoms and possible causes of syncope are briefly reviewed.

2.1.1 Definition of syncope

Syncope is defined as temporary loss of consciousness. It is better known as "fainting" or "passing out." It is often a sudden loss of postural tone followed by rapid spontaneous recovery. Recovery usually takes seconds to minutes. Syncope occurs in all age groups from pediatric to elderly, accounting for 3 percent of emergency room visits and 6 percent of hospital admissions every year (62). Many people have one episode of syncope in their lifetime and if symptoms of syncope do not repeat no treatment is necessary. Recurrent episodes, however, require diagnosis and treatment. Syncope itself will not hurt the person when he falls down and recovers the cerebral blood flow quickly. However, the sudden fall poses an injury threat.

2.1.2 Symptoms of syncope

Pre-syncopal symptoms: Pre-syncopal symptoms happen before the person completely loses consciousness. The person feels dizzy, lightheaded, warm, sweaty, nausea and has blurred vision or tunneled vision (can only look at the area in the front), palpitation etc. These can be used as warnings of syncope. Once the person has the above symptoms he should sit down or lie down to prevent him from developing syncope.

Syncope symptoms: During syncope there is a complete loss of consciousness. Some people will faint without any warning, i.e. without any presyncopal symptoms (19).

2.1.3 Causes of syncope

The direct reason of syncope is temporary insufficient blood flow to the brain. Though constituting only 2% of total body weight, the brain receives 15% of the cardiac output. Oxygen and glucose demand for brain is high when compared with other organs (except heart). A lack of blood flow for a few seconds will lead to syncope and for 3 – 4 min will lead to permanent brain damage.

Syncope can be put into two major classifications: cardiac syncope and non-cardiac syncope. In the case of cardiac syncope, the person has an irregular cardiac rhythm (arrhythmia) or abnormalities in the structure of the heart. The heart does not function properly so blood flow supply in the brain is inadequate. This is the most dangerous type of syncope. In the case of non-cardiac syncope, the person's heart function is normal. Non-cardiac syncope includes neurologic, psychiatric, orthostatic hypotension and neurally mediated syncope. Severe loss of blood flow, associated with blood loss, chronic diarrhea, and dehydration, will also lead to syncope.

2.1.4 Neurally mediated syncope

Neurally mediated syncope (NMS) is also called neurocardiogenic or vasovagal syncope and it is the most frequent cause of fainting. It is one type of non-cardiac syncope. In this type of syncope, the heart is working properly while the autonomic nervous system which controls the heart is not. NMS often occurs when blood pressure drops (hypotension) and the blood flow supplied to the brain is not enough (62).

Two most common phenomena observed before NMS is hypotension (low blood pressure) and bradycardia (slow heart rate). Prior to the onset of syncope, either blood pressure

and/or heart rate has a sudden drop suggesting that vagal tone is enhanced and sympathetic tone is diminished before syncope.

When the person moves from supine to standing position, the blood volume shifts to the lower extremities (like legs) because of the gravitational effects. The reflex mechanism like the baroreflex will adjust the cardiovascular system to try to restore the blood flow to the original level. The baroreceptors will detect the changes in blood pressure then through enhancing the sympathetic tone (increase heart rate and vascular resistance) and diminishing the parasympathetic tone the blood pressure and cerebral perfusion is restored. However, in the person who has syncope problems, the adaption is not adequate and cannot compensate the changes in blood pressure and cerebral perfusion caused by orthostatic responses.

There are several possible explanations for NMS (49), including:

-Ventricular theory. The blood pressure drop is detected by baroreceptors and the sympathetic activity is enhanced so the heart is beating faster and stronger, while the ventricle is already part empty (inadequate preload). Similar to Bezold-Jarisch Reflex, the onset of syncope involves an increase in vagal efferent discharge to the heart which causes bradycardia and hypotension (49, 62).

-Baroreflex dysfunction theory. Some researchers believe the reason for the syncope is the baroreflex dysfunction. Either baroreceptors can not detect the changes or the reflex cannot compensate for the hemodynamic changes (48).

-Respiration theory. Hyperventilation, hypocapnia and yawning have been reported were observed prior to the onset of syncope (52). It is possible that hypocapnia caused by hyperventilation might lead to reduction in CBF leading to syncope. The depth of

respiration also increases the blood pressure oscillations in presyncopal patients (18). Respiration might also play a role in the onset of syncope.

-Cerebral blood flow dysregulation. Cerebral autoregulation is an intrinsic property to maintain the cerebral blood flow in face of oscillations in systemic blood pressure. In case of impaired cerebral autoregulation, the blood flow cannot be maintained.

2.1.5 Tilt table test

Tilt table test is widely used in diagnosing syncope in both clinical setting and research laboratories. Tilt table test is designed to evaluate the orthostatic response based on the fact that prolonged standing could lead to venous pooling. In a tilt table test, the patient is strapped to a table, which is then tilted to a head up tilt position. During tilt, the subject is advised to do not move much. When the subject has any syncopal or presyncopal symptoms the result is considered a positive test. Contracting leg muscles will compress the venous vessels and since the venous valves are unidirectional, venous return is forced back towards the heart. In contrast to standing, during tilt table test the movement is passive and the skeletal muscle pump is inhibited.

2.1.6 Treatment for neurally mediated syncope

One episode of NMS usually does not need treatment. Repeated syncope may need medication. Several types of drugs have been used including beta blockers, serotonin uptake inhibitors, florinef and midodine. In 60-70% of the syncopal cases, these drugs help reduce the episodes of syncope (1). People who have syncope problems should drink plenty of water and be on a high-salt diet to prevent dehydration and syncope. When they have pre-syncopal symptoms they should lie down immediately with both legs elevated (62).

2.2 Cardio-respiratory interactions

In this section, cardiovascular and respiratory regulation related to our study will be reviewed.

2.2.1 Nervous control of cardiovascular system

Increase in sympathetic nervous system activity will lead to increase in heart rate (positive chronotropy) while parasympathetic or vagal activity will have the opposite effects. Increase in sympathetic activity will also lead to the enhancement of atrial and ventricular contractility (positive inotropy). The changes of sympathetic and parasympathetic activity are often reciprocal. An increase in heart rate involves an increase in sympathetic and a decrease in parasympathetic regulation of the SA-node. Sympathetic activity increase will also result in vasoconstriction and an increase in peripheral resistance.

2.2.2 Short-term regulation of blood pressure through baroreflex

Baroreflex is involved in short term regulation of blood pressure. The baroreceptors located in carotid sinuses and aortic arch will detect the stretch in the vessels and then send afferent signal through carotid sinus nerve (part of the glossopharyngeal nerve) and vagus nerves respectively to the nucleus of the tractus solitarius (NTS) in the medulla. Increase in blood pressure will lead to an increase in the frequency of baroreceptor nerve firing and will inhibit the vasoconstrictor regions in the medulla. This inhibition will result in peripheral vasodilation. By an increase in parasympathetic and decrease in sympathetic activity the heart rate is decreased. All of these changes help decrease the blood pressure and restore the blood pressure to the normal value. Regulation by the baroreflex is short-term and effective when the changes in blood pressure or cardiac output are abrupt. The long term regulation of blood pressure depends on fluid balance and the kidney. Long term regulation is not that important during investigation of

syncope related issues as syncope is likely an acute problem. Certain hormones, such as epinephrine and insulin, also affect heart rate and thus blood pressure.

2.2.3 Autonomic control of breathing

There are two types of chemoreceptors (for CO_2 and O_2): central and peripheral receptors. Central chemoreceptors, located at ventral surface of medulla are responsive to $PaCO_2$ by way of hydrogen ion concentration in cerebrospinal fluid (CSF). Central chemoreceptors increase ventilation in response to increased $PaCO_2$ level. Peripheral chemoreceptors, located in aortic arch and carotid bodies, are responsive to arterial partial pressure of oxygen (PaO_2) and $PaCO_2$. Peripheral chemoreceptors increase ventilation in response to decreases in PaO_2. Mechanoreceptors (lung stretch receptors), located in the chest wall and lungs, sense the lung volume change. The afferent signal sensed from the receptors is sent to the respiratory center in medulla and then efferent signal is sent to control the respiratory muscles to control breathing and adjust ventilation.

The regulation of breathing is dependent on different state of the body. For example, during sleep and wakefulness the breathing is differently regulated. This is due to a group of interneurons known as the reticular activation system that affect the controller by the state of alertness.

2.2.4 Respiration alters venous return

During inspiration, the intra thoracic pressure is decreased and thus the central venous pressure is decreased. The increase of the pressure gradient between extra thoracic and intra thoracic veins accelerates the venous return to the right atrium. During expiration, the flow decelerates. However, the momentum as well as the valves in the veins of the extremities prevents the blood from flowing backward. According to the Frank-Starling law of the heart, the heart adapts to the rate of venous return and pumps all the blood

from venous return, therefore when venous return is affected by respiration, cardiac output will be affected accordingly.

2.2.5 Gravity effects on cardiac output

When a person shifts from supine to the standing position, about 300-800ml (5) blood will go to the lower extremities (legs) because of gravitational effects, which is called venous pooling. This blood shift is caused by the compliance of the blood vessels. When a person stands, the blood in the vessels will distend the blood vessels because of gravitational effects. Since the compliance of venous vessels is much larger than arterial vessels, the distention is more prominent in venous vessels than in arterial vessels. This venous pooling will cause a decrease in cardiac output.

2.3 Cerebral hemodynamics

Syncope occurs when cerebral perfusion globally decreases. Glucose is the primary metabolic substrate of the brain (75). Brain tissue depends on adequate blood flow to provide enough glucose. Unlike other organs, brain tissue has no significant storage capacity for glucose, therefore, a decreased cerebral perfusion for only 3-5 seconds results in syncope.

Like the blood flow in other body parts, the cerebral blood flow will respond to both myogenic and metabolic regulation. The myogenic regulation of cerebral blood flow indicates that blood flow is maintained almost constant in face of the perfusion pressure oscillations. In human, when the blood pressure is within 60-160 mmHg, the blood flow will be relatively constant in a narrow range averaging 55ml/min/100g of brain (5) . This property of the brain is commonly referred to as cerebral autoregulation. During cerebral autoregulatuion, vascular smooth muscle contracts when pressure increases and the vessels are stretched. The smooth muscle will relax when the pressure decreases. Mean arterial pressure less than 60 mm Hg will result in the decrease of cerebral blood flow and

syncope. The metabolic regulation describes that the blood flow will be regulated by the local chemical environment, such as CO_2 tension. The cerebral vessels are very sensitive to CO_2 levels. Increase in $PaCO_2$ will lead to cerebral vasodilation and an increase in cerebral blood flow, and vice versa (9).

2.4 Spectral analysis of physiological signals

Power spectral analysis and analysis based on it such as transfer function and coherence are quantitative tools widely used in investigating physiologic and patho-physiological phenomena.

Power spectral analysis of heart rate and blood pressure is commonly used to investigate the role of the autonomic nervous system in cardiovascular system regulation. The very low frequency (below 0.04 Hz) reflects changes in thermal regulation. The low frequency (around 0.1 Hz) spectral power of heart rate is considered to be affected by both sympathetic and parasympathetic (vagal) systems, while the high frequency spectral power of heart rate (within respiratory frequency region) is considered to be mediated solely by the parasympathetic system via respiration (24).

Spectral analysis methods, such as transfer function and coherence between blood pressure, cerebral vascular resistance and cerebral blood flow have been used to investigate cerebral autoregulation (7, 33, 72). If the CBFV demonstrates large amplitude oscillations (higher CBFV variability) or blood pressure changes are more correlated with changes in CBFV (higher coherence and larger gain), this would indicate that CA is not functioning properly. Therefore, higher CBFV variabilities, higher coherence and larger gain are considered to be related to impaired CA.

Higher order spectral analysis, especially bispectral analysis, has also been widely used in processing physiological signals. Power spectral analysis does not provide any phase

information of the signals, whereas bispectra can determine whether two harmonically related frequency components are quadratically phase coupled.

Chapter 3 Methods

This chapter presents the information regarding subjects who participated in the studies, the experimental protocols, the instrumentation used and the experiment setup.

3.1 Subjects

All subjects were non-smokers and did not have any history of cardiovascular or lung diseases. The female subjects were not pregnant, did not use birth control pills and were in the pre-menopausal stage.

For experiment one, thirty-one healthy adults (male: 14, female: 17, mean age 27, range 20-41) participated in our study. When we started these studies, we had planned to assay for catecholamines and thus used IV placement in subjects who were enrolled at first. Subsequently, we determined not to pursue this analysis and thus subjects enrolled after an initial group of 8 subjects did not have an IV line.

For experiment two, 18 healthy adults (male: 10, female: 8, mean age 28, range 20-42) participated in our study.

All studies were approved by the Institutional Review Board at the University of Kentucky. All subjects gave written informed consent.

3.2 Experimental protocol

3.2.1 Protocol for experiment one

The experimental protocol, as shown in Figure 3.1, included four parts: Supine Control, Supine PRBS, Tilt PRBS and Tilt Control. In the first part (10 minutes), the subject was asked to lie down on a tilt table and breathe only room air. In the second part (10 minutes), the subject breathed either room air or room air plus 5% CO_2 according to a Pseudo Random Binary Sequence (PRBS). In the third part (10 minutes), the subject was passively tilted to a 70 degree head up tilt position, while still breathing either room air or room air plus 5% CO_2. In the fourth part (20 minutes), they breathed room air only. The total length for tilt was 30 minutes or less if the subject developed any pre-syncopal symptoms. If a subject developed any pre-syncopal symptoms, the tilt table was returned to supine immediately. At the end of the 30 minutes, the subject was tilted back to supine for a 10-min-recovery.

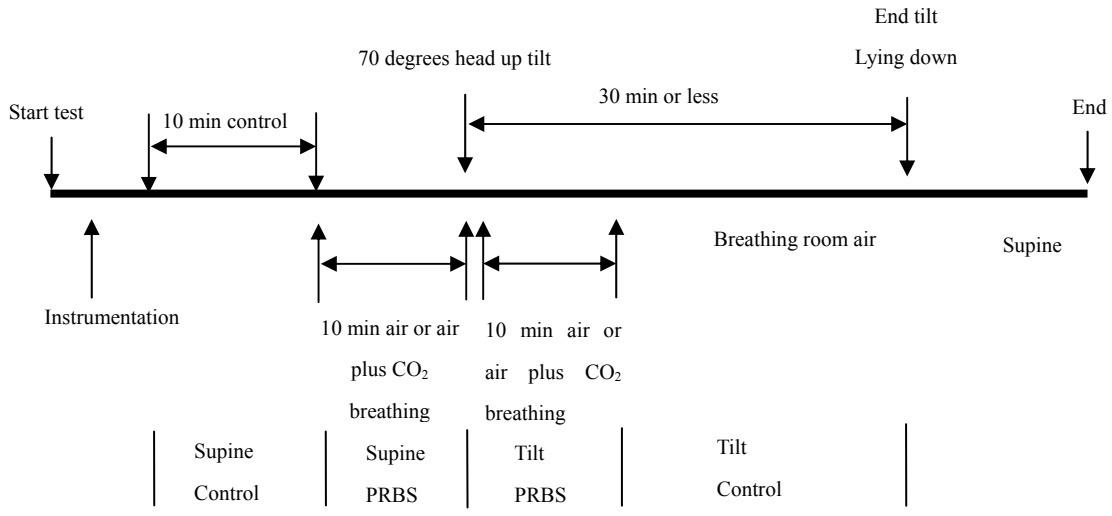

Figure 3.1 Schematic of the protocol for experiment one. The figure shows the four sections of the study from where data were collected: Supine Control; Supine PRBS; Tilt PRBS; and Tilt Control.

3.2.2 Protocol for experiment two

The protocol for experiment two is shown in Figure 3.2. Subjects were randomly assigned to a Control or Treatment group. Treatment group had 10 subjects and Control group had 8 subjects. After instrumentation, subjects from both groups were placed in supine position. Baseline data were collected for 10 minutes (stage 1). After collecting the baseline data, instantaneous tidal volume was calculated and projected on a screen along with a target breathing pattern. To maintain their CO_2 at a level similar to the level of CO_2 observed during baseline, peak value of the target breathing pattern was increased accordingly, while the respiratory rate was maintained constant. Subjects voluntarily controlled their breathing and tried to make their instantaneous tidal volume curve follow the target pattern for 5 minutes in supine position (stage 2). After stage 2 the subjects were passively tilted to a 70 degree head up tilt position for 30 minutes. All subjects breathed a mixture of air plus 2.5% CO_2 during the first 5 minutes of tilt (stage 3). They still controlled their breathing but the target pattern's peak value was increased to maintain their end-tidal CO_2 value to be relatively unchanged from the baseline data. Thereafter, subjects in the Treatment group were switched to breathe only room air, while subjects in the Control group continued breathing the CO_2 mixture. They kept controlling their breathing pattern while the peak volume remained unchanged for the rest of the study (stage 4). The protocol for the first three stages is same for both groups, while during stage 4, treatment group breathe only room air while control group breathe room air with 2.5% CO_2. If a subject developed any pre-syncopal symptoms, the tilt table was returned to supine position immediately.

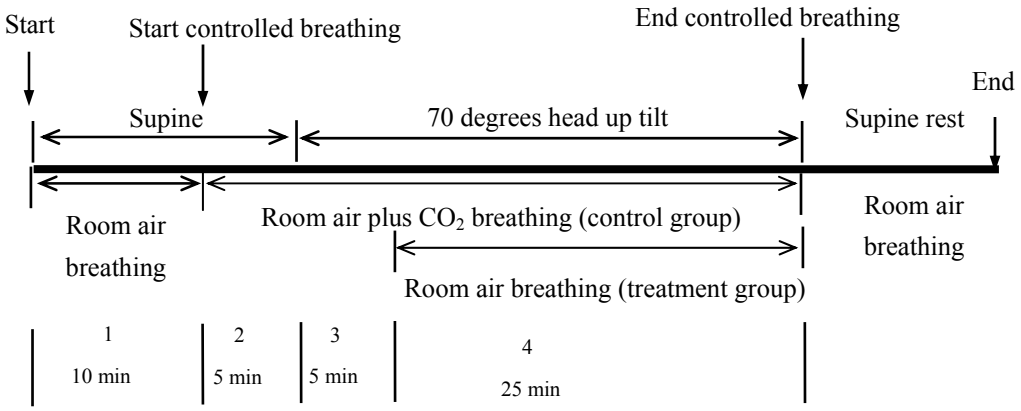

Figure 3.2 Schematic of the protocol for experiment two. The figure shows the four sections of the study from where data were collected. The only difference between treatment and control group is during stage 4.

3.3 Instrumentation

Lead II ECG (Monitor 90603A, Spacelab, Redmond, WA) was recorded. Continuous blood pressure waveform was recorded non-invasively from the middle finger in the left hand (Finapres BP monitor, Ohmeda, Madison, WI). A sling was used to hold the left hand at the heart level. An automated cuff blood pressure monitor was placed on the right arm for validating the blood pressure values from the Finapres BP monitor. The middle cerebral artery was insonated to measure CBFV by a Transcranial Doppler probe (Multigon Model 500M) at 2 MHz in the right middle temporal window. The probe was fixed by a headband. The subject breathed through a mouthpiece which was connected to pneumotachograph (Fleisch). A nose clip was used to insure that the subjects breathed only through their mouths. An infrared CO_2 monitor (Novametrix) was used to measure CO_2 fraction in inspired and expired gas. Tilt angle was measured by measuring the voltage across a potentiometer in a bridge circuit. All data were sampled at 500Hz by a data acquisition system (Windaq® DI-720).

3.4 Experimental setup

3.4.1 Experiment one

As shown in Figure 3.3, the subject breathed through a mouthpiece which was connected to two balloon valves. If one balloon is inflated then the other will deflate, such that only one balloon is inflated at one time. Balloon valve A was open to room air and valve B was connected to an airbag with air plus 5% CO_2. If balloon A is inflated (balloon B is deflated), the subject will breathe room air plus 5% CO_2; if balloon B is inflated (balloon A is deflated), the subject will breath room air. The inflating and deflating of the balloon were controlled by a PRBS. PRBS was generated such that the incidence of "0" and "1" is almost equal in a given time interval. PRBS was pre-generated and stored in the computer. The custom written program collected the airflow signal and detected the expiration (37). During each expiration, the program will send out either "0" or "1" through the D/A board different voltage was sent to an Automatic Controller (Hans Rudolph) of the balloons. If "1" is send out, the balloon will be inflated, otherwise if "0" is send out, the balloon will be deflated. One end of the valve was connected to an airbag with 5% CO_2 balanced with 21% O_2 and 74% N_2. The other end of the valve was open to room air. Since the incidence of "0" and "1" is almost equal, the chance of the subjects to breathe room air or room air plus 5% CO_2 is almost the same. Therefore, on the average the subjects breathed 2.5% CO_2.

The rational for using PRBS type input is that PRBS widens input spectrum which allows us to investigate the frequency response of the system in a wide frequency range. Since the signal is only changed during expiration, the upper frequency limit for the input spectrum is the inverse of averaged breath duration.

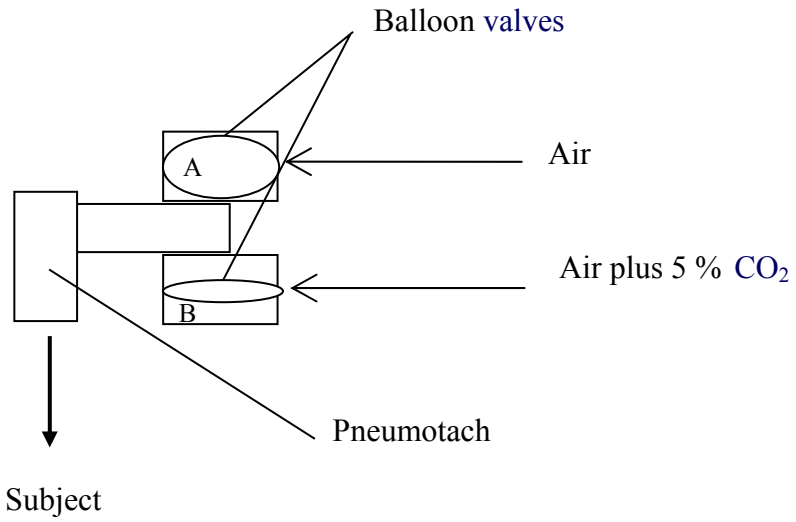

Figure 3.3 Setup for PRBS breathing. One of the two balloon valves is inflated and the other is deflated. The subject will breathe in air plus 5% CO2 as shown above.

The following variables were recorded during experiment one: Airflow, CO_2 level, ECG, Blood pressure, PRBS, Cerebral blood flow velocity, Tilt angle.

3.4.2 Experiment two

The subject's airflow and CO_2 level in their airflow were collected for the first 10 minutes (baseline data). The offline program in Matlab® calculated the average tidal volume, breath duration and end tidal CO_2 from the baseline data. Using a LabView® program, the target pattern was generated from combining two sine waves with different period as shown in Figure 3.4. The ascending part is the inspiration part and the descending part is the expiration part. The time duration for inspiration and expiration ratio is 2:3. The initial peak value for the target pattern was the average tidal volume calculated from the 10 min baseline data.

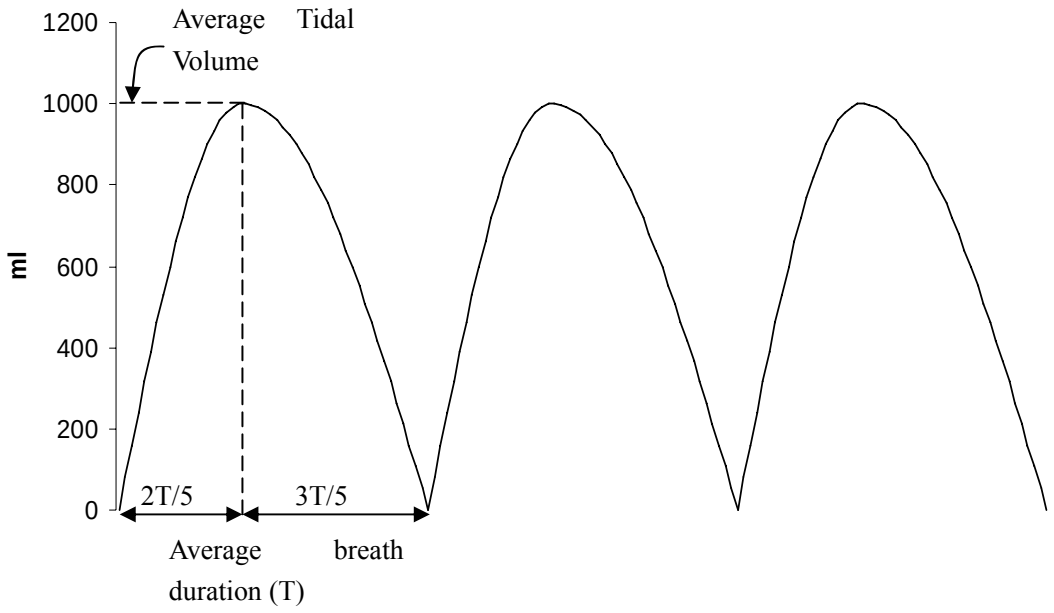

Figure 3.4 The target pattern generated from combining two sine waves.

The following variables were recorded during experiment two: airflow, CO_2 level, ECG, blood pressure, cerebral blood flow velocity, tilt angle.

Chapter 4 Data Analysis

4.1 Preprocessing procedure

From the airflow signal, the zero-crossing were located and the start and end of a breath were identified. The airflow signal within each breath was integrated to get instantaneous tidal volume. Within each breath, tidal volume (maximum value of the lung volume during that breath) and breath duration (the time between the start and the end of that breath) were calculated. Breath by breath ventilation ($\dot{V}_E$) was calculated as the ratio of tidal volume to breath duration. Inspired and $ETCO_2$ were detected from each breath. These breath by breath values were held constant during that breath, then sub-sampled at 5 Hz or sub-sampled at average breathing frequency for that particular subject.

From the ECG signal, we used an algorithm developed by Macdonald et. al.(43) to detect R peaks. Briefly, a band pass filter (20-60 Hz) was used to suppress baseline wandering and high frequency noise. The absolute value of the filtered signal was then compared with an automatically adjusting threshold. RR intervals were calculated as the time duration between two R peaks. Maximum and minimum values of the blood pressure during each beat were computed as systolic and diastolic blood pressure. Peak and average value of the cerebral blood flow within each beat was the peak (CBFP) and mean cerebral blood flow velocity. Blood pressures at the heart level adjusted by the height from the heart level to the eye level were used as estimation for BP_{MCA}. Cerebral vascular resistance index (CVR) is estimated as the ratio of BP_{MCA} to CBFM. These beat by beat values were held constant within each beat. The resulting piece-wise continuous signals were sub-sampled at 5 Hz.

The results from pre-processing sampled at 5Hz were used in spectral analysis, such as coherence, transfer function and bispectral analysis. Those results sampled at average breathing frequency were used in parametric system identification of ventilatory sensitivity to CO_2.

4.2 Parametric system identification

Similar to the methods used by Lai and Bruce(37), a generalized linear model as shown in Figure 4.1 was used to represent the ventilatory control system. In order to estimate the ventilatory response, a Box-Jenkins model was used (37, 41):

$$y(n) = \frac{B(q)}{F(q)}u(n-nk) + \frac{C(q)}{D(q)}e(n) \quad n = 1,2,...,N \tag{4.2.1}$$

In equation 4.2.1, u(n) is the input of the system, which, for open loop or controller responses is $ETCO_2$ (an approximation of P_aCO_2 (4, 6)), and for the closed loop responses, the input is inspired volume of CO_2 (inspired CO_2 fraction multiplied by tidal volume). In equation 4.2.1, y(n) is the output of the system $\dot{V}_E$, e(n) is random noise, n represents (re-sampled) breath number, nk is time delay between output and input (representing circulation time between the lungs and the site of the chemoreceptors), and N is the total number of breaths. The letters B, C, D, and F represent polynomials in a shift operator q.

$$B(q) = b_0 + b_1q^{-1} + b_2q^{-2} + ... + b_{nb}q^{-nb}; \quad F(q) = 1 + f_1q^{-1} + f_2q^{-2} + ... + f_{nf}q^{-nf};$$

$$C(q) = 1 + c_1q^{-1} + c_2q^{-2} + ... + c_{nc}q^{-nc}; \; D(q) = 1 + d_1q^{-1} + d_2q^{-2} + ... + d_{nd}q^{-nd}; \tag{4.2.2}$$

The orders of polynomials *B, C, D, and F* are *nb, nc, nd, nf*. We used a prediction error method (PEM) to estimate model parameters *nn*= [*nb nc nd nf nk*]. Similar to the method used by Lai and Bruce (37), optimal parameter values were determined by starting from initial values of *nn*=[1 0 0 1 1] and increasing one of these five values by 1 each time until *nn*=[4 3 3 3 4]. The selection of optimal nn parameters was based on a combination of three criteria: final prediction error (FPE), whiteness of residuals and lack of statistically significant correlation between the input signal and residuals. Because our protocol for experiment one for ventilatory sensitivity assessment was very similar to that used by Lai and Bruce, we confirmed that the selected model was consistent with that reported by them. To get better estimates of model parameters at lower frequencies (37), we included data during last five minutes of Supine Control with those during Supine PRBS to calculate ventilatory response during supine posture. Similarly, data during Tilt PRBS and the first five minutes during Tilt Control were used to calculate ventilatory response during tilt.

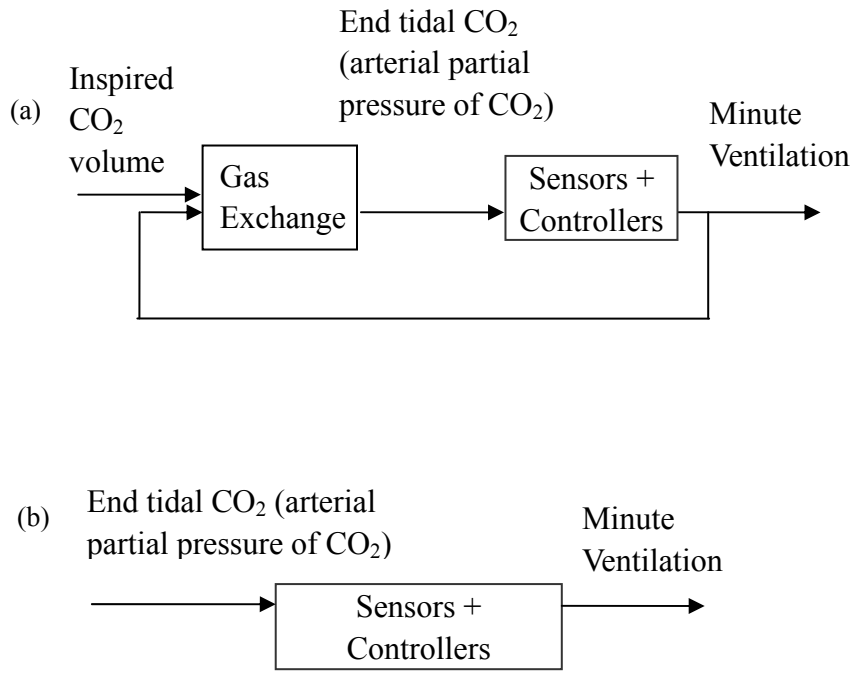

Figure 4.1 Schematic of parametric models assumed for ventilatory control based on results of Lai and Bruce(37). Parameters for these models were estimated using a procedure described in the appendix. (a) Minute ventilation responses to changes in inspired CO_2 volume, which we refer to as close-loop response; (b) Minute ventilation responses to changes in end tidal CO_2 (arterial partial pressure of CO_2), which we refer to as open-loop response.

4.3 Baroreflex sensitivity estimation

We used sequence analysis method to estimate sensitivity of the baroreflex (26). First of all, in beat by beat systolic blood pressure sequences, we identified those sequences contained three or more monotonic increasing or decreasing beats. Secondly using one beat delay in beat by beat RR interval, we identified those sequences in RR intervals when blood pressure was increasing, RR interval also increased, and when blood pressure was decreasing, RR interval also decreased. Once all these qualified sequences were identified, we plotted all the points within a sequence on a plane with blood pressure as X axis, RR interval as Y axis, and then estimated the slope of the sequences with least

square error method for each qualified sequence. The average value of all the slopes was used as an estimate of the sensitivity of baroreflex.

4.4 Spectrum, transfer function and coherence

Auto-spectrum was calculated using Welch's method with 120-second window length, 50% overlap and Hamming window (68) . The auto-spectrum was normalized by the total area under the auto-spectrum curve. Heart rate variability, blood pressure variability were both calculated by the same method.

Transfer functions were estimated as the ratio of cross-spectrum of the input and output of the signal to auto-spectrum of input signal

$$H(f) = Sxy(f) / Sxx(f) \qquad (4.4.1)$$

Where Sxx(f) is the auto spectrum of input, Sxy(f) is cross spectrum between input and output. The absolute value of H(f) is the gain of the transfer function.

Coherence was estimated by the following equation

$$C(f) = | Sxy(f) |^2 / [Sxx(f)*Syy(f)] \qquad (4.4.2)$$

Where Sxx(f) is the auto spectrum of input, Syy(f) is the auto spectrum of output and Sxy(f) is the cross spectrum between input and output.

The auto-spectrum, transfer functions and coherencies were integrated within different frequency ranges. The frequency band below 0.04Hz was considered very low frequency (VLF) region, around 0.1Hz was considered as low frequency (LF) region and within respiratory frequency region was considered high frequency (HF) region.

4.5 Bispectra estimation

Bispectra were estimated by an approach similar to that described previously (56). As the spectrum is defined as the Fourier transform of the auto-correlation, similarly the bispectrum is defined as the 2-D Fourier transform of the third-order cumulant. The bispectrum at frequency coordinate (f_1, f_2) is estimated as the average value of a triple product of three discrete Fourier transforms at frequencies f_1, f_2 and f_1+f_2 as given in equation (4.5.1).

$$B_{xyz}(f_1, f_2) = \frac{1}{M}\sum_{k=1}^{M} {}^{x}S_k(f_1)^{y}S_k(f_2)^{z}S_k^{*}(f_1 + f_2), \qquad (4.5.1)$$

where * denotes conjugation, and

$${}^{x}S(f) = \sum_{n=1}^{N} X(n)\exp\left(\frac{-j2\pi nf}{N}\right). \qquad (4.5.2)$$

Data were segmented into 120-second long segments with 50% overlap. A Hanning window was used to reduce truncation effects. For all of the subjects who developed pre-syncopal symptoms during Tilt control, the average duration before the onset of symptoms was 13 minutes. To keep variances consistent for bispectra estimation, we used data from first 13 minutes during Tilt Control for the group of subjects who did not have any symptoms. In order to minimize the effects of differences in absolute variabilities among subjects, we divided each bispectra by the largest value within that bispectrum in the frequency region (0.04-0.3 Hz). All bispectra were normalized to values between 0 and 1. To quantify the degree of phase coupling, bispectral surfaces were integrated within different frequency bandwidths (four combinations of a low frequency band (LF, 0.04-0.15Hz) and a high frequency band (HF, 0.15-0.3Hz)). These four regions were named as regions I (f_1: LF; f_2: LF), II (f_1: HF, f_2: LF), III (f_1: HF, f_2: HF)

and IV (f_1: LF, f_2: HF).We integrated frequencies up to 0.3 Hz in the high frequency band because the bispectral powers for frequencies larger than 0.3 Hz were relatively small. Since auto-bispectra are symmetrical along the diagonal, integration was conducted only in regions I, II and III

We present an example here to illustrate how amplitude modulation type phenomenon can lead to changes in bispectra, and thus produce a change in phase coupling (69).

Consider two signals $x_1(t)$ and $x_2(t)$.

$$x_1(t) = \sin(f_1t+\theta_1)+ \sin(f_2t+\theta_2)+ 0.5\cos((f_1-f_2)t+ \theta_3)+ 0.5\cos((f_1+f_2)t+ \theta_4)$$

$$x_2(t) = \sin(f_1t+\theta_1) + \sin (f_2t+\theta_2) + \sin(f_1t+\theta_1)* \sin(f_2t+\theta_2)$$

$$= \sin (f_1t+\theta_1) + \sin (f_2t+\theta_2) + 0.5\cos ((f_1-f_2)t+ (\theta_1-\theta_2))- 0.5\cos((f_1+f_2)t+ (\theta_1+ \theta_2)).$$

Where f_1=0.28 Hz, f_2=0.06 Hz, θ_1, θ_2, θ_3, θ_4 are random phases. Both x_1 and x_2 have energies at four frequencies f_1, f_2, f_1+f_2 and f_1-f_2, but the difference between them is that in $x_1(t)$ the phases are all random while in $x_2(t)$ the phase at frequency f_1+f_2 is $\theta_1+ \theta_2$, and at frequency f_1-f_2 the phase is $\theta_1-\theta_2$ which is the result of modulation of f_1 by f_2. Therefore, x_2 is phase coupled at frequencies f_1 and f_2. $x_1(t)$ and $x_2(t)$ are shown in Figure 4.2(i) and (iii). Spectra of x_1 and x_2 are shown in Figure 4.2 (ii) and (iv). As seen from the figure, both signals have same spectra although they have different phases. Bispectra between these signals were estimated as described in equation 4.5.1 and shown in Figure 4.3 (a) and (b). The figure shows that the phase coupling in signal x_2 is much larger than that in signal x_1. The figure also shows the symmetry that is present in the auto-bispectra. There are two peaks seen in each half of the bispectra, one is at coordinate (f_1, f_2) while the other is at (f_1-f_2, f_2), because $(f_1-f_2)+f_2=f_1$ while $(\theta_1-\theta_2)+\theta_2=\theta_1$. Note that f_1 is within the high frequency region (0.15-0.30Hz) and f_2 is within the low frequency region

(0.04-0.15Hz), we selected signals in these frequency regions to simulate the type of coupling observed in our study.

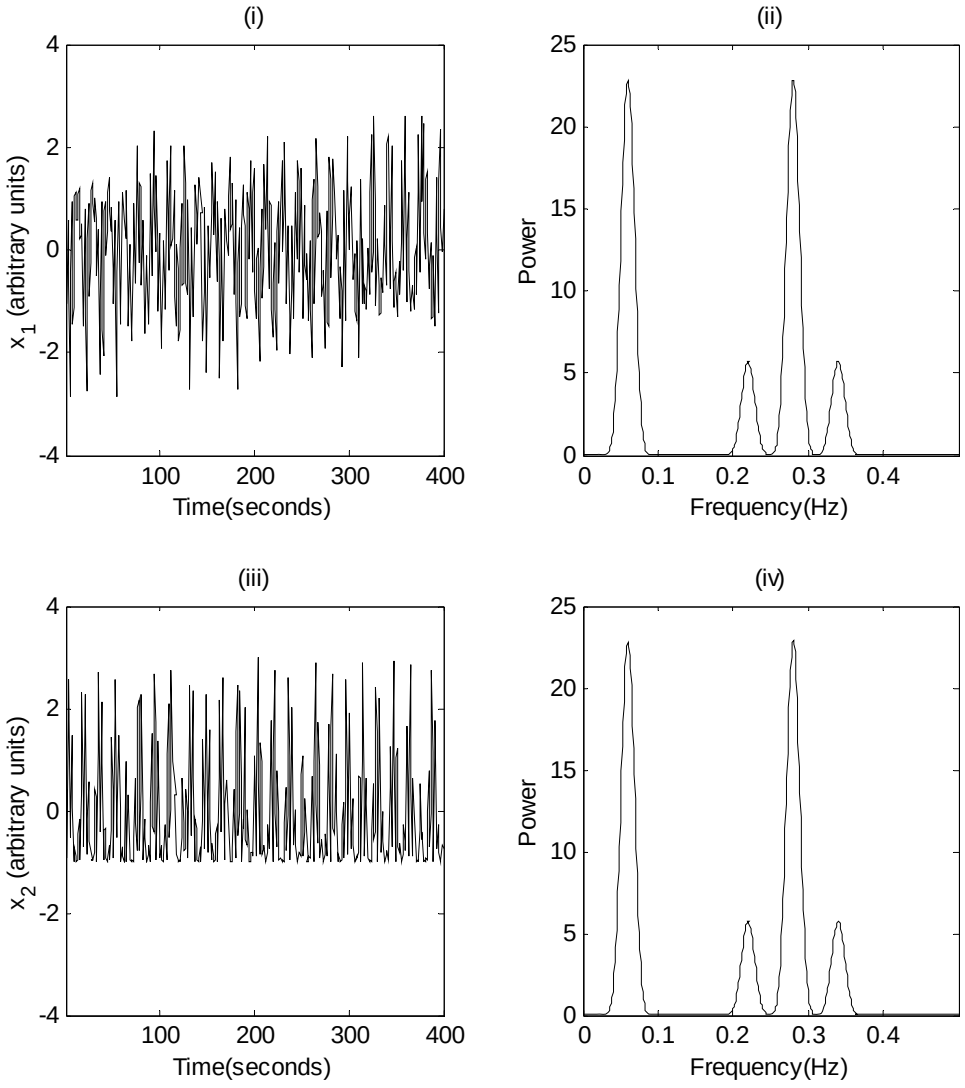

Figure 4.2 Two test signals (x_1 and x_2) are shown in Figure 4.2(i) and (iii). Spectra of x_1 and x_2 are shown in Figure 4.2 (ii) and (iv). As seen from the figure, both signals have same spectra although they have different phases.

Figure 4.3 a

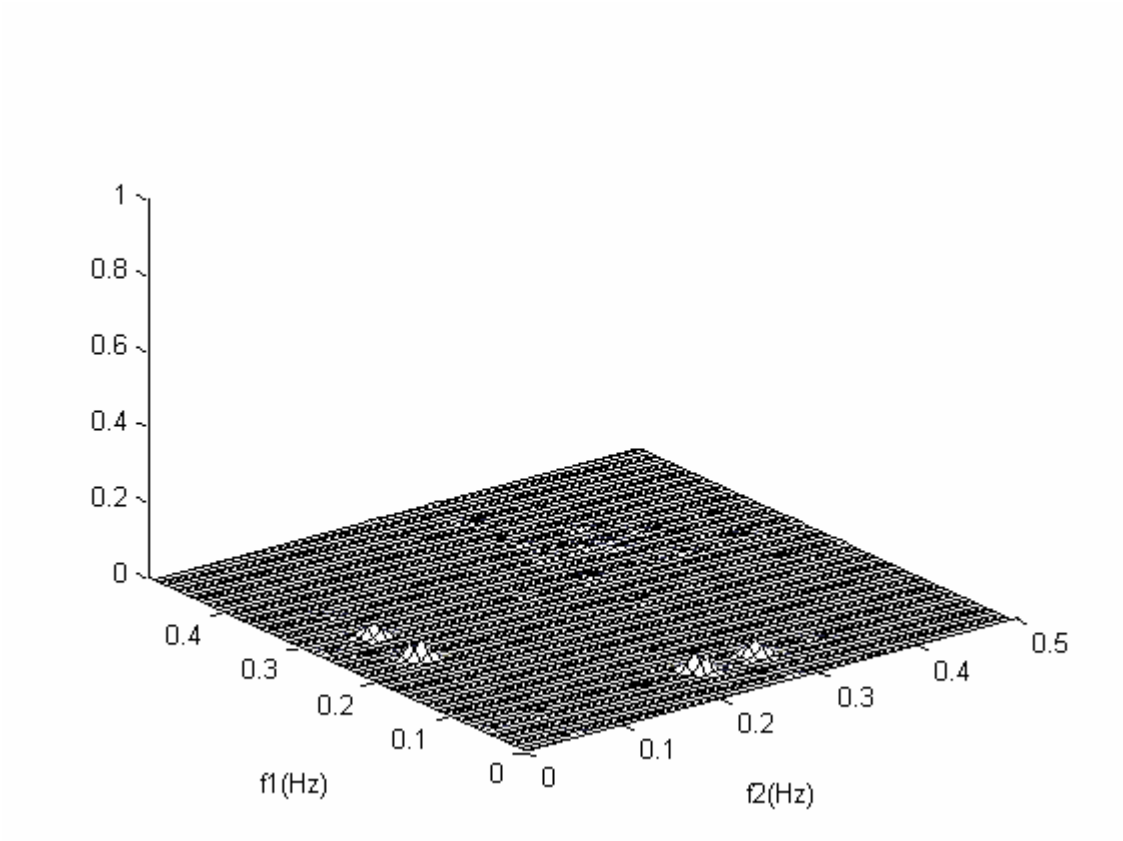

Figure 4.3 b

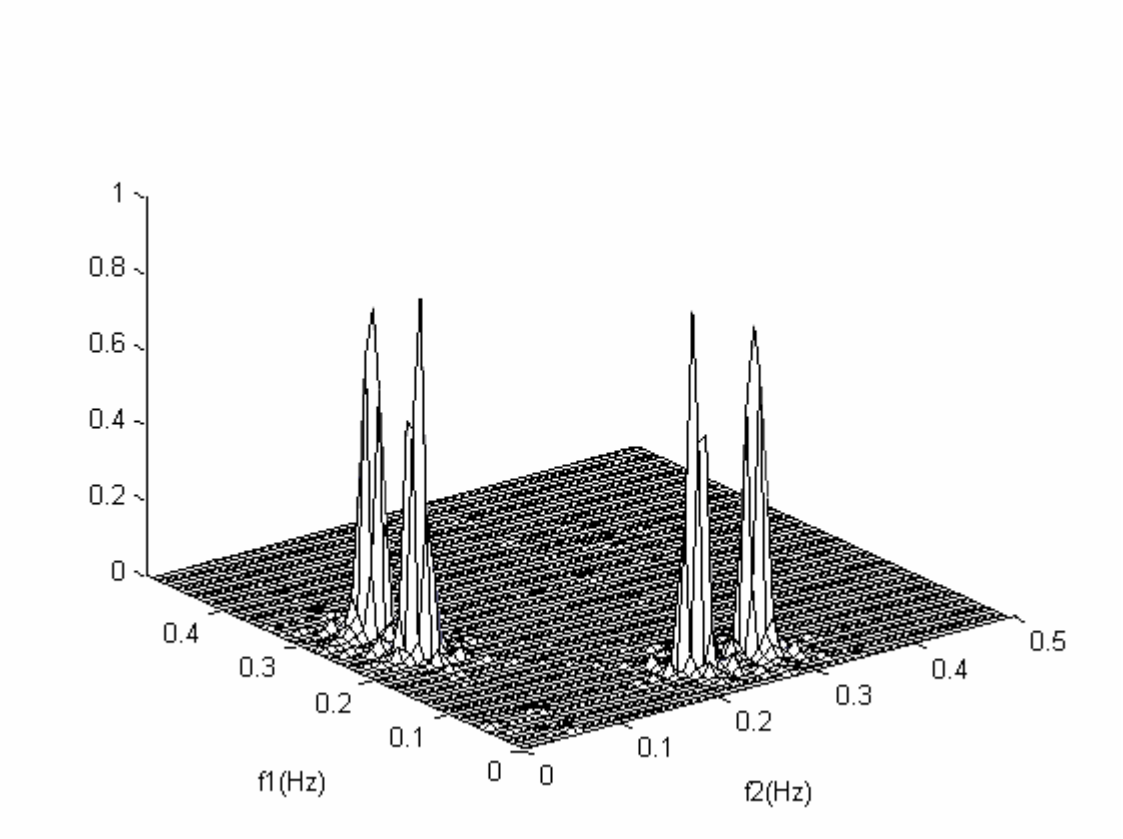

Figure 4.3 Bispectra for signals x_1 (Figure 4.3a) and x_2 (Figure 4.3b). The figure shows that the phase coupling in signal x_2 is much larger than that in signal x_1. The figure also shows the symmetry that is present in the auto-bispectra. There are two peaks seen in each half of the bispectra, one is at coordinate (f_1, f_2) while the other is at (f_1-f_2, f_2), because (f_1-f_2)+f_2=f_1 while (θ_1-θ_2)+θ_2=θ_1.

4.6 Statistics

Differences between groups were compared using a t test assuming un-equal variances. Differences between the stages were compared using paired t test. A p value of < 0.05

was considered significant. Two-way ANOVA test (gender and stage are two factors) was used to test whether gender had significant effects on mean cerebral blood flow.

Chapter 5 Results

5.1 Experiment one

Six subjects developed pre-syncopal symptoms during Tilt Control. The other 24 subjects did not have any presyncopal symptoms. Based on the outcome of tilt test, we divided subjects into two groups; a Presyncopal and a Non-presyncopal group. One subject of the Presyncopal group developed presyncopal symptoms early during Tilt Control, about 2 minutes after onset of Tilt Control. Since we did not have enough data during Tilt Control, data from this subject were not used for the Tilt Control section. The results for the presyncopal group during Tilt Control are from five subjects. The CBFV signal for two subjects in the non-presyncopal group was not of quality comparable to that from other subjects, therefore, CBFV signals from these two subjects were not used for calculating the results related to CBFV.

5.1.1 Mean values

For the 24 non-presyncopal subjects, the mean values of their cardio-respiratory parameters are shown in Table 5.1. Mean heart rate and blood pressure increased during tilt compared to that during Supine Control. Relative to Supine Control, mean heart rate decreased during Supine PRBS, likely a consequence of adaptation. There was no difference in BP between Supine Control and Supine PRBS (Table 5.1). BP increased during tilt compared to that during Supine Control. Neither peak cerebral blood flow nor mean cerebral blood flow changed during Supine PRBS yet decreased during tilt relative to Supine Control. As expected, $\dot{V}_E$ and Vt increased during both PRBS (Supine and Tilt) compared with during Supine Control. $\dot{V}_E$ was also higher during Tilt Control relative to that during Supine Control. Compared with Supine Control, $ETCO_2$ increased during

Supine PRBS and decreased by about 4 mm Hg during Tilt Control. There was no increase in $ETCO_2$ during Tilt PRBS compared with during Supine Control, likely due to a decrease in mean $ETCO_2$ produced by tilt.

Table 5.1 Mean values for cardio-respiratory parameters in the non-presyncopal subjects (N=24). Values are shown as Mean ± SEM. *denotes the difference between Supine PRBS and Supine Control is significant. † denotes the difference between Tilt PRBS and Supine Control is significant. ‡ denotes the difference between Tilt Control and Supine Control is significant.

Non-presyncopal subjects (N=24)	Supine Control	Supine PRBS	Tilt PRBS	Tilt Control
Heart rate (beats/min)	74.1 ± 2.5	$72.2^{*} \pm 2.5$	$87.2^{\dagger} \pm 2.3$	$91.3^{\ddagger} \pm 2.4$
MBP (mmHg)	90.9 ± 2.5	91.9 ± 2.3	$102.6^{\dagger} \pm 3.5$	$105.7^{\ddagger} \pm 4.2$
CBFP (cm/s)	84.9 ± 3.5	85.6 ± 3.7	$73.4^{\dagger} \pm 3.2$	$72.9^{\ddagger} \pm 2.8$
CBFM (cm/s)	73.3 ± 3.2	74.3 ± 3.3	$64.7^{\dagger} \pm 2.9$	$64.5^{\ddagger} \pm 2.4$
V_t (ml)	582.6 ± 39.9	$630.6^{*} \pm 37.1$	$686.3^{\dagger} \pm 50.0$	614.4 ± 31.9
Resp rate (breaths/min)	13.6 ± 0.5	13.9 ± 0.6	14.2 ± 0.6	14.2 ± 0.6
$\dot{V}_E$ (L/min)	7.63 ± 0.4	$8.62^{*} \pm 0.5$	$10.0^{\dagger} \pm 0.5$	$8.47^{\ddagger} \pm 0.4$
$ETCO_2$(mmHg)	46.9 ± 0.9	$49.4^{*} \pm 0.9$	47.4 ± 0.9	$42.9^{\ddagger} \pm 1.0$

As shown in Table 5.2, the mean value changes in presyncopal subjects were similar to those of non-presyncopal subjects. Some changes are not significant, which might relate to the limited number of subjects in this group.

Table 5.2 Mean values for cardio-respiratory parameters in the presyncopal subjects (N=5). Values are shown as Mean ± SEM. * denotes the difference between Supine PRBS and Supine Control is significant. † denotes the difference between Tilt PRBS and Supine Control is significant. ‡ denotes the difference between Tilt Control and Supine Control is significant. ^{s} denotes the difference between non-presyncopal and presyncopal group is significant.

Presyncopal subjects (N=5)	Supine Control	Supine PRBS	Tilt PRBS	Tilt Control
Heart rate (beats/min)	69.1 ± 4.3	68.4 ± 3.7	$90.5^{\dagger}$ ± 5.8	$95.7^{\ddagger}$ ± 4.0
MBP (mmHg)	86.9^{s} ± 2.6	88.8^{s} ± 1.5	91.2^{s} ± 2.0	92.9^{s} ± 1.6
CBFP (cm/s)	97.2 ± 6.7	97.4 ± 5.7	$87.7^{\dagger, s}$ ± 6.0	$83.3^{\ddagger, s}$ ± 4.6
CBFM (cm/s)	86.1^{s} ± 5.7	86.4^{s} ± 5.0	$79.7^{\dagger,s}$ ± 5.2	$75.6^{\ddagger,s}$ ± 4.2
V_t (ml)	726.6 ± 99.6	768.2^{s} ± 33.9	$909.8^{\dagger,s}$ ± 78.5	780.3 ± 113.3
Resp rate (breaths/min)	12.5 ± 1.3	13.7 ± 0.5	13.4 ± 1.0	13.4 ± 1.3
$\dot{V}_E$ (L/min)	8.7^{s} ± 0.4	$10.6^{*,s}$ ± 0.4	$12.0^{\dagger,s}$ ± 0.52	10.1 ± 1.0
$ETCO_2$(mmHg)	44.9 ± 2.9	47.8^{*} ± 3.0	44.7 ± 3.0	$38.5^{\ddagger}$ ± 2.8

5.1.2 Impulse responses of ventilatory control of CO_2

To determine orthostatic modification of ventilatory sensitivity, we compared open and closed loop ventilatory responses to CO_2 disturbances between Supine PRBS and Tilt PRBS for both presyncopal and non-presyncopal group. The typical model parameters for open loop non-presyncopal group were nn= [1 2 2 1 2]. Figure 5.1a shows $ETCO_2$ in one subject during the four stages of the study. As expected there was an increase in ETCO2 during Supine PRBS and Tilt PRBS. Figure 5.1b shows $\dot{V}_E$ across the study (dashed line) and $\dot{V}_E$ predicted by the fitted model (solid line). The overlap between the two traces shows that the model predicted changes in ventilation acceptably.

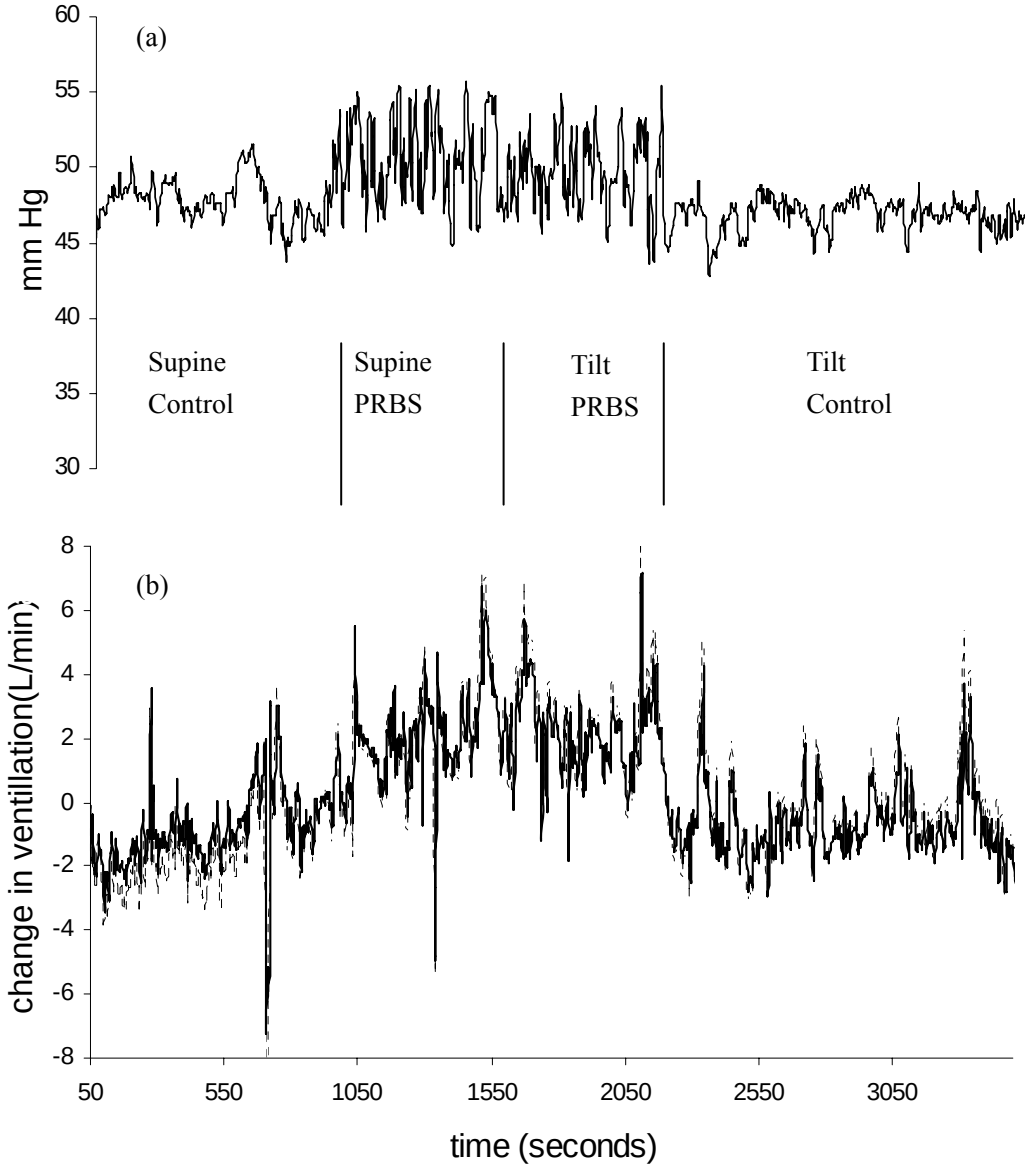

Figure 5.1 The top panel (a) shows an example of end tidal CO_2 in a non-presyncopal subject across the four states of the study, Supine control, Supine PRBS, Tilt PRBS and Tilt control. The bottom panel (b) shows change in ventilation (dashed) during the four states and predicted change in ventilation using the fitted model (solid). The overlap between the two traces shows that the model predicted changes in ventilation acceptably.

From the model, we computed an impulse response of the ventilatory control system to a single breath perturbation in $ETCO_2$ of 1 mmHg. Figure 5.2 shows open loop impulse responses in one typical subject from the non-presyncopal group during Supine PRBS (thin line) and Tilt PRBS (thick line). The impulse response during tilt showed an increase in peak values and decrease in decay time (time for the response to decrease by 50%) relative to supine. We computed gains, peak values and decay times from the impulse responses as indexes of sensitivity of the control system. As shown in Figure 5.3, the control system gain (integral of the impulse response) was significantly higher ($p<0.005$) during tilt (0.73 ± 0.10 L/Min/mmHg) compared with that during supine (0.46 ± 0.08 L/Min/mmHg). Peak values were also higher ($p<0.05$) during tilt (0.10 ± 0.01 L/Min/mmHg) relative to supine (0.06 ± 0.01 L/Min/mmHg). Decay times of the responses were shorter during tilt (43.6 ± 4.99 seconds) relative to that during supine (53.4 ± 10.1 seconds), this difference, however, was not significant. The closed loop responses did not show any differences between supine and tilt. There were no significant differences between presyncopal and non-presyncopal subjects in impulse responses.

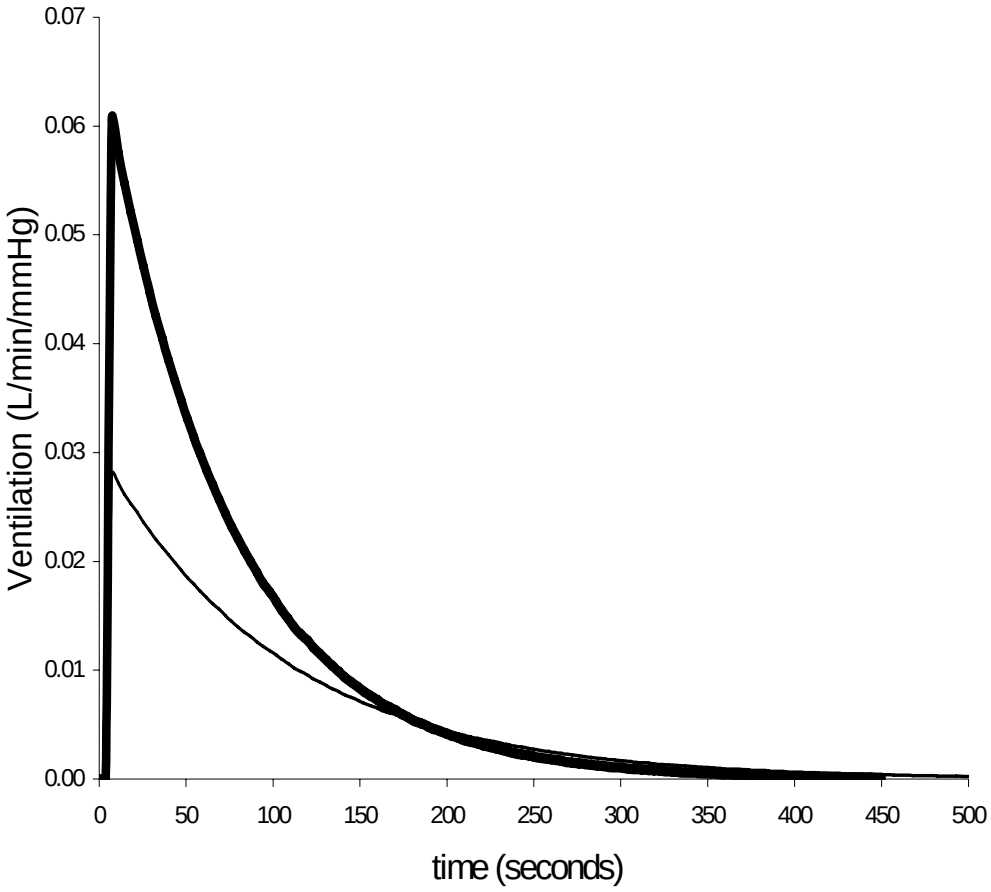

Figure 5.2 Open loop impulse responses in a non-presyncopal subject during Supine PRBS (thin line) and Tilt PRBS (thick line). The responses show an increase in peak value and decrease in decay time (time for the response to decrease by 50%) during tilt relative to that during supine.

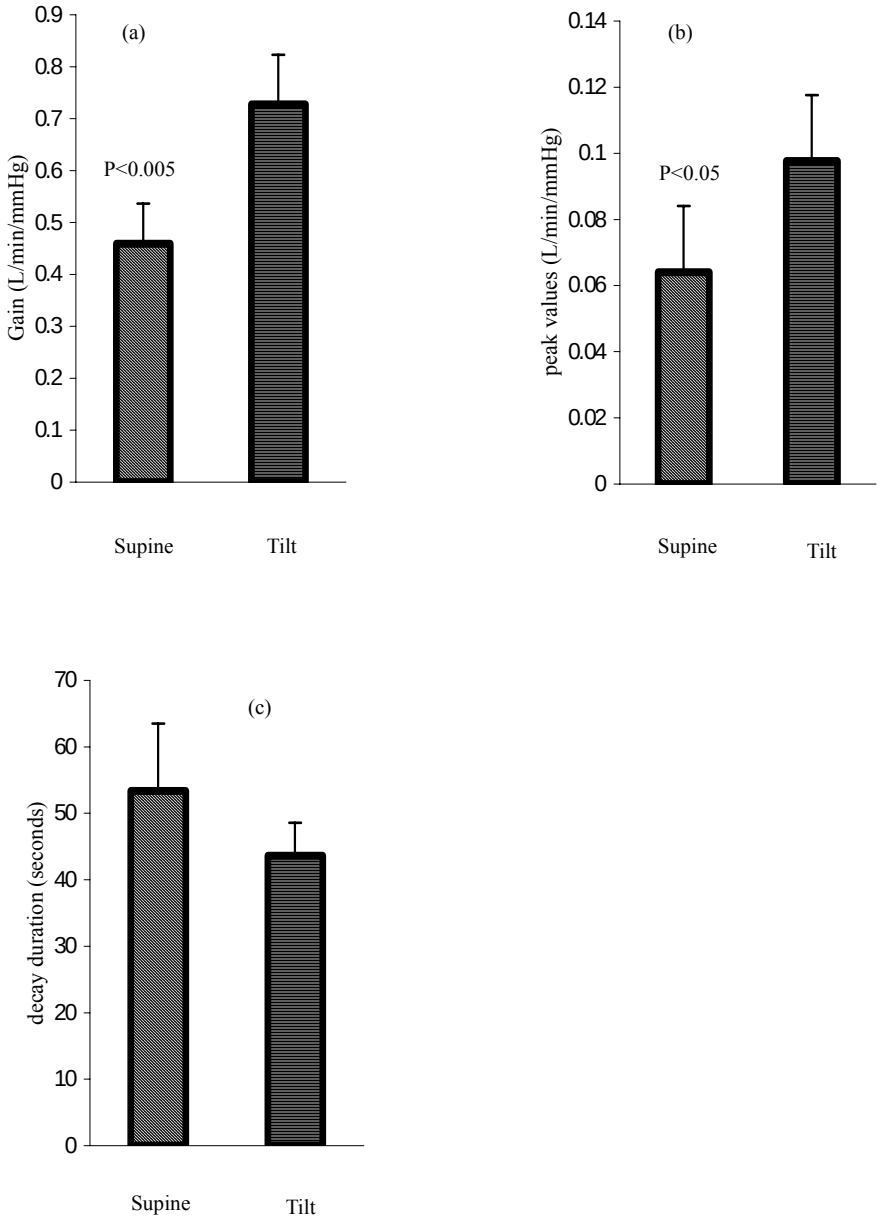

Figure 5.3 Integrals (a), peak values (b) and 50 % amplitude decay time (c) for non-presyncopal group average (N=24) open loop impulse responses. The responses show that integral of the impulse response and peak values were larger in tilt than in supine ($p < 0.05$). The impulse responses decayed faster in tilt than supine (c) but the difference was not significant.

5.1.3 Transfer function between end tidal CO_2 and ventilation

To verify and to complement changes in ventilatory responses that we obtained using parametric estimates, we used a non-parametric transfer function estimate. Figure 5.4 showed the average transfer function magnitude between $ETCO_2$ and $\dot{V}_E$ from non-presyncopal subjects (N=24). The transfer functions showed higher magnitude at most frequencies below the Nyquist frequency of 0.12 Hz (Since the average respiratory rate is about 14 breaths/min, the average breathing frequency is 0.24 Hz and the Nyquist frequency is half of the breathing frequency). We integrated the transfer function magnitudes over all frequencies between 0 and 0.12 Hz to quantify an index of ventilatory response. The average integrated transfer function values during Supine PRBS (0.22 ± 0.02 L/min/mmHg) were larger than during Tilt PRBS (0.29 ± 0.02 L/min/mmHg) (Mean±SEM) ($p < 0.05$). The figure shows that the difference in transfer function magnitudes between Supine and Tilt was more pronounced in the frequency region between 0.08 and 0.1 Hz. The average of the transfer functions magnitude within this frequency region was also significantly higher ($p < 0.01$) during tilt than supine. Note that the estimates for near zero (DC) frequencies are unreliable due to removal of mean during computation of the transfer functions.

Using a similar method, we estimated the transfer function between $ETCO_2$ and $\dot{V}_E$ for the presyncopal subjects (N=6) during Supine PRBS and Tilt PRBS. Unlike non-presyncopal group, there were no significant differences between supine and tilt for presyncopal group. When comparing between groups, as shown in Figure 5.5, it is obvious that at most frequencies the mean value for the transfer function gain is higher for presyncopal subjects than non-presyncopal subjects during supine. Integrated transfer function gain in the frequency region 0.08-0.11Hz were higher for presyncopal subjects

than non-presyncopal subjects during supine ($p<0.05$). There were no significant differences between groups during tilt. The presyncopal group started with a higher gain and did not increase further during tilt; while the non-presyncopal group started with a lower gain, then the gain was enhanced during tilt.

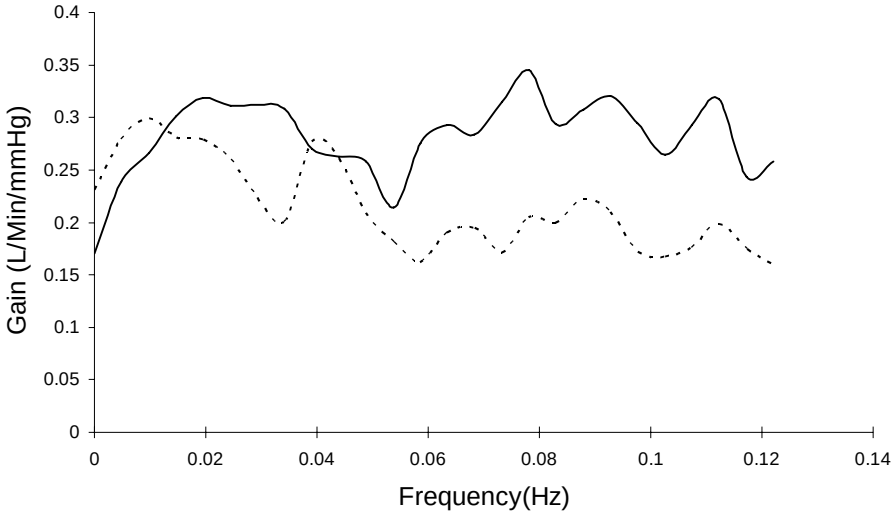

Figure 5.4 Non-presyncopal group average (N=24) transfer function gain between $ETCO_2$ and $\dot{V}_E$ during Supine PRBS (dashed) and Tilt PRBS (solid). Note that for almost all frequencies the gain was larger in tilt than in supine. Differences in gain were largest in a frequency region approximately between 0.08 and 0.1 Hz. Note that the estimates for near zero (DC) frequencies are unreliable due to removal of mean during computation of the transfer functions.

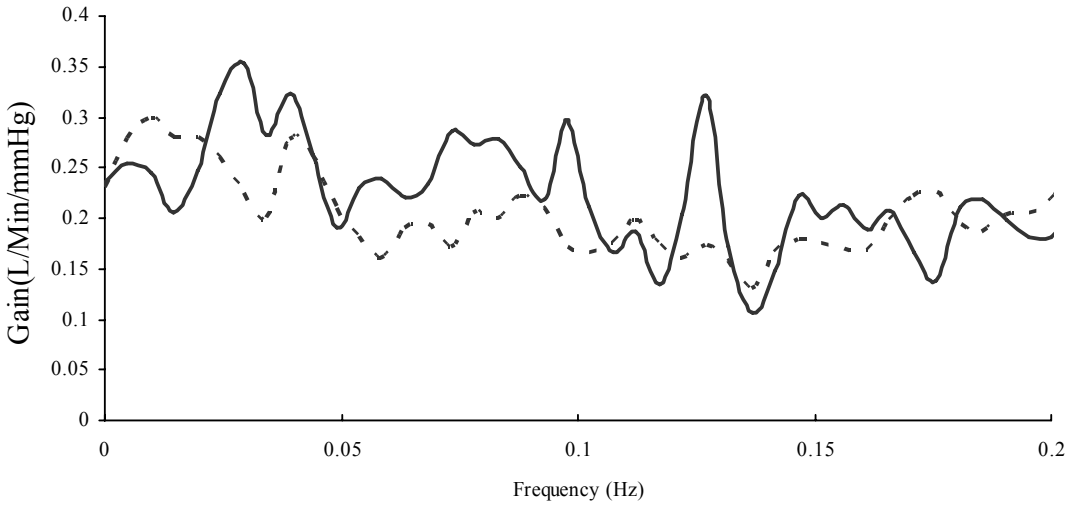

Figure 5.5 Average transfer function gains between $ETCO_2$ and $\dot{V}_E$ for non-presyncopal group (dashed) and presyncopal group (solid) during Supine PRBS. Note that for almost all frequencies the gain was larger in presyncopal group than in non-presyncopal group.

To show that PRBS widens the input spectrum, in our case the spectrum of $ETCO_2$, we include Figure 5.6. As shown in Figure 5.6, during PRBS stimulation (pink), the $ETCO_2$ spectrum had more power within a larger frequency range between 0 and 0.15 Hz than during Supine Control (blue). These results show that PRBS input did widen the input spectrum as expected.

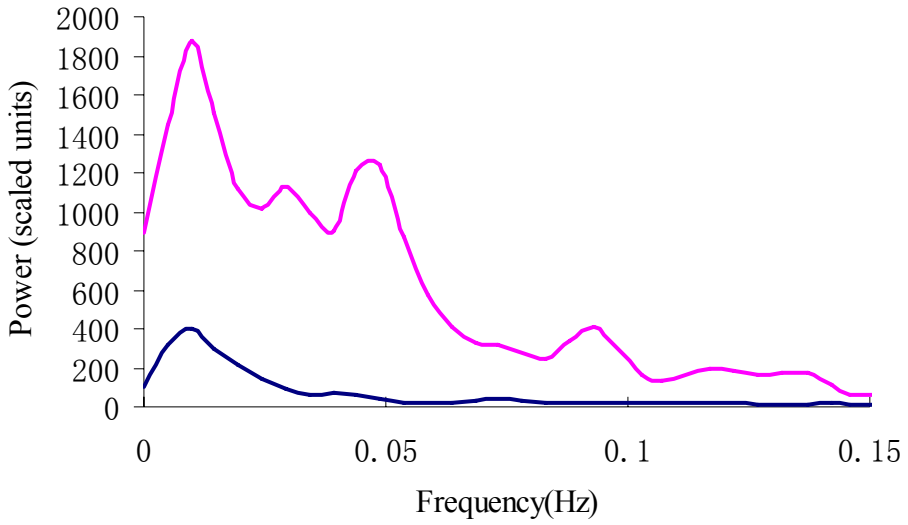

Figure 5.6 Power spectrum for $ETCO_2$ during Supine PRBS (pink) and Supine Control (blue).

5.1.4 Baroreflex sensitivity, heart rate and blood pressure variability

In non-presyncopal subjects, baroreflex sensitivity increased from 5.5 msec/mmHg during supine to 17.6 msec/mmHg during tilt ($p<0.001$). Similarly, in pre-syncopal subjects, baroreflex sensitivity increased from 6.5 during supine to 21.8 msec/mmHg during tilt ($p=0.01$)

Figure 5.7 shows the averaged RR interval spectra for non-presyncopal subjects (N=24) (a) and for presyncopal subjects (N=6) (b) during the four stages of our study. The distribution of power seen in these spectra reveals frequency regions where these signals oscillated. We note that spectra from pre-syncopal group show more pronounced peaks in very low, low and high frequency regions relative to those seen in spectra from the non-presyncopal group. It is possible that variations in intrinsic breathing frequencies among the larger pool in non-presyncopal group averaged the power over wider frequency range.

Figure 5.7 a

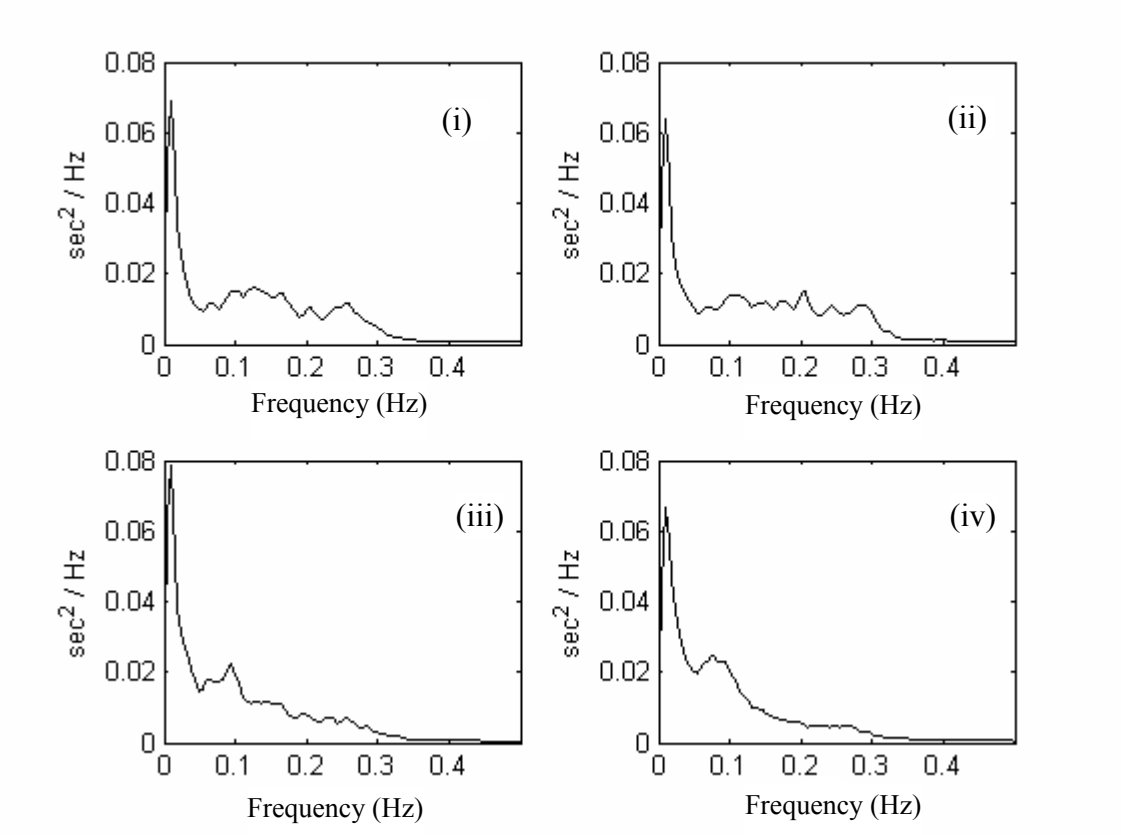

Figure 5.7 b

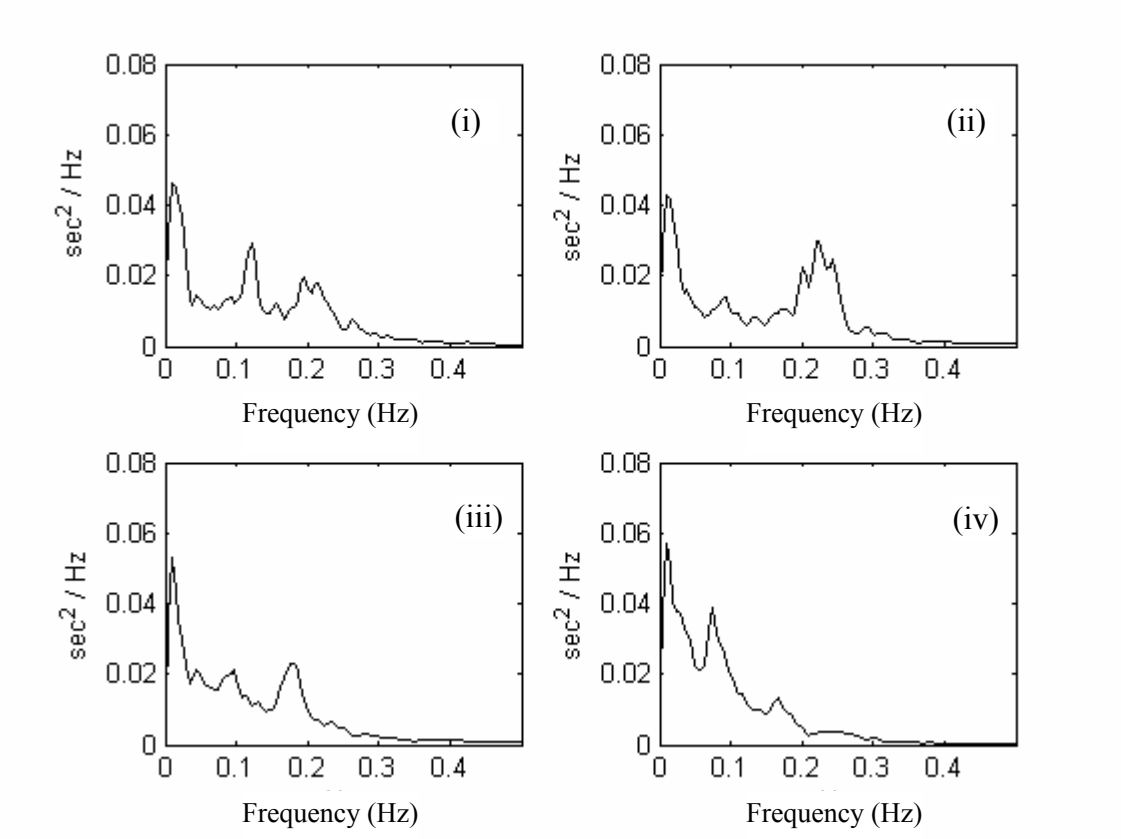

Figure 5.7 The average heart rate variability for non-presyncopal subjects (N=24) (a) and for presyncopal subjects (N=6) (b) during the four stages of our study.(i) Supine Control (ii) Supine PRBS (iii) Tilt PRBS (iv) Tilt Control.

As an index of parasympathetic activity, we computed respiratory synchronous heart rate variability for the non-presyncopal subjects, which decreased during tilt from 1.08 to 0.47 AU, $p < 0.01$, a 57 % decrease which was comparable to those reported previously, i.e. 60% and 77% (Patwardhan et al.(54) and Laitinen et al (38)).

Figure 5.8 shows the average of MBP spectra during Supine Control (dashed) and Tilt Control (solid) for non-presyncopal subjects. As expected, blood pressure oscillations within the LF region centered at 0.1 Hz increased during tilt ($p < 0.01$).

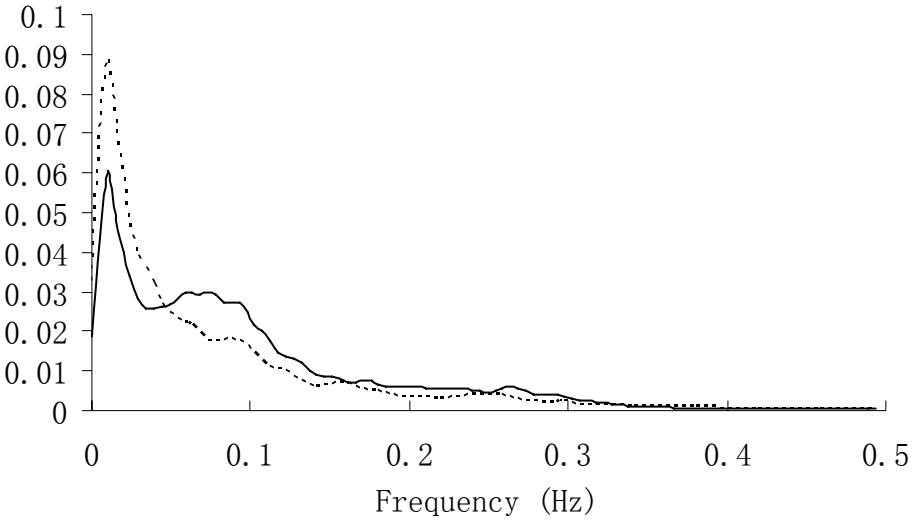

Figure 5.8 Average (N=24) of mean blood pressure variability during Supine Control (dashed) and Tilt Control (solid) for non-presyncopal subjects. As expected, blood pressure oscillations within the LF region centered at 0.1 Hz increased during tilt ($p < 0.01$).

5.1.5 Gender-related differences in non-presyncopal subjects

We selected age-matched 10 male and 10 female subjects from the non-presyncopal group. The mean values of CBFM, heart rate, MBP, ventilation and $ETCO_2$ are listed (Mean± SEM) in tables 5.3 (Men) and 5.4 (Women) for the four stages of the study. Results from two-way ANOVA test shows that the factor of gender had significant

effects on CBFM ($p<0.05$). Women had higher CBFM than men (a difference of almost 10cm/s) during Supine Control and Supine PRBS. During Tilt PRBS, CBFM for both groups was almost the same, while during Tilt Control, the mean value for women was higher, but the difference (5 cm/s) was smaller compared with that observed during the supine position. For both groups, CBFM had a small but significant increase during Supine PRBS compared with Supine Control and significant decrease during tilt. Heart rate, blood pressure and ventilation were increased during tilt for both groups, as expected. $ETCO_2$ was increased during Supine PRBS and decreased during Tilt Control for both groups (68).

Table 5.3 Mean values for male subjects (N=10). [a] significant difference between Supine PRBS and Supine Control; [b] significant difference between Tilt PRBS and Supine Control; [c] significant difference between Tilt Control and Supine Control.

Male	Supine Control	Supine PRBS	Tilt PRBS	Tilt Control
CBFM (cm/s)	67.0 ± 4.5	$68.8^{a} \pm 5.1$	66.4 ± 4.8	$62.5^{c} \pm 4.5$
Heart Rate (beats/min)	74.6 ± 4.7	$72.2^{a} \pm 4.5$	$89.9^{b} \pm 4.0$	$94.5^{c} \pm 4.1$
MBP (mmHg)	96.1 ± 3.7	95.1 ± 3.2	$100.6^{b} \pm 4.2$	$104.3^{c} \pm 4.2$
Ventilation (L/Min)	7.9 ± 0.7	8.4 ± 0.8	$9.7^{b} \pm 0.9$	8.5 ± 0.7
$ETCO_2$ (mmHg)	48.2 ± 1.7	$50.8^{a} \pm 1.5$	48.7 ± 1.1	$44.3^{c} \pm 1.7$

Table 5.4 Mean values for female subjects (N=10). [a] significant difference between Supine PRBS and Supine Control; [b] significant difference between Tilt PRBS and Supine Control; [c] significant difference between Tilt Control and Supine Control;

* significant difference between men and women.

Female	Supine Control	Supine PRBS	Tilt PRBS	Tilt Control
CBFM (cm/s)	$76.7^{*} \pm 3.5$ (*p=0.07)	$78.3^{*,a} \pm 3.6$ (*p=0.07)	$65.6^{b} \pm 3.9$	$67.5^{c} \pm 2.99$
Heart Rate (beats/min)	72.1 ± 3.5	70.5 ± 3.5	$82.9^{b} \pm 3.5$	$87.0^{c} \pm 3.66$
MBP (mmHg)	85.4 ± 4.0	89.4 ± 3.3	$97.8^{b} \pm 3.6$	$100.0^{c} \pm 4.2$
Ventilation (L/Min)	7.6 ± 0.5	$8.9^{a} \pm 0.7$	$10.0^{b} \pm 0.9$	$8.3^{c} \pm 0.5$
$ETCO_2$ (mmHg)	46.2 ± 1.2	$48.8^{a} \pm 1.2$	46.9 ± 1.3	$42.1^{c} \pm 1.2$

Figure 5.9 shows averaged coherencies between mean blood pressure (MBP) and mean cerebral blood flow (CBFM) during Supine Control for men (thin line) and women (thick line). Integrated coherence within 0.03-0.10 Hz and 0.22-0.31 Hz showed that women had significantly higher coherence than men during Supine Control (p=0.05 and 0.01). As shown in Figure 5.10, transfer function gains were higher in women (thick line) than men (thin line) in frequency regions 0.03-0.14 Hz and 0.22-0.31 Hz during Supine Control. The differences in integrated gains within these regions were significant (p=0.0045 and 0.0015).

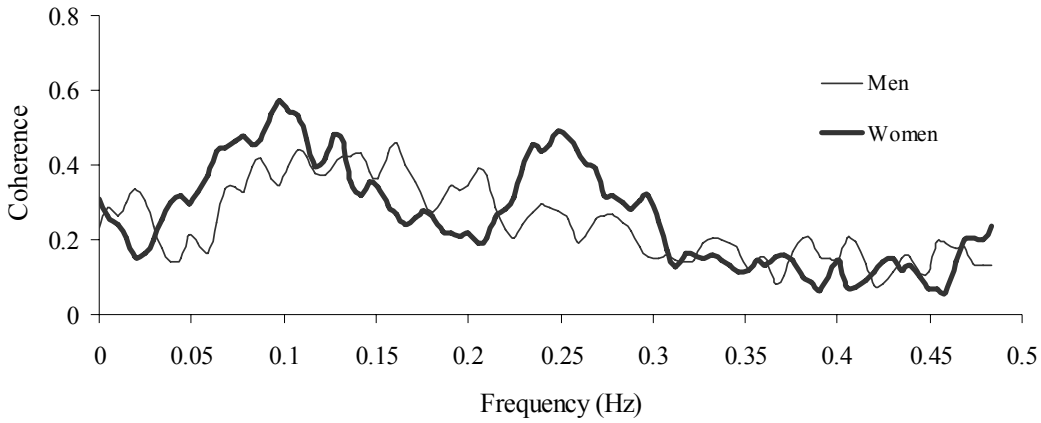

Figure 5.9 Averaged coherencies between mean blood pressure (MBP) and mean cerebral blood flow (CBFM) in female (thick line) and male (thin line) subjects during Supine Control.

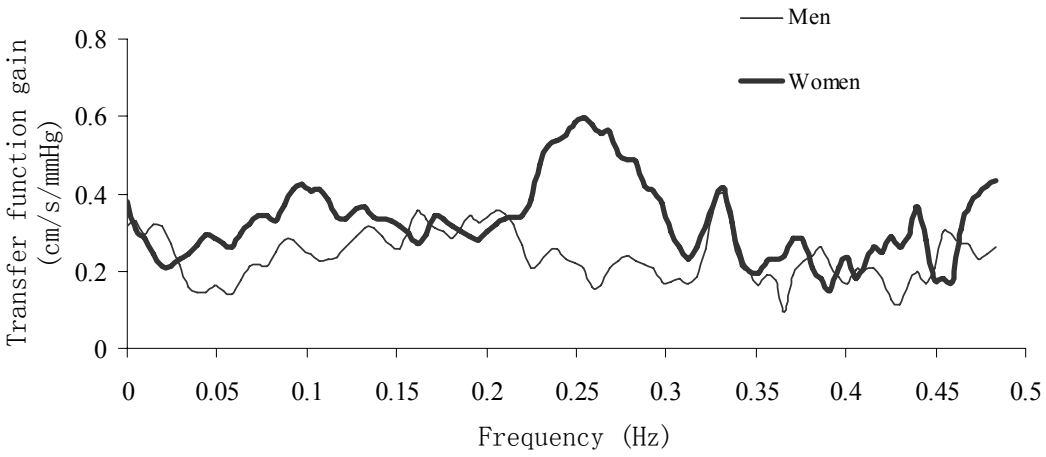

Figure 5.10 Averaged transfer function gains between mean blood pressure (MBP) and mean cerebral blood flow (CBFM) in female (thick line) and male subjects (thin line) during Supine Control.

As shown in Figure 5.11, men had significantly higher coherence than women during Tilt PRBS between 0.05-0.28 Hz (p=0.0013). As shown in Figure 5.12, between 0.05-0.26 Hz men had significantly higher coherence than women during Tilt Control (p=0.016). The transfer function gain for men during Tilt PRBS tended to be larger than women but the difference was not significant. The transfer function gain in Tilt Control also did not show significant differences between women and men.

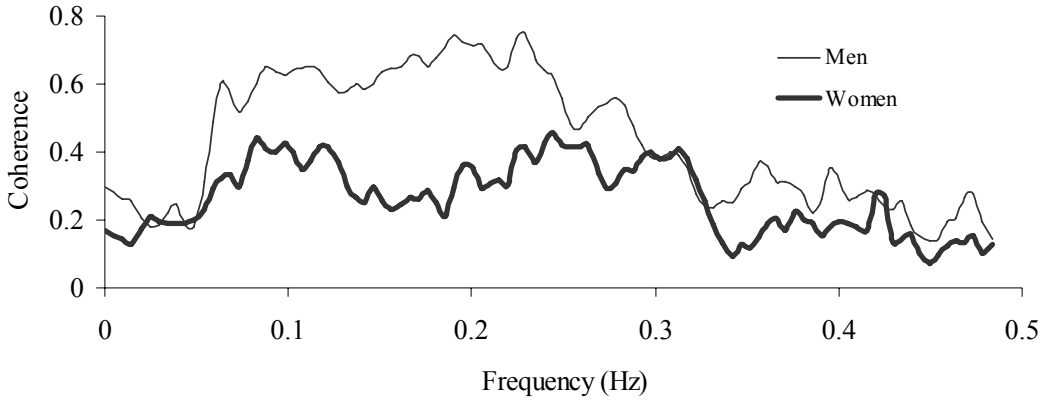

Figure 5.11 Average coherencies between mean blood pressure (MBP) and mean cerebral blood flow (CBFM) in women (thick line) and men (thin line) during Tilt PRBS.

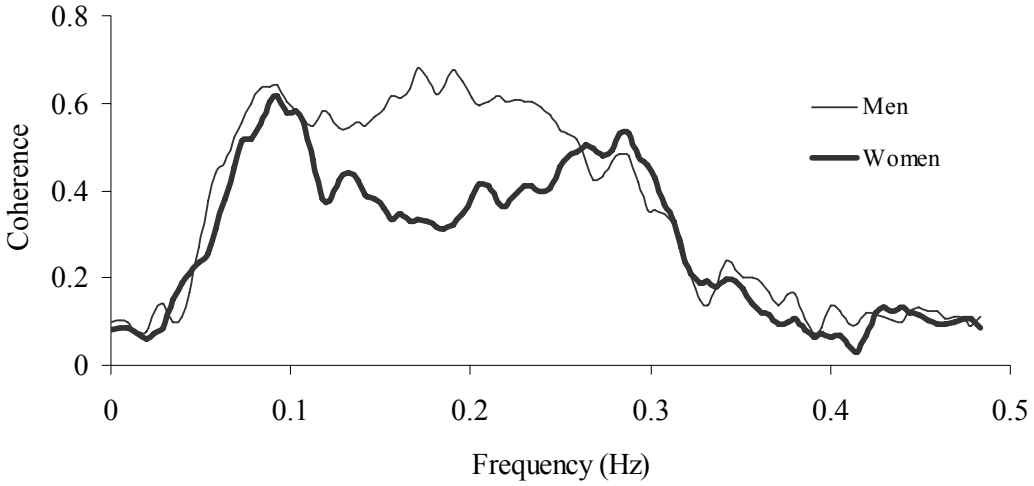

Figure 5.12 Average coherencies between mean blood pressure (MBP) and mean cerebral blood flow (CBFM) in women (thick line) and men (thin line) during Tilt Control.

5.1.6 Bispectrum estimation

Figure 5.13 shows an example of the normalized auto-bispectrum calculated from RR intervals in one non-presyncopal subject during the four sections of study. The auto-bispectra are symmetric around the diagonal ($f_1=f_2$), therefore only half of the bispectral surfaces are shown in the figure; the other half is shown as zero. The figure shows concentration of power at low frequencies, as expected from the nature of RR interval variability. Changes in the phase coupling during PRBS are also evident: phase coupling is seen at relatively higher frequencies during Supine PRBS (panel ii) but is concentrated at very low frequencies during Tilt PRBS (panel iii).

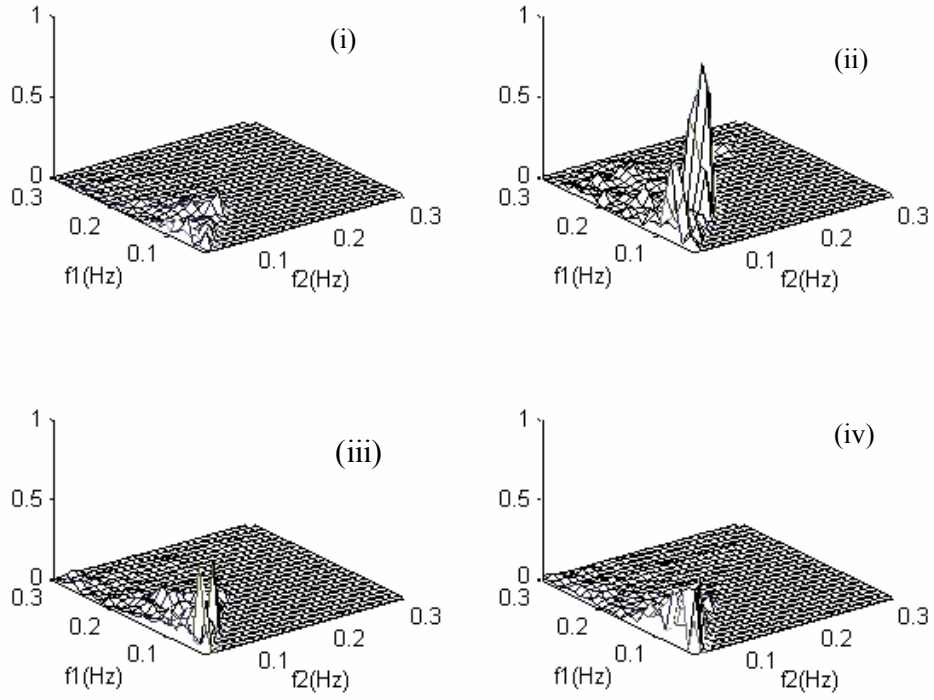

Figure 5.13 Normalized auto-bispectra for RR intervals from one typical subject in the non-presyncopal group during each stage of the study (i-Supine Control; ii-Supine PRBS; iii-Tilt PRBS; iv-Tilt Control). The auto-bispectra are symmetric around the diagonal (f_1=f_2), therefore, only half of the bispectral surfaces are shown in the four panels. The figure shows concentration of power at very low frequencies. Changes in the phase coupling during PRBS are also evident, at higher frequencies during Supine PRBS (panel ii) and concentration of power at very low frequencies during Tilt PRBS (panel iii).

To quantify the degree of phase coupling between frequencies, we integrated bispectra within different frequency regions defined by frequencies ranges (f_1 and f_2). The integrated bispectral values were then compared for statistically significant differences as follows: The effects of orthostatic and chemoreflex modulation of phase coupling were compared within the non-presyncopal and the presyncopal groups across all four sections of the study (Tables 5.5 and 5.6). To determine changes in phase coupling prior to the onset of presyncope, a between-groups comparison was made during each section of the study (Table 5.6).

Table 5.5 Integrated bispectra for the non-presyncopal subjects (N=24). † Significant difference between Supine PRBS and Supine Control; ‡ Significant difference between Tilt PRBS and Supine Control; * Significant difference between Tilt Control and Supine Control.

RR	Supine Control	Supine PRBS	Tilt PRBS	Tilt Control
I	36.87±4.92	47.2†±5.5	30.89±4.7	21.13*±3.09
II	41.03±6.21	64.3†±8.92	28.47‡±6.2	14.14*±2.6
III	15.15±2.99	25†±4.93	8.454‡±2.2	3.457*±0.78
SBP				
I	12.35±1.8	12.2±1.94	33.67‡±4.1	32.54*±3.95
II	8.909±1.7	7.74±1.55	29.88‡±7.5	20.9*±3.07
III	2.278±0.5	1.96±0.52	10.81‡±4.4	5.04*4±0.8
RR-SBP				
I	62.36±6.92	75.1†±6.62	70.93±7.4	51.93±5.35
II	41.05±5.72	60.3†±7.92	34.2±5.4	20.04*±3.65
III	15.02±2.93	23.3†±4.61	15.53±3.4	7.849*±1.64
IV	24.33±3.44	33.2†±5.1	28.9±4.9	17.64*±2.9
RR-Vt				
I	44.95±5.78	60.7†±7.87	57.89‡±6.7	41.5±6.06
II	26.98±3.98	48†±8.21	26.51±4.2	15.32*±2.72
III	5.739±1.18	11.2†±2.84	5.757±1	3.52±0.72
IV	9.889±1.3	16.5†±2.81	12.41‡±2	8.954±1.71
CBFM-$ETCO_2$				
I	13.53±2.1	41.3†±5.67	62.45‡±6.5	25.89*±4.9
II	5.85±0.83	16.1†±2.53	26.94‡±3.5	11.64*±2.84
III	1.37±0.19	3.73†±0.58	6.016‡±0.8	2.648*±0.59
IV	3.955±0.79	11.5†±1.49	17.16‡±2.6	6.765*±1.32
CBFM-SBP				
I	23.63±3.5	34.5†±5.56	76.45‡±5.8	46.15*±5.39
II	10.66±1.74	13.2†±2.28	29.57‡±2.5	19.15*±2.19
III	4.276±0.82	5.35±0.98	14.15‡±1.7	7.465*±0.94
IV	9.757±1.55	14.2†±2.45	34.56‡±4.7	16.94*±1.68

Table 5.6 Integrated bispectra for presyncopal subjects (N=6). † Significant difference between Supine PRBS and Supine Control; ‡ Significant difference between Tilt PRBS and Supine Control; * Significant difference between Tilt Control and Supine Control; [a] Significant difference between non-presyncopal and presyncopal subjects.

RR	Supine Control	Supine PRBS	Tilt PRBS	Tilt Control
I	22.08±7.19	27.48 [a] ±8.78	16.06 [a] ±5.05	14.4±5.36
II	24±8.18	39.3±12.4	13.53 [a] ±5.51	5.29[a,*]±1.56 (*p=0.06)
III	11.51±5.31	20.62†±6.65	5.82±3.46	1.01[a,*]±0.26 (*p=0.06)
SBP				
I	14.02±3.93	11.67±2.5	45.71‡±11.6	41.93*±5.50
II	6.16±1.65	7.67±2.22	40.89‡±17.4	18.67*±4.77
III	1.34±0.47	1.41±0.41	13.68±7.04	2.98 [a, *]±0.81
RR-SBP				
I	40.3 [a]±9.37	46.97 [a]±13.1	48.26±14	35.19±9.21
II	26.48±6.47	46.17±15.4	24.8±11.2	8.72 [a,*]±1.93 (*p=0.06)
III	9.03±2.62	17.05†±4.63	15.33±9.39	2.44 [a, *]±0.44
IV	12.12 [a]±2.30	18.41 [a]±4.83	19.8±9.32	7.09[a]±1.81
RR-Vt				
I	32.9±10.01	53.99±16.4	53.3±13.8	29.99±4.17
II	19.77±5.77	46.61†±15.8	25.01±9.05	8.00 [a, *]±1.59
III	4.28±1.27	10.34†±3.41	7.011±4.01	1.88 [a]± 0.31
IV	7.31±2.48	11.56±3.33	9.9±3.81	5.04 [a]± 0.89
CBFM-$ETCO_2$				
I	8.43±2.52	28.1†±9.37	44.24‡±10.3	33.48±13.16
II	4.16±1.59	16.17†±6.48	16.85 [a, ‡]±4.42	11.4±4.90
III	1.12±0.5	4.10±2.26	3.28 [a, ‡]±0.84	2.38±1.05
IV	2.68±0.99	8.94†±2.54	10.05 [a, ‡]±2.55	7.43±3.41
CBFM-SBP				
I	27.5±11.26	30.57±10.1	61.04‡±15.2	66.04 [a, *]±6.27
II	14.38±6.72	18.19†±7.09	20.05±5.04	19.19±1.14
III	5.42±2.44	9.66±5.97	11.38‡±4.62	5.95±0.48
IV	10.26±4.26	14.86†±5.13	23.06±7.02	16.21±3.13

Figure 5.14 shows contour plots of group averaged RR interval auto-bispectra. The non-presyncopal group's averaged RR interval bispectra are shown in Figure 5.14 (a), and those from the presyncopal group are in 5.14 (b). There was an enhanced coupling of frequencies less than 0.1 Hz with those greater than 0.1 Hz during Supine PRBS for both groups which probably reflected altered chemoreflex control. The contours in panel iii and iv show the orthostatic effects. As given in Table 5.5, in non-presyncopal group in all frequency regions phase coupling increased during Supine PRBS while phase coupling decreased during Tilt PRBS and Tilt Control, relative to Supine Control. As given in Table 5.6, we observed a similar pattern of change in the presyncopal group as in the non-presyncopal group. The increase in phase coupling during Supine PRBS in frequency region III was significant and the decreases in phase coupling during Tilt Control, within frequency regions II and III were not significant at our threshold of $p=0.05$ (they were marginally significant with $p=0.06$). Comparison between groups showed that phase coupling in RR interval was smaller in the presyncopal group than the non-presyncopal group during Supine PRBS within frequency region I, during Tilt PRBS within regions I and II, and during Tilt Control within frequency regions II and III.

Figure 5.14 a

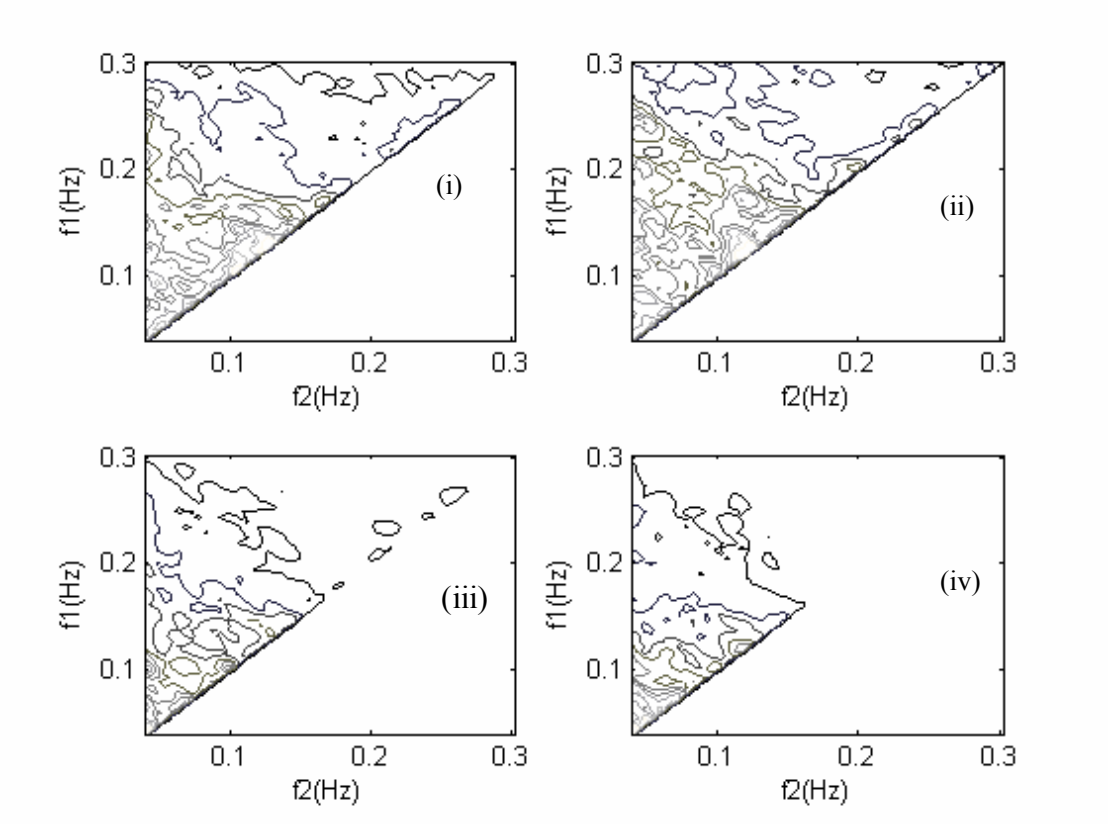

Figure 5.14 b

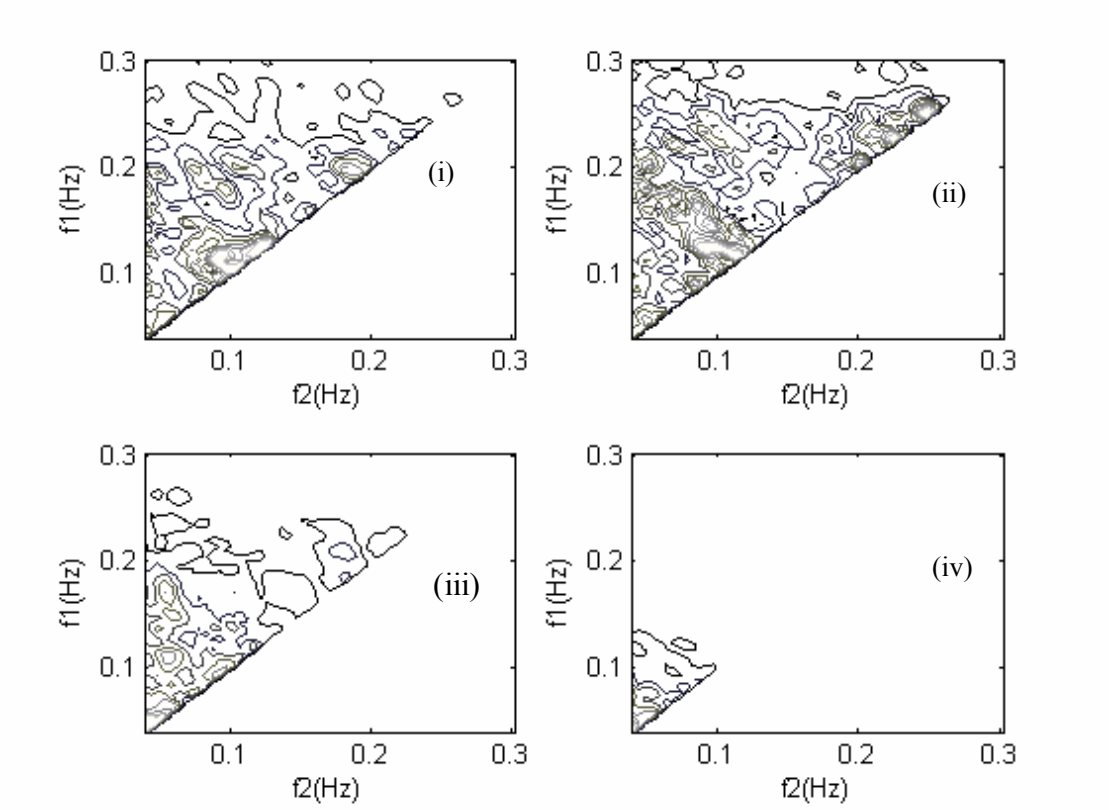

Figure 5.14 Contour plots of group averaged RR interval auto-bispectra (i-Supine Control; ii-Supine PRBS; iii-Tilt PRBS; iv-Tilt Control). (a) shows the averaged (N=24) bispectra for the non-presyncopal group. The contours in panel iii and iv show the orthostatic effects. (b) shows the averaged (N=6) bispectra of the presyncopal group. As shown in panel (iv) during Tilt Control, there was a marked reduction in the spread of contours relative to that during Tilt PRBS (panel iii).

Figure 5.15 shows contour plots of group averaged Systolic blood pressure (SBP) auto-bispectra in a format similar to that in Figure 5.14. The non-presyncopal group's averaged SBP bispectra are shown in Figure 5.15 (a), and those from the presyncopal group are in 5.15 (b). Figure 5.15 shows that relative to RR intervals, the phase coupling within SBP was confined to lower frequencies. Comparison between the contours in panels i, ii with iii and iv of the figures show that phase coupling in both groups increased significantly during tilt within almost all the frequency regions (except

for presyncopal subjects during Tilt PRBS within region III) . Comparison between groups showed, the phase coupling was lower for the pre-syncopal than for the non-presyncopal group during Tilt Control within region III (0.15-0.30, 0.15-0.30Hz).

Figure 5.15 a

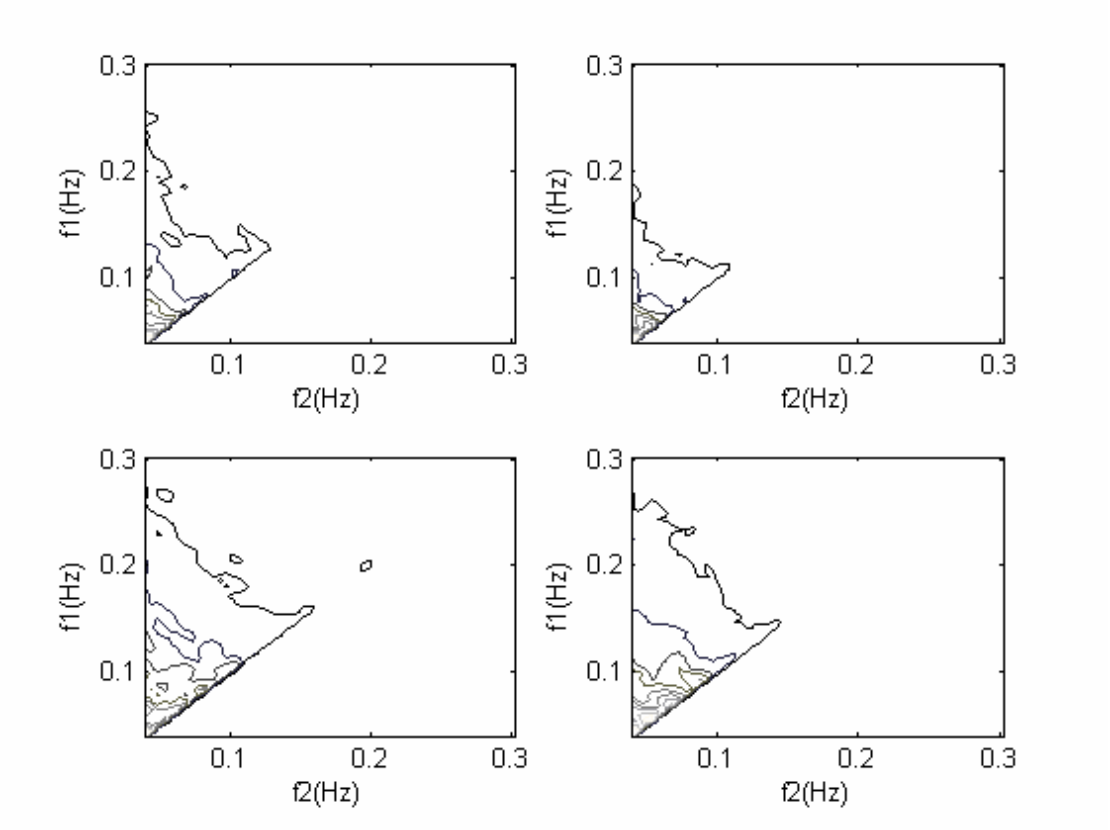

Figure 5.15 b

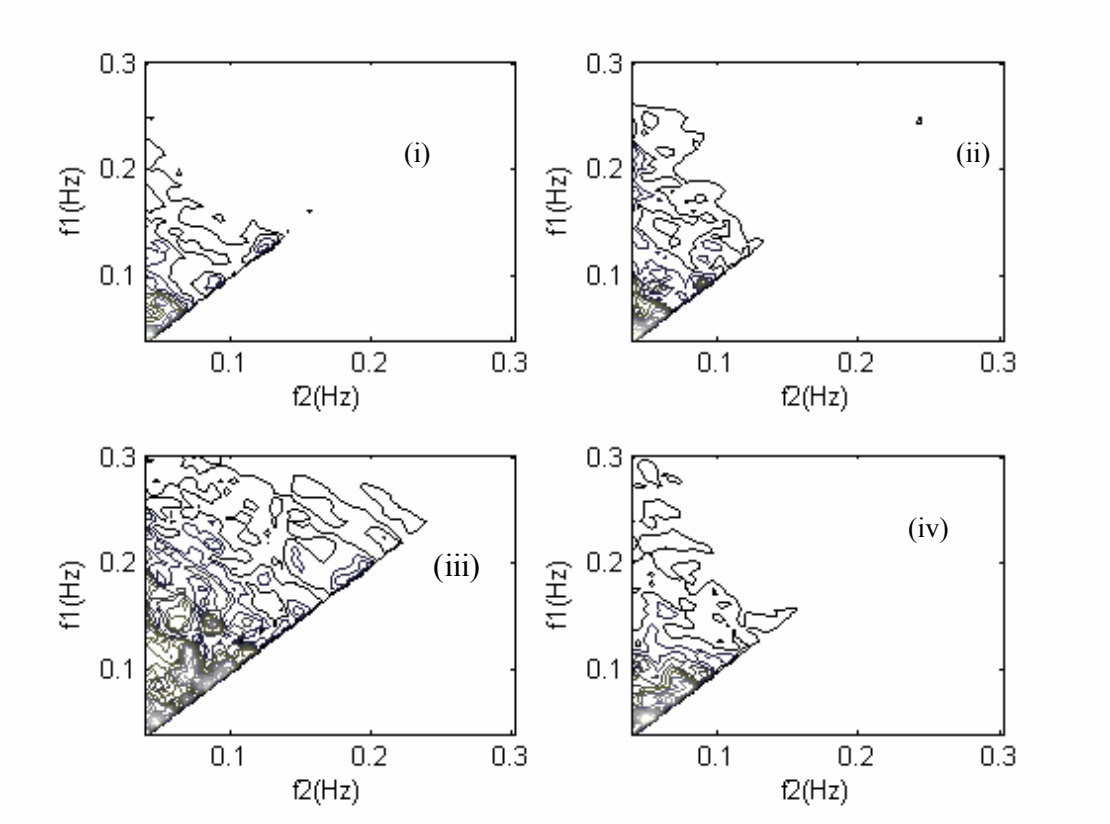

Figure 5.15 Contour plots of group averaged systolic blood pressure (SBP) auto-bispectra (i-Supine Control; ii-Supine PRBS; iii-Tilt PRBS; iv-Tilt Control). Figure 5.15 (a) shows the averaged (N=24) bispectra for the non-presyncopal group. Comparison between the contours in panels i, ii with iii and iv of the figure show that tilt increased phase coupling. Figure 5.15 (b) shows the averaged (N=6) bispectrum for the presyncopal group. There was a noticeable increase in the spread of contours in presyncopal group relative to that in the non-presyncopal group in all stages.

The cross-bispectra are not symmetric, therefore, the bispectra were estimated over the entire frequency range, i.e. 0.04-0.3, 0.04-0.3 Hz. The group averaged bispectra between RR interval and SBP are shown in Figure 5.16. It is obvious that the low frequencies were more modulated by high frequency during Supine PRBS for presyncopal group than non-presyncopal group. As shown in Table 5.5 and Table 5.6, for both groups, during Supine PRBS, phase coupling between RR interval and SBP increased in all the frequency regions, while during Tilt Control, phase coupling decreased. Comparisons between groups showed that the presyncopal group had a lower degree of coupling than non-presyncopal group during Supine Control and Supine PRBS in region I and IV, during Tilt Control in region II, III and IV.

Figure 5.16 a

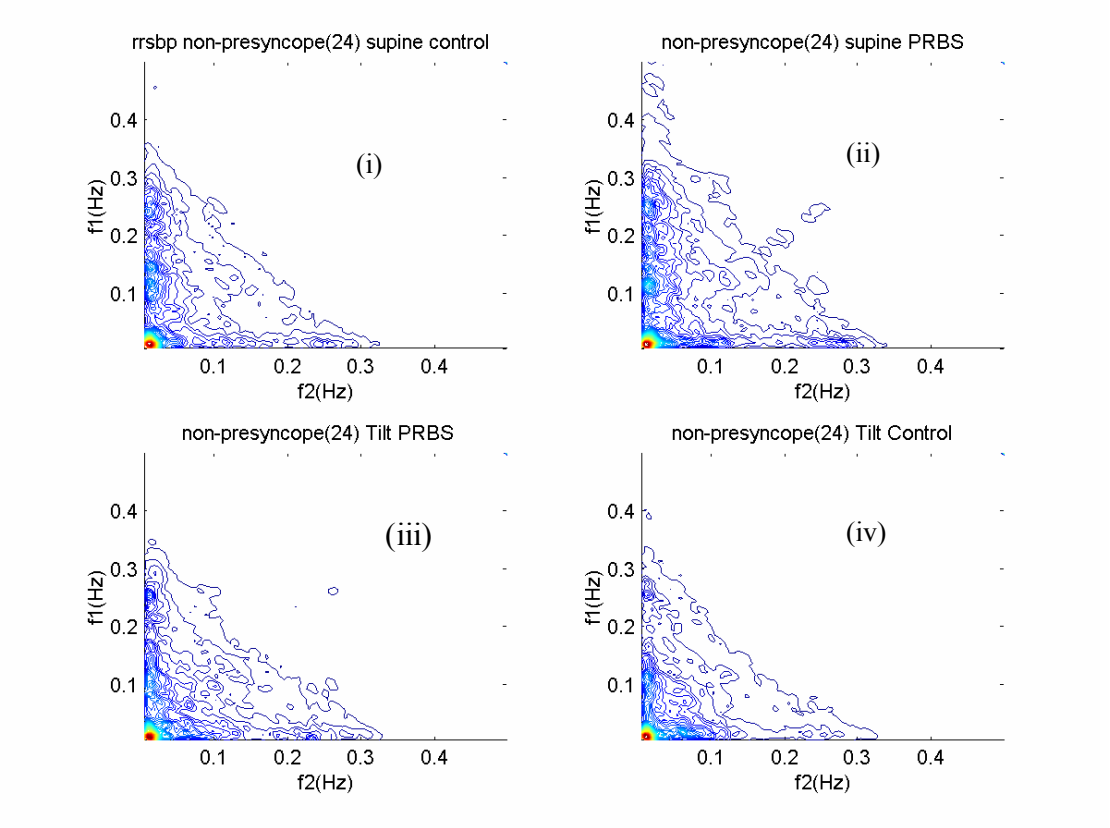
rrsbp non-presyncope(24) supine control
(i)
non-presyncope(24) supine PRBS
(ii)
non-presyncope(24) Tilt PRBS
(iii)
non-presyncope(24) Tilt Control
(iv)
f1(Hz)
f2(Hz)
0.1
0.2
0.3
0.4

Figure 5.16 b

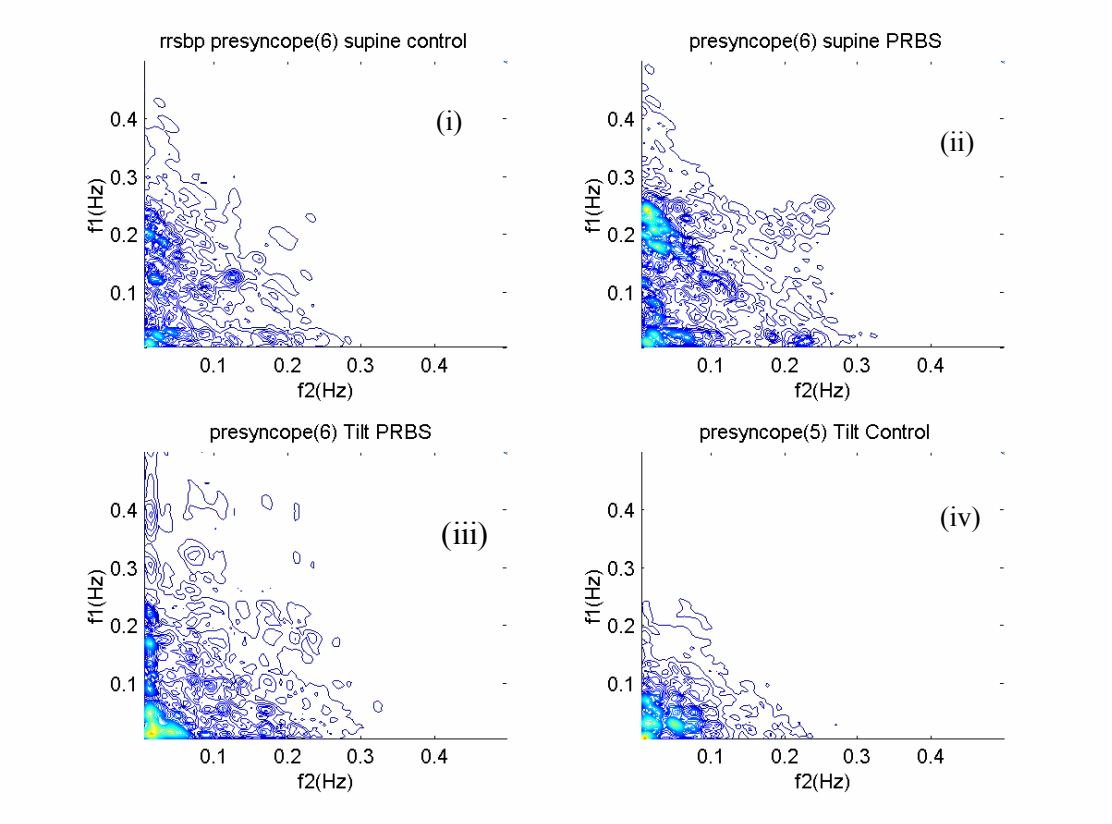

Figure 5.16 Contour plots of group averaged cross-bispectra between RR interval and systolic blood pressure (RR-SBP) (i-Supine Control; ii-Supine PRBS; iii-Tilt PRBS; iv-Tilt Control). Figure 5.16 (a) shows the averaged (N=24) bispectra for the non-presyncopal group. Figure 5.16 (b) shows the averaged (N=6) bispectrum for the presyncopal group.

To investigate cardio-respiratory interactions, we calculated cross-bispectra between RR-interval and Tidal volume, the results of which are shown in Figure 5.17. During Supine PRBS, we observed increased phase coupling between RR interval and Tidal volume for both groups within all the frequency regions (except for presyncopal subjects within region I and IV). For both groups during Tilt control in region II, modulation of higher frequencies in RR interval (f_1: 0.15-0.3Hz) by lower frequencies in Tidal volume (f_2: 0.04-0.15Hz) decreased. During Tilt PRBS, we observed enhanced phase coupling in region I and IV for the non-presyncopal subjects. During Tilt Control, the phase coupling was lower in pre-syncopal than in non-presyncopal group in frequency region II, III and IV.

Figure 5.17 a

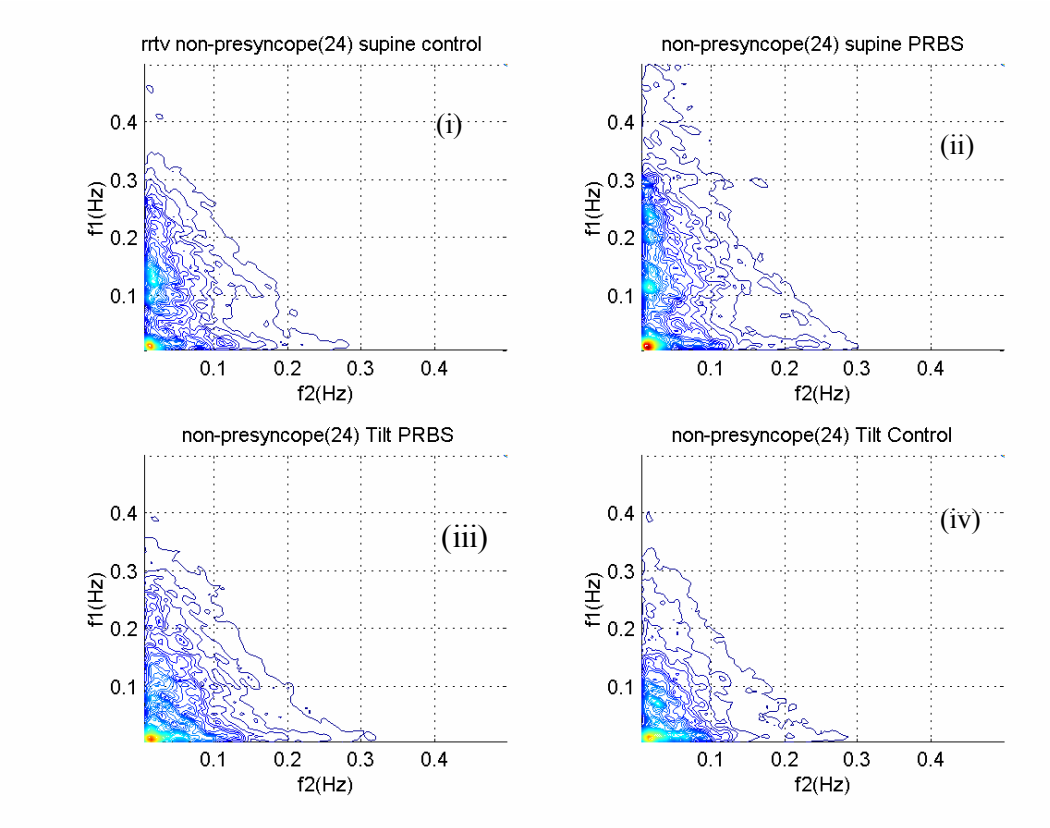

Figure 5.17 b

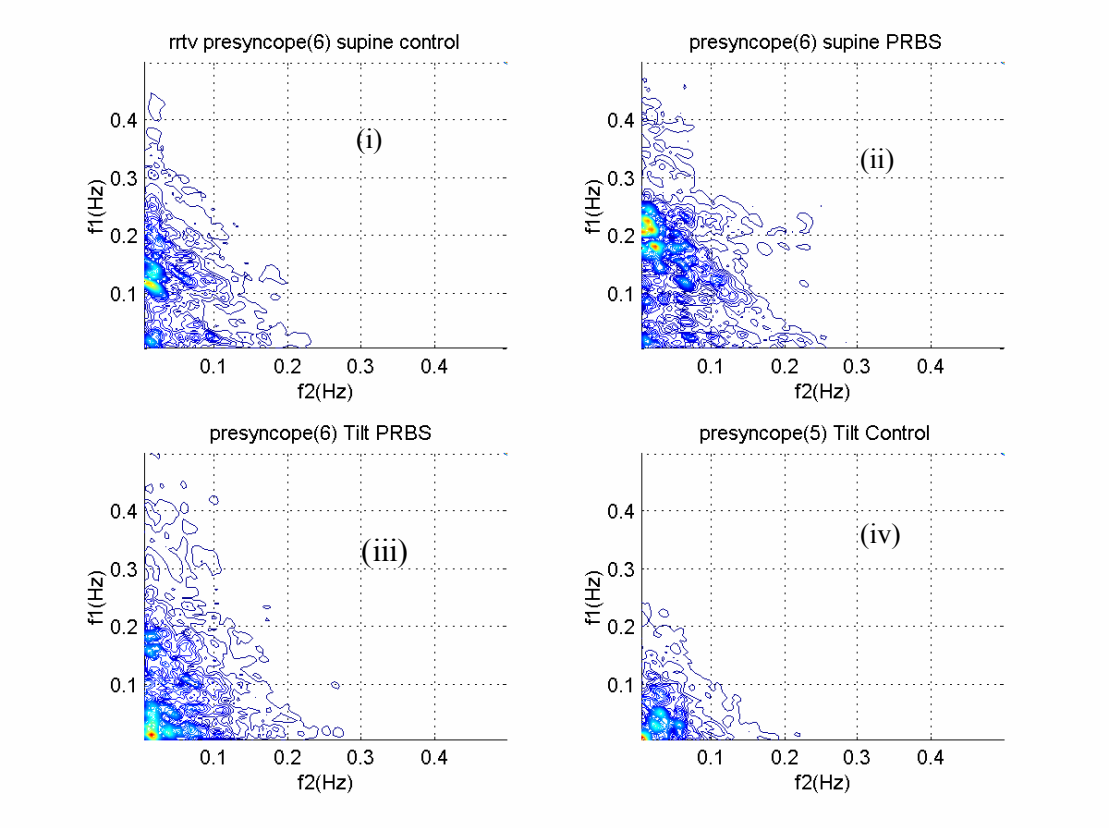

Figure 5.17 Contour plots of group averaged cross-bispectra between RR interval and tidal volume (RR-V_t) (i-Supine Control; ii-Supine PRBS; iii-Tilt PRBS; iv-Tilt Control). Figure 5.17 (a) shows the averaged (N=24) bispectra for the non-presyncopal group. Figure 5.17 (b) shows the averaged (N=6) bispectrum for the presyncopal group.

As shown in Figure 5.18, we calculated cross-bispectra between CBFV and $ETCO_2$ to investigate the effects of arterial partial pressure of CO_2 on CBFV. Cross-bispectra between CBFV and $ETCO_2$ showed that, in non-presyncopal subjects (Table 5.5), relative to Supine Control, phase coupling increased during Supine PRBS, Tilt PRBS and Tilt Control in all frequency regions. In presyncopal group, the changes in phase coupling showed a similar trend to changes in the non-presyncopal group (within some frequency regions the changes were not significant). Between-groups comparison showed that the presyncopal group had a lower phase coupling compared to non-presyncopal group during Tilt PRBS in frequency regions II, III and IV.

Figure 5.18 a

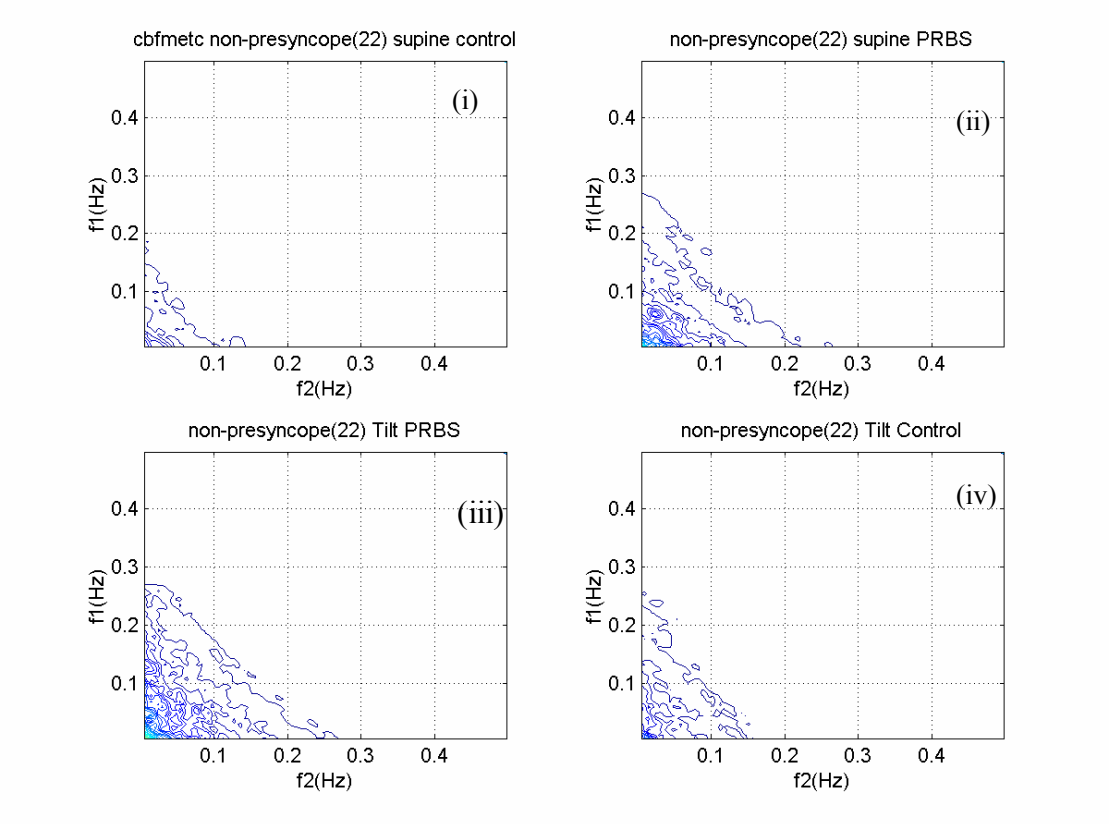

Figure 5.18 b

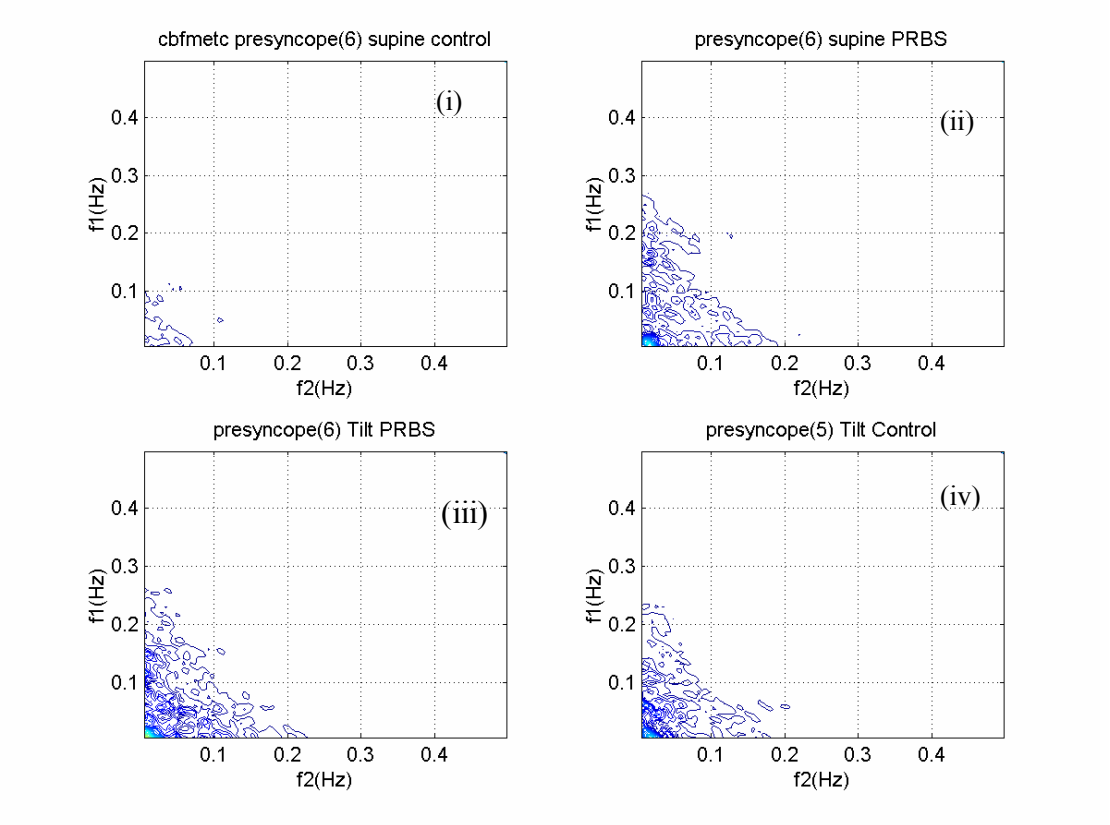

Figure 5.18 Contour plots of group averaged cross-bispectra between CBFM and $ETCO_2$ volume (CBFM-$ETCO_2$) (i-Supine Control; ii-Supine PRBS; iii-Tilt PRBS; iv-Tilt Control). Figure 5.18 (a) shows the averaged (N=24) bispectra for the non-presyncopal group. Figure 5.18 (b) shows the averaged (N=6) bispectra for the presyncopal group.

In order to determine changes in cerebral autoregulation, we calculated cross-bispectrum between CBFV and SBP as shown in Figure 5.19. Relative to Supine Control, phase coupling increased in the non-presyncopal group during Supine PRBS, Tilt PRBS and Tilt Control in all frequency regions (Table 5.5). Changes in the presyncopal group were similar but the difference was not significant in some frequency regions. Comparisons between groups showed that during Tilt Control pre-syncopal subjects had higher phase coupling than non-presyncopal subjects within frequency region I (Table 5.6).

Figure 5.19 a

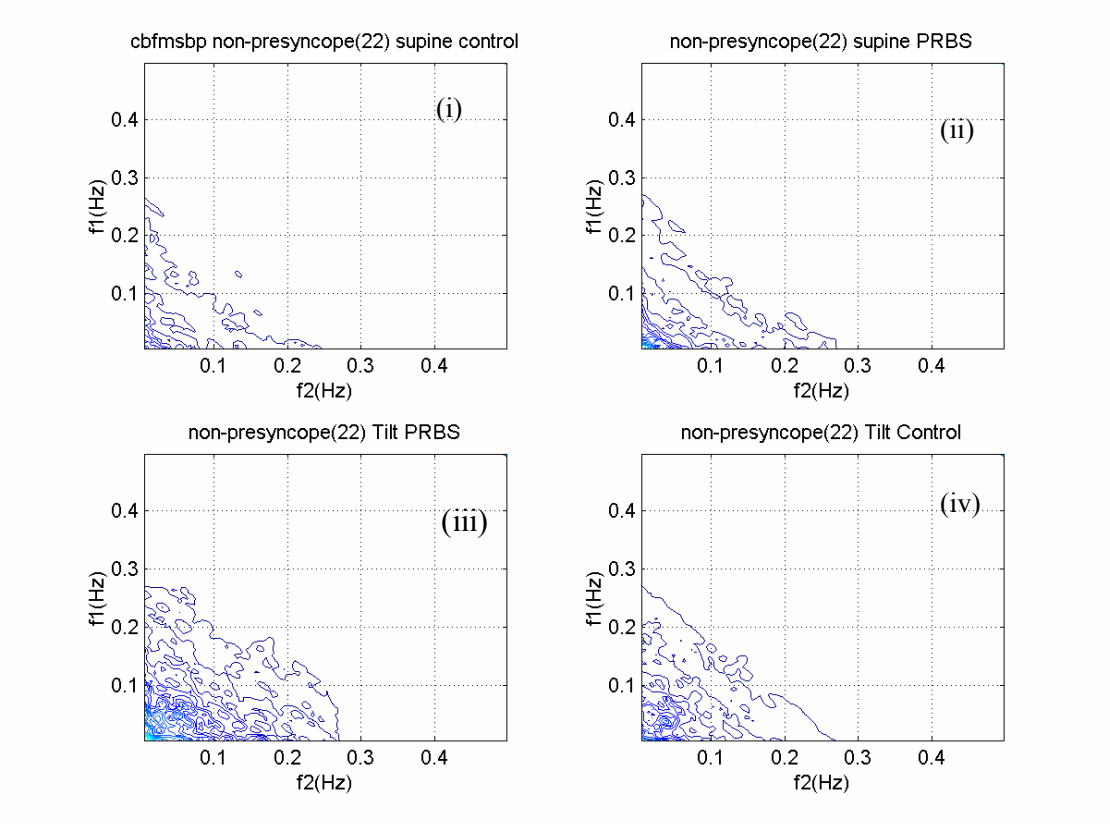

Figure 5.19 b

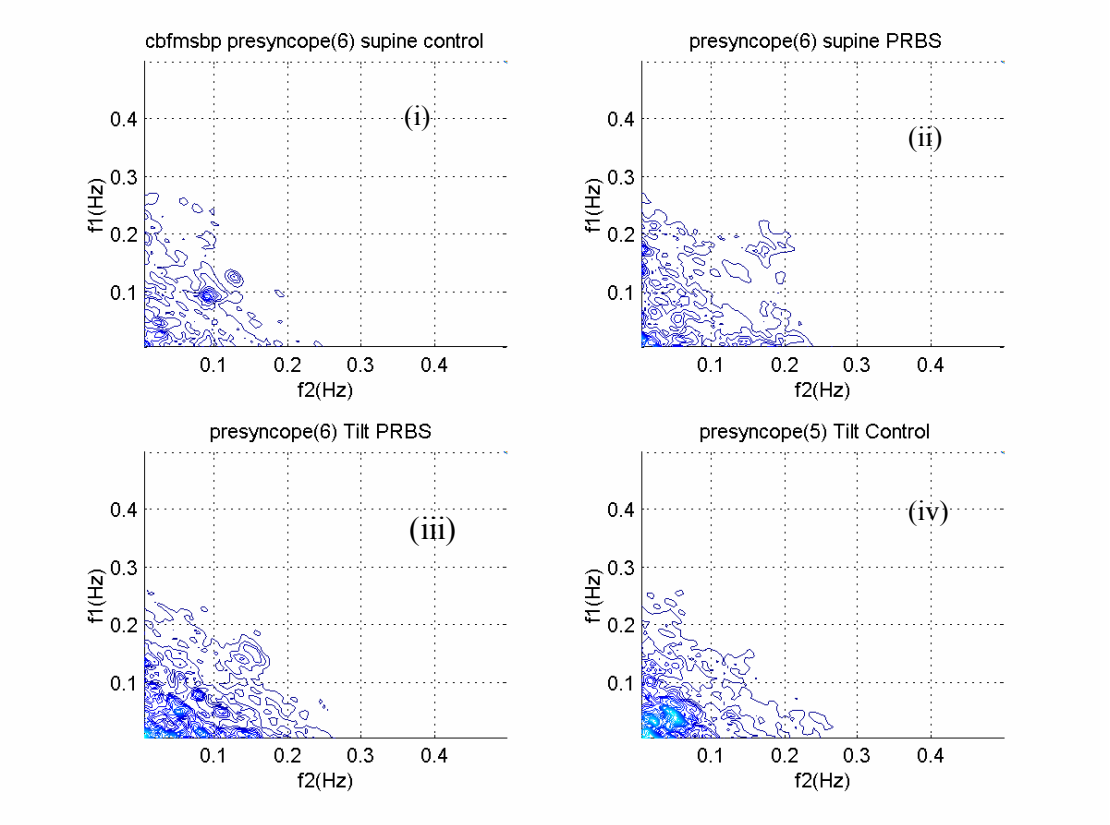

Figure 5.19 Contour plots of group averaged cross-bispectra between CBFM and SBP (CBFM-SBP) (i-Supine Control; ii-Supine PRBS; iii-Tilt PRBS; iv-Tilt Control). Figure 5.19(a) shows the averaged (N=24) bispectra for the non-presyncopal group. Figure 5.19 (b) shows the averaged (N=6) bispectra for the presyncopal group.

5.2 Experiment two (effects of hypocapnia on cerebral autoregulation)

Two out of the eighteen subjects developed presyncopal symptoms during stage 4 of experiment two. Both of them were in treatment group. Since the number of subjects who developed presyncope was not adequate to perform any statistical analysis, we used data from the 16 non-presyncopal subjects to report results from experiment two. Eight of these subjects were in the treatment group and the other eight were in the control group.

5.2.1 Mean values

Mean values of cardio-respiratory parameters are shown for treatment group (Table 5.7) and control group (Table 5.8) during all four stages of our study. As expected, $ETCO_2$ decreased significantly (47 to 36.6 mmHg) during stage 4 of the study compared with stage 1 for treatment group. While ETCO2 for control group did not change (48 to 48.4 mmHg) during stage 4 compared with stage 1. Blood pressure did not change for both groups. During tilt (stage 3 and 4), subjects in both groups increased their heart rate. CBFM in both groups increased during stage 2 and decreased during stage 4 compared with stage 1. Tidal volume, ventilation and respiratory rate were almost same for both groups in stage 3 and 4. Comparison between groups showed that during stage 4, treatment group had significant lower $ETCO_2$ level than control group.

Table 5.7 Mean values for treatment group in experiment two (N=8). *Significant difference between stage 2 and stage 1; †Significant difference between stage 3 and stage 1; ‡Significant difference between stage 4 and stage 1; ^{s} Significant difference between treatment and control group.

Mean values of:	Stage 1	Stage 2	Stage 3	Stage 4
Heart rate (beats/min)	69.8 ± 4.0	$70.9^{*} \pm 4.3$	$85.8^{\dagger} \pm 4.6$	$92.1^{\ddagger} \pm 5.4$
BP_{MCA} (mmHg)	77.3 ± 4.0	79.5 ± 4.76	82.4 ± 7.45	86.5 ± 6.5
CBFP (cm/s)	85.4 ± 6.0	89.2 ± 6.7	80.5 ± 5.5	70.8 ± 5.1
CBFM (cm/s)	76.7 ± 5.1	$80.3^{*} \pm 5.9$	73.6 ± 4.8	$65.5^{\ddagger} \pm 4.4$
V_t (ml)	659 ± 42.7	$925.5^{*} \pm 66.9$	$936^{\dagger} \pm 59.1$	$900^{\ddagger} \pm 64.2$
Resp rate (breaths/min)	11.7 ± 0.8	$12.5^{*} \pm 0.6$	$12.8^{\dagger} \pm 0.7$	$12.1^{\ddagger} \pm 0.6$
$\dot{V}_E$ (L/min)	7.6 ± 0.2	$11.5^{*} \pm 0.8$	$11.7^{\dagger} \pm 0.3$	$11.0^{\ddagger} \pm 0.5$
$ETCO_2$ (mmHg)	47 ± 2.1	48.1 ± 1.7	45.5 ± 1.5	$36.6^{\ddagger,s} \pm 2.1$

Table 5.8 Mean values for control group in experiment two (N=8). *Significant difference between stage 2 and stage 1; †Significant differences between stage 3 and stage 1; ‡Significant difference between stage 4 and stage 1.

Mean values of:	Stage 1	Stage 2	Stage 3	Stage 4
Heart rate (beats/min)	66.4 ± 5.2	67.7 ± 6.6	$82.0^{\dagger} \pm 6.1$	$87.0^{\ddagger} \pm 7.0$
BP_{MCA} (mmHg)	70.6 ± 5.2	74.4 ± 6.8	74.6 ± 5.9	78.3 ± 5.0
CBFP (cm/s)	90.0 ± 3.1	$96.2^{*} \pm 2.9$	80.2 ± 3.4	$76.3^{\ddagger} \pm 2.6$
CBFM (cm/s)	78.7 ± 2.5	$84.9^{*} \pm 2.6$	72.8 ± 2.8	$69.4^{\ddagger} \pm 2.0$
V_t (ml)	650 ± 47.2	$882.1^{*} \pm 51.5$	$924^{\dagger} \pm 66.6$	$940^{\ddagger} \pm 73.2$
Resp rate (breaths/min)	13.3 ± 1.2	13.2 ± 1.0	13.4 ± 1.0	13.2 ± 1.0
$\dot{V}_E$ (L/min)	8.3 ± 0.5	$10.6^{*} \pm 0.6$	$12.1^{\dagger} \pm 0.7$	$12.1^{\ddagger} \pm 0.6$
$ETCO_2$ (mmHg)	48 ± 1.7	$51.9^{*} \pm 1.8$	48.5 ± 2.0	48.4 ± 1.9

Ventilation and end tidal CO_2 across the four stages of our study from one typical subject in the treatment group is shown in Figure 5.20. Top panel shows ventilation. Bottom panel shows end tidal CO_2. It is clear that from these figures, end tidal CO_2 decreased while ventilation was relatively constant which means the subject had hypocapnia with minor changes in the ventilation.

The coefficients of variation were calculated as the ratio of variation in the signals to mean values of the signals, which is an indicator of relative changes in the signals. A lower value of coefficient of variation means relatively less variation. The coefficients of variation for tidal volume in treatment group decreased from 0.26 ± 0.04 (stage 1, spontaneous breathing) to 0.16 ± 0.04 (stage 4, controlled breathing). The coefficients of variation of ventilation and respiratory rate in treatment group decreased from 0.004 to 0.002 and from 0.22 ± 0.04 to 0.12 ± 0.03 (Mean $\pm$ SEM). We can see the coefficients of variation for tidal volume, ventilation and respiratory rate decreased during controlled breathing for treatment group which means the variation for those parameters during controlled breathing were less.

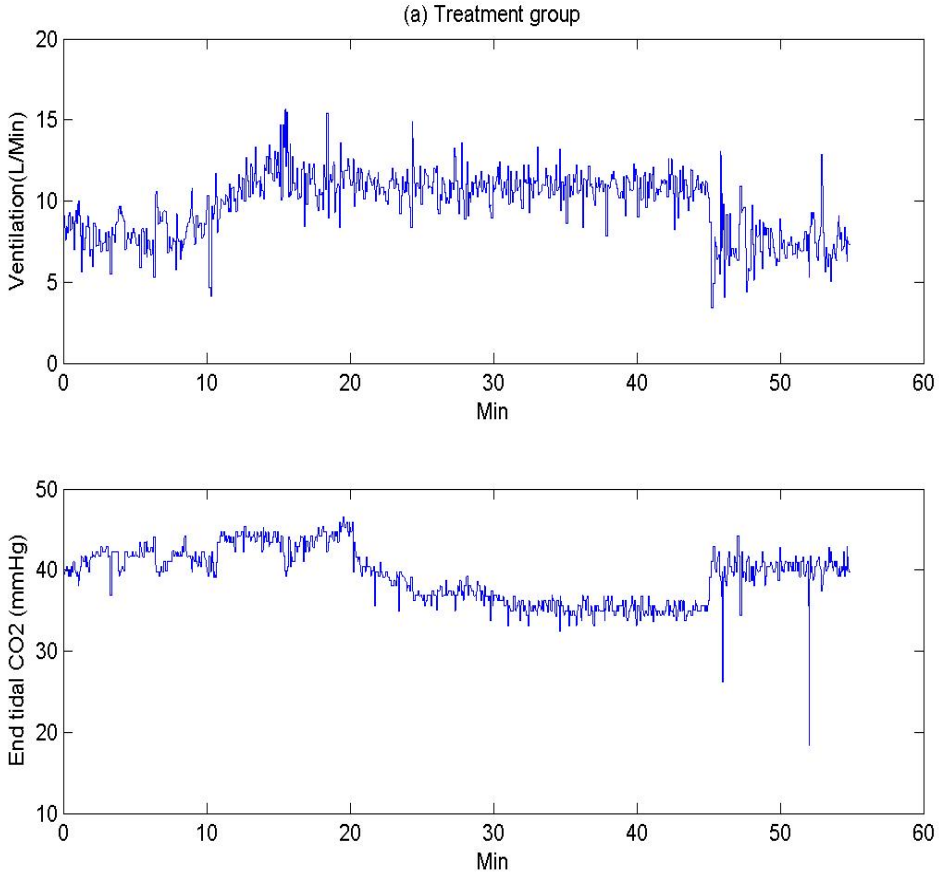

Figure 5.20 Ventilation (Top) and $ETCO_2$ (Bottom) from one typical subject in the treatment group. It is clear from these figures that the subject's $ETCO_2$ decreased while his ventilation was almost constant which means the subject had hypocapnia with minor changes in the ventilation.

Similar to Figure 5.20, ventilation (Top) and ETCO2 (bottom) from one subject in the control group is shown in Figure 5.21. As shown in the figure, the subject controlled the ventilation and the ETCO2 level was maintained. The coefficients of variation for tidal volume in control group decreased from 0.31 ± 0.04 (stage 1, spontaneous breathing) to 0.18 ± 0.04 (stage 4, controlled breathing). The coefficients of variation of ventilation and respiratory rate in control group decreased from 0.003 to 0.002 and from 0.19 ± 0.01 to 0.14 ± 0.02 (Mean $\pm$ SEM).

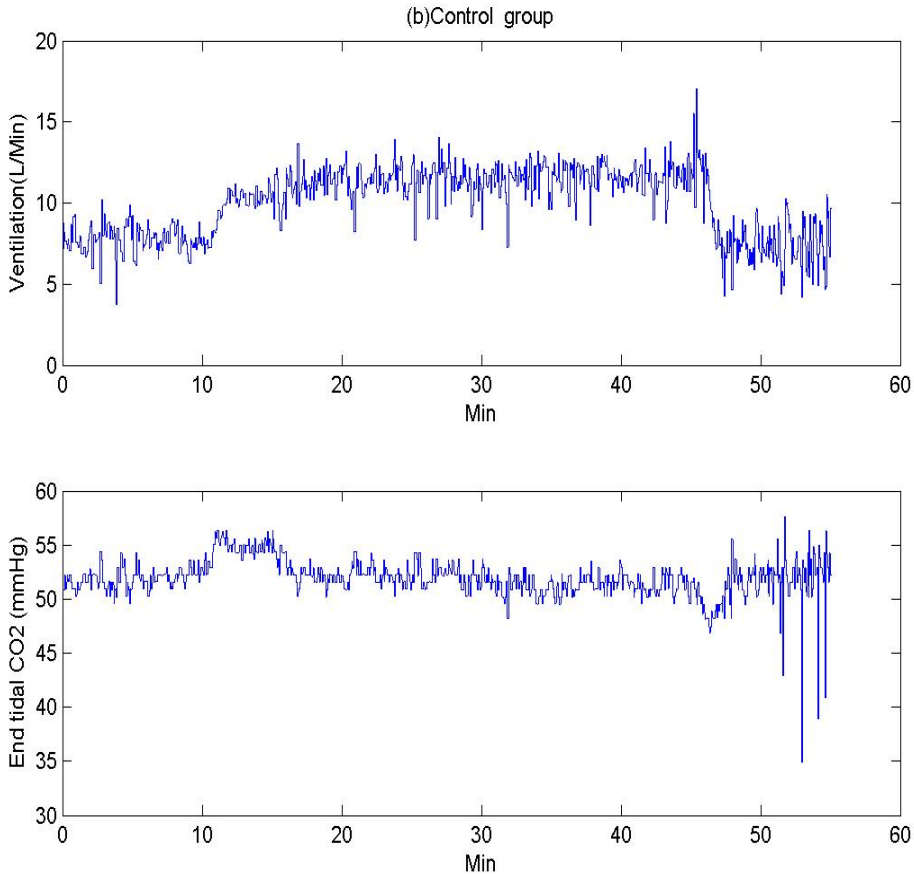

Figure 5.21 Ventilation (Top) and $ETCO_2$ (bottom) from one typical subject in the control group. As seen from this figure, the subject controlled the ventilation yet the CO_2 level was normal.

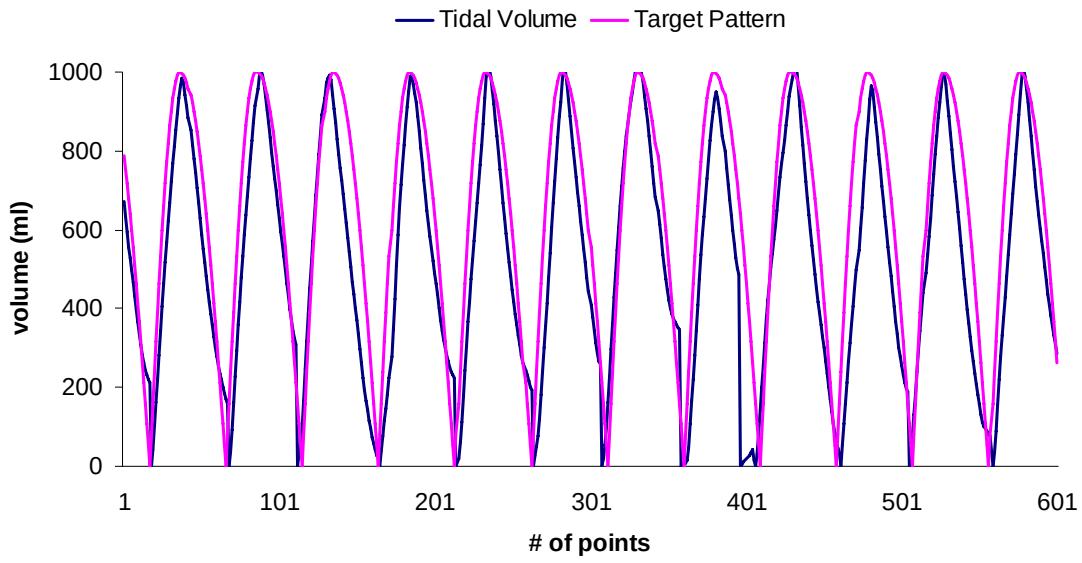

Figure 5.22 Target pattern (pink) and instantaneous tidal volume (blue) from one subject during voluntarily controlled breathing.

Figure 5.22 shows how the subject followed the generated pattern. The red curve is the target pattern generated by our Labview® program and the blue curve is the subjects' instantaneous tidal volume calculated as the integrated airflow during each breath and was reset to zero after each breath. From this figure, we can see the subject followed the pattern acceptably.

5.2.2 Auto-spectra of CBFM, BP_{MCA} and CVR

The averaged auto-spectra of CBFM, BP_{MCA} and CVR are shown in Figure 5.23. As shown in Figure 5.23, low frequency power is concentrated within region 0.04-0.15Hz, high (respiratory) frequency power is concentrated within region 0.15-0.32Hz, therefore the auto-spectra of CBFM, BP_{MCA}, and CVR were integrated within LF(0.04-0.15Hz) and

HF (0.15-0.32Hz) frequency regions; then the integrated values were compared for statistically significant differences as follows: To determine how hypocapnia will affect CA, a between-group comparison was performed during the stage 4 of the study. Power spectra during stage 4 were compared with that during stage 1 (baseline data) within each group. The results are shown in Table 5.9.

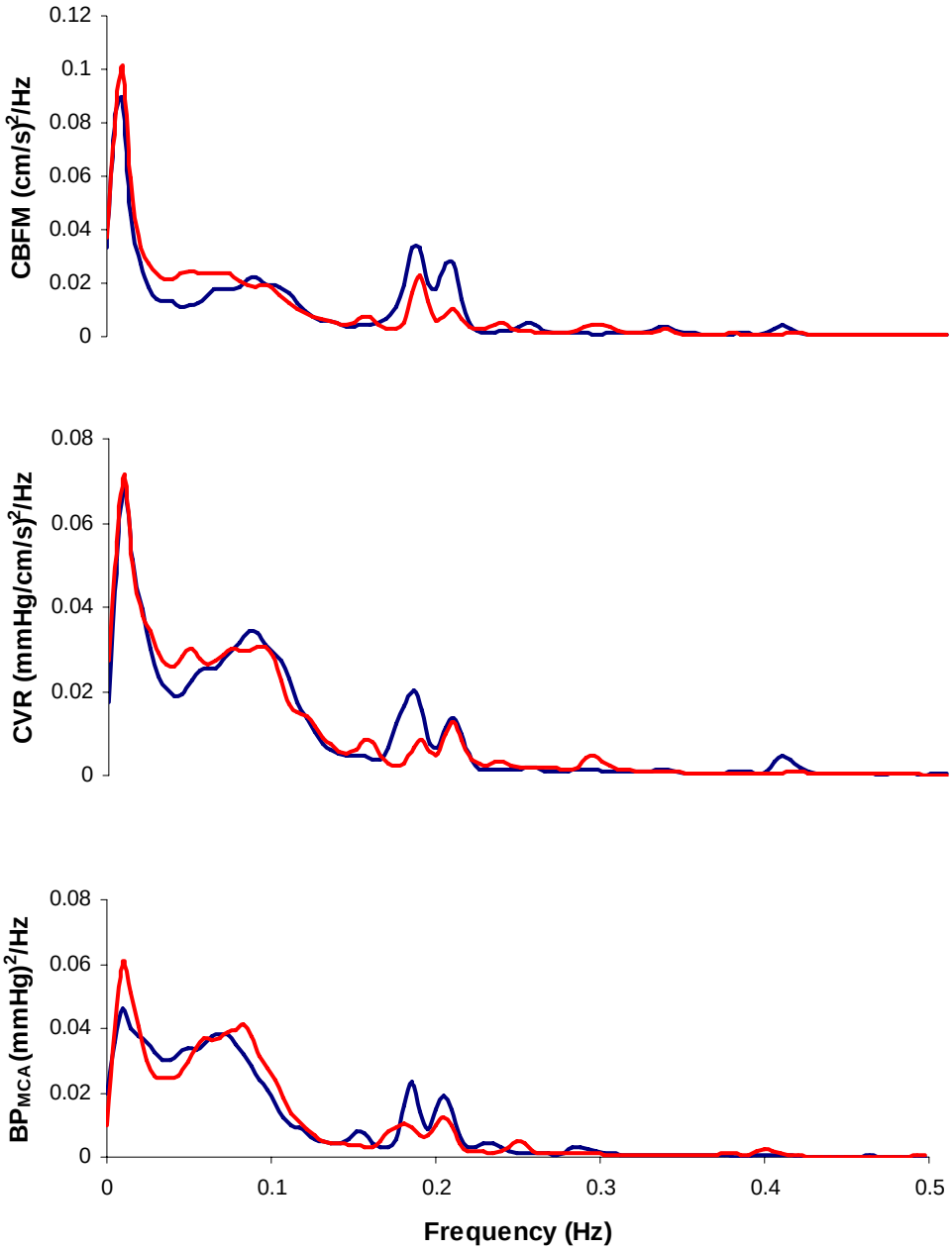

Figure 5.23 Averaged auto-spectra of CBFM, BP_{MCA}, CVR for Treatment (blue) and Control (red) group.

Table 5.9 Integrated averaged auto-spectra within low and high frequency regions for CBFM, BP_{MCA} and CVR for the Treatment and Control group during stage 1 and stage4. LF denotes frequency region 0.04-0.15Hz and HF denotes frequency region. 0.15Hz-0.32Hz. † significant differences between stage 1 (Treatment_1) and stage 4 (Treatment_4) of the treatment group; ‡ significant differences between stage 1 (Control_1) and stage 4 (Control_4) of the Control group.

Auto-spectra		Treatment_1	Treatment_4	Control_1	Control_4
CBFM	LF	0.27 ± 0.022	0.31±0.040	0.29±0.018	$0.37^{\ddagger}$±0.052
	HF	0.14 ±0.019	$0.27^{\dagger}$±0.052	0.14 ±0.016	0.17±0.041
BP_{MCA}	LF	0.33 ± 0.057	$0.54^{\dagger}$±0.040	0.33± 0.047	$0.51^{\ddagger}$±0.048
	HF	0.084 ± 0.024	0.13±0.015	0.073 ±0.017	$0.18^{\ddagger}$±0.044
CVR	LF	0.34 ± 0.056	$0.49^{\dagger}$±0.044	0.33± 0.034	$0.496^{\ddagger}$±0.061
	HF	0.11 ± 0.017	0.16±0.039	0.10± 0.018	0.13±0.020

There were no significant differences in the spectra of CBFM, BP_{MCA} and CVR between two groups during stage 4. For treatment group, integrated spectra of CBFM were higher during stage 4 than that during stage 1 in the HF region. For Control group, integrated spectra were higher during stage 4 than stage 1 in LF region. For both groups, in LF region, the power in BP_{MCA} and CVR during stage 4 was higher than during stage 1. For Control group, the power in HF region of BP_{MCA} is also higher during stage 4 than during stage 1.

5.2.3 Coherence and transfer function gain between BP_{MCA} and CBFM

Comparisons of coherence between two groups and within group between stage 4 and 1 are shown in Table 5.10. Group averaged coherencies between BP_{MCA} and CBFM during stage 4 are shown in Figure 5.24. Red curve shows control group and blue curve shows treatment group. There were no significant differences between two groups. Within HF region, the treatment group had a lower coherence during stage 4 than stage 1.

Table 5.10 Integrated averaged coherence within low and high frequency regions between BP_{MCA} and CBFM/CVR for the Treatment and Control group during stage 1 and stage 4. LF denotes frequency region 0.04-0.15Hz and HF denotes frequency region. 0.15Hz-0.32Hz. † significant differences between stage 1 (Treatment_1) and stage 4 (Treatment_4) of the treatment group; ‡ significant differences between stage 1 (Control_1) and stage 4 (Control_4) of the Control group.

Coherence		Treatment_1	Treatment_4	Control_1	Control_4
BP_{MCA}-CBFM	LF	8.90 ±1.45	9.74±1.56	9.47 ± 1.37	11.47±1.31
	HF	14.25 ± 1.48	11.03†±1.14	13.34±1.49	12.10 ±1.11
BP_{MCA}-CVR	LF	16.64 ±1.89	20.69†±0.79	18.69±1.15	20.01±0.90
	HF	18.89 ± 1.85	23.04†±1.82	19.81± 2.06	24.69‡±0.95

Comparisons of transfer function gain between two groups and within group between stage 4 and 1 are shown in Table 5.11. Both groups had a higher gain during stage 4 compared with baseline data within LF and HF region. As shown in Figure 5.25, transfer function gain from BP_{MCA} to CBFM during stage 4 was lower in the treatment group than control group within LF region.

Table 5.11 Integrated averaged transfer function gain within low and high frequency regions between BP_{MCA} and CBFM/CVR for the Treatment and Control group during stage 1 and stage4. LF denotes frequency region 0.04-0.15Hz and HF denotes frequency region. 0.15Hz-0.32Hz. † significant differences between stage 1 (Treatment_1) and stage 4 (Treatment_4) of the treatment group; ‡ significant differences between stage 1 (Control_1) and stage 4 (Control_4) of the Control group; * significant differences between Treatment and Control group during stage 4.

Transfer function gain		Treatment_1	Treatment_4	Control_1	Control_4
BP_{MCA}-CBFM	LF	10.07± 1.14	$5.37^{\dagger}$±0.63	11.03 ±1.34	$7.59^{\ddagger,*}$ ±0.68
	HF	24.49 ±3.72	$10.63^{\dagger}$±1.80	21.84 ±1.99	$11.30^{\ddagger}$±1.085
BP_{MCA}-CVR	LF	0.35 ±0.023	$0.41^{\dagger}$±0.021	0.34 ±0.0079	$0.38^{\ddagger}$±0.013
	HF	0.53 ±0.06	0.54±0.039	0.45 ±0.028	0.51±0.026

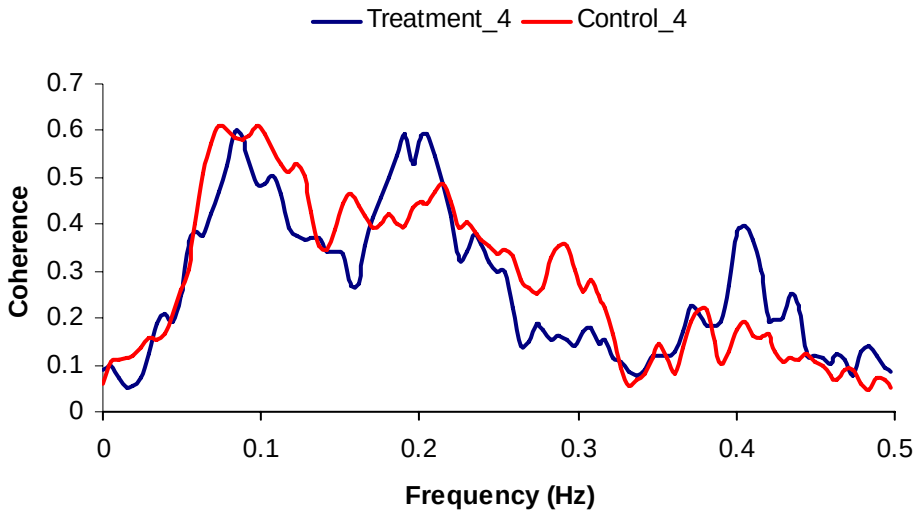

Figure 5.24 Averaged coherencies between BP_{MCA} and CBFM during stage 4. Red curve represents control group and blue represents treatment group.

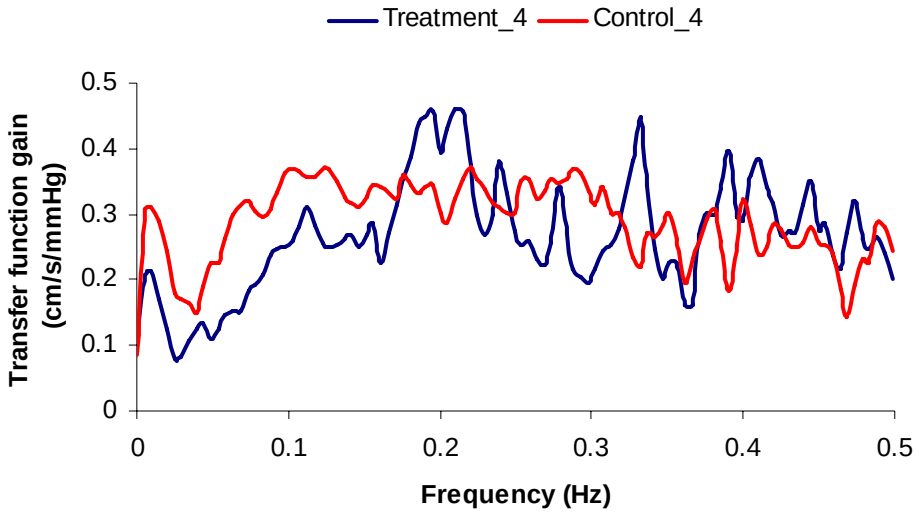

Figure 5.25 Averaged transfer function gain for Control group (Red) and Treatment group (Blue) between BP_{MCA} and CBFM during stage 4.

5.2.4 Coherencies and transfer function gain between BP_{MCA} and CVR

As shown in Table 5.10 and Figure 5.26, there were no significant differences between two groups in coherence between BP_{MCA} and CVR during stage 4. For both groups, the coherence during stage 4 was higher than baseline data in HF region. For treatment group, the coherence is higher during stage 4 than baseline data in LF region.

As shown in Table 5.11 and Figure 5.27, there were no significant differences between two groups in transfer function gain between BP_{MCA} and CVR during stage 4. For both groups the gain during stage 4 was higher than baseline data in LF region.

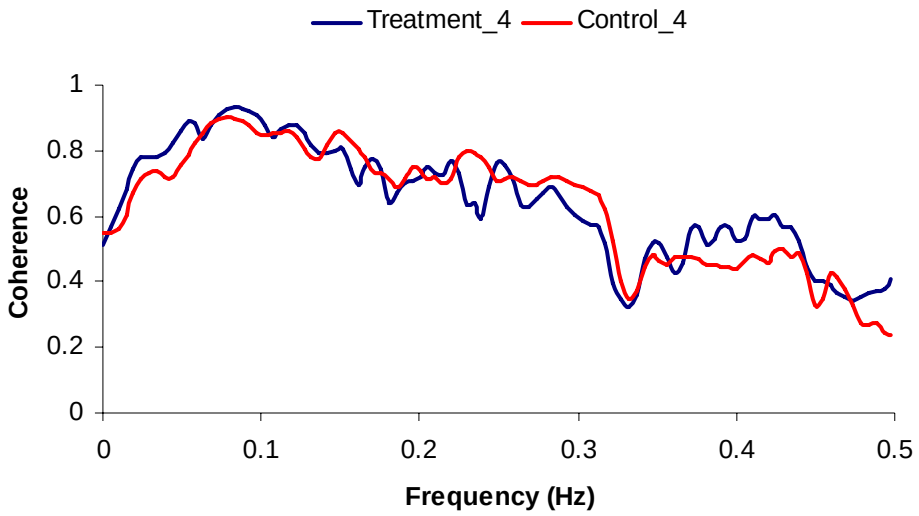

Figure 5.26 Averaged coherencies for Control group (Red) and Treatment group (Blue) between BP_{MCA} and CVR during stage 4.

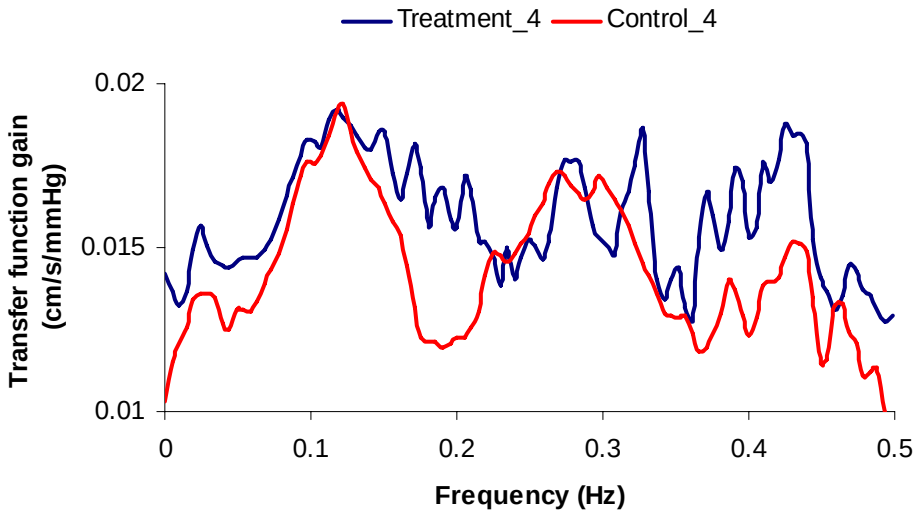

Figure 5.27 Averaged transfer function gain for Control group (Red) and Treatment group (Blue) between BP_{MCA} and CVR during stage 4. Red curve denotes control group and blue denotes treatment group.

Chapter 6 Discussion

6.1 Ventilatory sensitivity to CO_2

The main finding of this part of our study was that the dynamic sensitivity of the ventilatory control system to perturbations in CO_2 was enhanced during tilt. Combined with the decrease in mean levels of $ETCO_2$ and an increase in minute ventilation, our results suggest that during tilt there may be a change in the 'set point' of $PaCO_2$.

As discussed by Serrador et al (60), the reduction of $ETCO_2$ during tilt may be due to three mechanisms; active hyperventilation, which is an increase in alveolar ventilation relative to CO_2 production, increase in ventilation relative to cardiac output, and redistribution of tissue CO_2 stores. It is also possible that engagement of the vestibular reflex causes an increase in ventilation, which may also contribute to the decrease in $ETCO_2$ (35). Irrespective of the mechanisms that result in the reduction of $ETCO_2$, our objective was to investigate how the CO_2 control system adapts to, or accommodates, this decrease.

Our results showed that gain and peak values of the impulse response increased significantly during tilt relative to during supine, while the decay times showed a tendency to decrease (non-significant). Each of these three measures indicated that the ventilatory response to $ETCO_2$ was enhanced during tilt. Serrador et al (60) observed that CO_2 production may slightly increase after 20 minutes of supine posture preceding tilt. This observation combined with an increased dynamic sensitivity of the control system would predict against the observed decrease in $ETCO_2$. A possible mechanism that would

account for these changes in sensitivity and ventilation is a decrease in the set point of CO_2. The set point of CO_2 is the level of CO_2 against which the afferent signal from CO_2 receptors is compared (presumably at the sites of central regulation) in order to adjust respiratory effort. Yoshizaki et al (71) had a similar explanation using a steady state breathing technique to assess the sensitivity of the CO_2 control system during tilt. Yoshizaki et al observed that the slope of the ventilatory response to CO_2 perturbations remained unchanged during tilt while the curve was shifted leftward. They concluded that the increase in minute and alveolar ventilation during tilt combined with unaltered controller sensitivity indicated a change in CO_2 regulatory set point. Different methods in assessing system sensitivity may have contributed to the differences in the sensitivity assessments by Yoshizaki et al (71) and our results. Consistent with our observations, Jordan et al (27) also reported that the respiratory response to hypercapnia was enhanced during tilt using steady state CO_2 breathing. Initial results from a previous investigation where we studied a small number of young adults and adolescent subjects using a similar procedure also showed an increase in ventilatory sensitivity(58).

Collectively, our and others' results suggest that the target value for CO_2 regulation may change during tilt. Our experiment cannot provide information regarding the mechanisms via which the set point may change. However, we consider that additive excitatory neural influences due to arousal state during tilt may have contributed to the increased ventilation observed during tilt even though the CO2 levels were smaller. These types of neural influences were modeled as an Alertness Factor by Longobardo et al (42) in their recent modeling study. Another possible explanation for this change in "set point" could be that ventilation control is nonlinear. The "set point" model is based on a linear approximation. Changes in the "set point" actually reflect changes in the parameters of the nonlinear system. "Set point" gives us a way to visualize those changes, but may not directly point to the corresponding physiological changes.

In contrast to open loop or controller responses, there were no significant differences in comparison of closed loop responses between supine and tilt. Because of feedback loop, closed loop responses are less sensitive to changes in controller sensitivity than the open loop responses. Therefore, a likely explanation for not observing changes in closed loop responses is that our experiment was not sensitive enough to detect these differences.

We observed blunting of the baroreflex sensitivity from 17.6 msec/mmHg to 5.5 msec/mmHg during tilt. Sequence analysis method was used to estimate the baroreflex sensitivity, similar to the method used by Iellamo et al (26). It has been shown that hyperventilation by itself, without any changes in $ETCO_2$, can decrease baroreflex sensitivity (66) from 13 msec/mmHg to 9 msec/mmHg. In a study by Laitinen et al.(38), baroreflex sensitivity decreased from around 24 to 5 ms/mmHg. In their study subjects were also tilted to 70-degree head up tilt position but only for 13 minutes. A slightly larger decrease in baroreflex sensitivity was observed in our study. Baroreflex sensitivity, in our study, was calculated during Tilt Control, i.e. during 10 to 30 minutes from the onset of tilt. It is possible that the increased duration of tilt, combined with increased ventilation due to washout of residual from inspired CO_2, at least in the early part of tilt control, might have contributed to the slightly larger decrease seen in our study.

In order to further verify our results obtained through the parametric method, we used a non-parametric method to estimate the ventilatory responses to $ETCO_2$ perturbations. As shown in Figure 5.25, we found the transfer function gains were larger during tilt than supine in almost all frequencies from DC to 0.12 Hz. These results provide further support for our interpretation that the controller sensitivity (transfer function gain) was augmented during tilt. The transfer functions showed that the differences between responses during supine and tilt were more pronounced in the frequency region centered around 0.09 Hz. Spectral results from blood pressure provide possible explanation for increase in controller gain in this frequency region. Previous studies (53, 57) have shown

that amplitudes of oscillations in mean and diastolic blood pressures at frequencies around 0.1 Hz increase significantly during tilt. Results from our current study also showed increase in amplitude of oscillations within this frequency range. Additionally, within comparable frequency range, oscillations in cerebral blood flow have also been shown to increase in amplitude during tilt (11). It is possible, therefore, that the increase in amplitude of oscillations in pressure during tilt may translate into oscillations in perfusion within the tissue where CO_2 sensors are located. These changes in the perfusion pressure may result in oscillations in sensed levels of CO_2. Although speculative, the above explanation is consistent with our observations: the responses to $ETCO_2$ (resulting ultimately from sensed arterial CO_2) levels were augmented during tilt, while no change in ventilatory response to inspired CO_2 levels. If the above effect did play a role, then it is possible that the central controller sensitivity may not have increased but the response or output increased because of increased afferent signaling secondary to increased oscillations in perfusion pressure.

This part of our study has several limitations. We estimated responses during PRBS perturbations of lengths shorter than those used by others (37). Because of the possibility of development of presyncope we used shorter periods for PRBS stimulation. However, we ensured that the estimated responses from our study were comparable to those studies that used longer data records. Additionally, as discussed by Lai and Bruce (37) use of binary CO_2 stimulation levels requires assumption of linearity of responses. This is an assumption also shared by most of the previously studies involving estimates of ventilatory sensitivities. In our study $ETCO_2$ was used as the surrogate of $PaCO_2$. Results of previous studies (4, 6) suggest that the correlation between $ETCO_2$ and $PaCO_2$ may change during tilt, and that postural changes in $PaCO_2$ may be blunted with respect to those of $ETCO_2$. However, in these studies (4, 6), direct measurement of $PaCO_2$ confirmed that $PaCO_2$ also decreased during tilt. It is possible, therefore, a part of the

increase in sensitivity indicated by our results may be attributed to a change in correlation between $PaCO_2$ and $ETCO_2$.

In summary, our results suggest that the dynamic ventilatory response to perturbations in $ETCO_2$ is augmented during tilt relative to supine. The increase in ventilatory sensitivity during head up tilt may produce more oscillations in ventilation. Our results suggest, therefore, chemoreflex may play a role in the genesis of ventilatory oscillations prior to the onset of pre-syncopal symptoms during head up tilt (39).

6.2 Gender differences in cerebral autoregulation

Consistent with previous studies (3, 45), women had higher CBFM during supine than men. CBFM decreased during tilt in both groups. For similar reduction in $ETCO_2$ (women: 46-42mmHg; men: 48-44mmHg), women had a larger drop in CBFM than men (women: 76.74 to 67.52 cm/s; men: 66.99 to 62.52 cm/s). A higher CO_2 reactivity in women (32) may contribute to the larger drop in CBFM in women.

During Supine Control, women had a higher coherence between MBP and CBFM than men within a frequency region 0.03-0.10 Hz and 0.22-0.31 Hz. In a similar frequency region, the averaged transfer function gain between MBP and CBFM for women was also higher than for men during Supine Control. Higher coherence observed in women indicated that MBP for women was more related to CBFM than for men. Higher transfer function gain suggested that for the same amount of changes in MBP, CBFM changed more in women. Collectively, all these results suggested a less efficient CA in women than in men during supine rest. These differences in cerebral auto-regulation are likely influences from different hormone levels between women and men. Kastrup et. al. (31) reported that the higher CBFM and higher CO_2 vasodilator capacitances were diminished by indomethacin. Since indomethacin is a prostacyclin inhibitor, Meyer and Rauch (47) suggested that higher prostacyclin from cerebral arterial endothelium may attribute to

higher CBFV in women, and may be related to estrogen effects. During Tilt PRBS and Tilt Control the coherencies were significantly higher for men than for women, which was not expected. Additionally, during tilt, the differences in CBFM disappeared.

In summary, gender-related differences in CA did exist and gender may need to be considered as a factor in investigating CA.

6.3 Bispectral analysis

Our objective in using the bispectral analysis was to investigate alterations in non-linear phase coupling among cardio-respiratory signals in response to baro and chemo reflex stimuli. We explored these changes in non-linear cardio-respiratory interactions in presyncopal group and non-presyncopal group. We estimated auto-bispectra of RR intervals, SBP, and cross-bispectra between RR-SBP, RR-V_t, CBFM-$ETCO_2$ and CBFM-SBP. Our results showed that both RR interval and SBP phase coupling was lower in the presyncopal group than in non-presyncopals prior to onset of presyncopal symptoms.

Previous studies (8, 14, 22) have shown nonlinear components in the regulation of heart rate and blood pressure. Braun et. al (8) demonstrated that nonlinear components do exist in heart rate variability of healthy subject . However, physiological origins of these nonlinear components are not clearly identified. Kanters et. al. (28) concluded that nonlinear dynamics in heart rate does not come from respiration since nonlinear dynamics in heart rate existed even with fixed breathing rates. However, in Kanters' study, only breathing rate was controlled not tidal volume or ventilation. A previous study (55) clearly showed that variations in tidal volume, produced as an amplitude modulation, without changes in breathing rate, can importantly change the low frequency component of RR interval. Therefore, we cannot conclude that nonlinear components do not relate to respiration activity. Gonzalez et. al. (22) found that nonlinear components in

RR interval variability in rats appeared to be influenced more by parasympathetic activity while that in SBP variability seemed to be related to respiration via a non-neural pathway. Dabire et. al. (14) used pharmacological blockers and recurrence plots to determine that nonlinear indexes of RR intervals in normotensive rats increased when parasympathetic activity was blocked. The index of nonlinear coupling that we used (bispectral power) is different from previous indexes, therefore the physiologic correlates of our bispectral phase coupling index are not entirely clear from previous studies, but may be determined from the orthostatic response in non-presyncopal group.

We observed in the non-presyncopal subjects that phase coupling in RR interval decreased and phase coupling in SBP increased during tilt. It is generally accepted that the normal orthostatic response includes a decrease in vagal tone and a slight enhancement in sympathetic activity. Our results suggest that a decrease in RR interval phase coupling is related to decrease in vagal activity while increase in SBP phase coupling is related to increased sympathetic activity. We observed that the RR interval phase coupling decreased in both groups during Tilt Control compared to that with during Supine Control. In the presyncopal group, the RR interval phase coupling was lower compared with non-presyncopal group during Tilt Control in the frequency region II (0.15-0.3, 0.04-0.15 Hz) and III (0.15-0.3, 0.15-0.3Hz). These observations suggest that vagal input to cardiovascular regulation was diminished in both groups, however, the decrease in presyncopal group prior to onset of presyncopal symptoms was more pronounced than that in the non-presyncopal group. In both groups the SBP phase coupling increased during Tilt Control compared with during Supine Control. The presyncopal group had a lower SBP phase coupling in region III (i.e. high frequency region, 0.15-0.3, 0.15-0.3 Hz) during Tilt Control than non-presyncopal group. These observations suggest that sympathetic activity increased for both groups however subjects who developed pre-syncope increased it less than the non-presyncopal group. In a previous study by Convertino et al.(12), they also reported sympathetic withdrawal and

vagal tone enhancement prior to presyncope. Although our results also suggest diminished sympathetic activity in presyncopal group prior to the onset of presyncope, our results do not suggest an increase in vagal activity.

We observed that, in non-presyncopal subjects, stimulating the chemoreflex during supine (Supine PRBS) resulted in increased phase coupling between RR-intervals and SBP. During Tilt Control, the coupling decreased in both groups. Comparison between groups showed that the presyncopal group had a lower phase coupling compared with non-presyncopal group. Previous results suggest that RR-SBP coupling may involve respiration via the parasympathetic system (22). It is possible that stimulation of the chemoreflex affected respiratory pattern and, through either mechanical coupling or via the parasympathetic efferents, decreased phase coupling between RR interval and SBP. Although the physiological interpretation of coupling between RR and SBP is not entirely clear, a possible link may be mechanical via amplitude modulation type phenomenon. As discussed by Witte et al (69), the phase coupling estimated by bispectrum, also referred to as quadratic phase coupling (QPC), can result from amplitude modulation. An example discussed by Witte et al illustrates this point clearly. We provide this example here briefly: considering two signals A and B such that $A=\sin(2\pi f_1 t+\theta_1)$; $B= \sin(2\pi f_2 t+\theta_2)$; if A modulates B, and the resultant signal is added to A to obtain a new signal H(t), H(t) then includes power at frequencies f_1, f_2, f_2-f_1 and f_2+f_1. If the phase relations ($\theta_1+ \theta_2$, $\theta_2-\theta_1$) remain relatively unchanged, then the bispectrum of H(t) will have power at frequencies f_1,f_2. According to the above operation, power in a bispectrum indicates a fixed phase relation between θ_1, θ_2 and also a non-linear coupling between frequencies. Reduced coupling between RR and SBP and RR and Tidal volume observed in the presyncopal group during Tilt Control, therefore, suggests that some degree of disassociation of cardio-respiratory interaction. This interpretation is consistent with the results of a study by Lipstiz et al. (39) who used complex demodulation to show that cardio-respiratory interaction decoupled before the onset of syncope.

Arterial partial pressure of CO_2 (of which $ETCO_2$ is a surrogate) and SBP are two important factors affecting CBFV. In both groups, we observed that both tilt and stimulating the chemoreflex enhanced phase coupling between CBFM and $ETCO_2$. These results suggest a larger role of CO_2 tension mediated changes in CBFV via amplitude modulation type phenomenon during PRBS (where $ETCO_2$ and, therefore, arterial partial pressure of CO_2 changed by design) and during tilt compared with Supine Control. Between-group comparison showed that the presyncopal group had less coupling during Tilt PRBS compared with non-presyncopal group. These results suggest that this amplitude modulation type coupling was less effective in presyncopals. We have previously reported (33), that the CO_2 reactivity to CBFV was less in the presyncopal group. Whether the decrease in reactivity was related to the decreased modulation of CBFV is not entirely clear.

Cross-bispectrum between CBFV and SBP may reflect nonlinear dynamics in cerebral autoregulation. We observed an increase in the phase coupling during tilt (Table I). Comparison between groups showed that the phase coupling between CBFM and SBP during Tilt Control was higher in the presyncopal group than the non-presyncopal group, which may reflect diminished cerebral autoregulation. Our previous studies using linear methods (33), reported that presyncopal subjects had higher coherence and gain between SBP and CBFM which also suggested diminished CA. This result from our previous studies is consistent with our current interpretation.

An advantage of using bispectral analysis is that it allows us to explore nonlinear components within cardio-respiratory variables. Our results clearly show that such components do exist within these regulatory systems and that they will be affected by orthostatic stress, further, they are different based on the response to orthostatic stress (i.e. occurrence of pre-syncope). Whether such indexes are better predictors than others of pre-syncope remains unclear, however, our results provide support for such investigation.

Further investigation using these indexes is warranted to explore physiological origins of non-linear phase coupling within cardio-respiratory signals.

6.4 Hypocapnia effects on cerebral autoregulation

Our main findings in this part of the study were that in the transfer function gain between BP_{MCA} and CBFM in the treatment group was lower than control group in the LF region. The transfer function gain between BP_{MCA} and CBFM for the treatment group was lower than the control group in LF in stage 4 which suggest that the oscillations in BP_{MCA} are less transferred into the changes in CBFM during hypocapnia than normocapnia. Greater transfer gain between BP_{MCA} and CBFM suggested impaired autoregulation (72). Our results, therefore, mean hypocapnia improved the autoregulation compared with normocapnia.

We observed for both groups BP_{MCA} power increased during stage 4 relative to stage 1 in the LF region. The increase might come from tilt effects. Similar to the results from experiment one, the blood pressure variability increased in the LF region during tilt compared with during supine.

We observed peaks in the auto-spectrum of BP_{MCA} CVR and CBFM corresponding to the respiratory frequencies and their multiple harmonics as shown in Figure 5.23. In the coherence between BP_{MCA} and CBFM, we also observed peaks in similar frequency regions. As seen from Figure 5.24, in the treatment group the peaks at respiratory frequency region (around 0.22Hz) were very obvious. While in the control group, this is not so obvious. These results suggest that during controlled breathing both blood pressure and CBFV were modulated at the respiratory frequency, similar to the result from a recent study by Eames et. al. (15).

In a recent study by Edwards et. al (17), they used similar dynamic method to investigate the CA. In their study, auditory signal was used to fix the breathing rate at 15 breaths/min along with an ETCO2 forcing system to maintain the $ETCO_2$ level. Their results showed the gain for BP_{MCA} and CVR was enhanced with hypocapnia and diminished with hypercapnia compared with normocapnia indicating improved cerebral autoregulation under hypocapnia and impaired autoregulation in hypercapnia. Our analysis did not show significant differences for relation between BP_{MCA} and CVR between the two groups. The conclusion we obtained from the relation between BP_{MCA} and CBFM is consistent with theirs. In another study by Edwards et. al. (16), they used an ARMA model to investigate the interactions of CO_2 level and BP_{MCA} oscillation on cerebrovascular response simultaneously. In their study, subjects breathed in two breaths of CO_2 balanced with air to elicit the responses. They suggested when CO_2 level increased the cerebrovascular responsiveness to changes in CO2 or BP_{MCA} was reduced. These results also suggested that during normocapnia compared with hypocapnia the CA was less efficient. A recent study (46)also reported that, compared with normocapnia, hypocapnia helped more subjects restore CA during isoflurane-induced impairment of CA. However, as mentioned before, hypocapnia is expected to increase CVR, thus the CBF is expected to decrease accordingly, which may support an increase in the probability of developing syncope. Therefore, whether improved CA during hypocapnia indicates increased or decreased probability of developing syncope remains unclear.

In summary, our results showed decreased variabilities in CBFM in VLF region, lower gain between BP_{MCA} and CBFM in the HF region. All the above results showed improved CA during hypocapnia compared with during normocapnia when changes in ventilation were minimized. Whether impaired CA is related to an increased probability of developing syncope needs to be further investigated.

References

1. Syncope, Part 3 - Treatment of Syncope. http://heartdisease.about.com/cs/arrhythmias/a/Syncope3.htm [Sep. 10th, 2005].
2. **Aaslid R, Lindegaard KF, Sorteberg W, and Nornes H**. Cerebral autoregulation dynamics in humans. *Stroke* 20: 45-52, 1989.
3. **Ackerstaff RG, Keunen RW, van Pelt W, Montauban van Swijndregt AD, and Stijnen T**. Influence of biological factors on changes in mean cerebral blood flow velocity in normal ageing: a transcranial Doppler study. *Neurol Res* 12: 187-191, 1990.
4. **Anthonisen NR, Bartlett, J. R., Tenney S. M.** Postural effect on ventilatory control. *J Appl Physiol* 20: 191-196, 1965.
5. **Berne RM, and Levy MN**. *Principles of Physiology*. C.V. Mosby, 1999.
6. **Bjurstedt H, Hesser, C.M., Liljestrand, G., Matell G.** Effects of posture on Alveolar-Arterial CO_2 and O_2 Differences and on Alveolar Dead Space in Man. *Acta Physiol Scand* 54: 65-82, 1962.
7. **Blaber AP, Bondar RL, Moradshahi P, Serrador JM, and Hughson RL**. Inspiratory CO2 increases orthostatic tolerance during repeated tilt. *Aviat Space Environ Med* 72: 985-991, 2001.
8. **Braun C, Kowallik P, Freking A, Hadeler D, Kniffki KD, and Meesmann M**. Demonstration of nonlinear components in heart rate variability of healthy persons. *Am J Physiol* 275: H1577-1584, 1998.
9. **Busija DW, and Heistad DD**. Factors involved in the physiological regulation of the cerebral circulation. *Rev Physiol Biochem Pharmacol* 101: 161-211, 1984.
10. **Censi F, Calcagnini G, Strano S, Bartolini P, and Barbaro V**. Nonlinear coupling among heart rate, blood pressure, and respiration in patients susceptible to neuromediated syncope. *Ann Biomed Eng* 31: 1097-1105, 2003.
11. **Chern CM, Kuo TB, Sheng WY, Wong WJ, Luk YO, Hsu LC, and Hu HH**. Spectral analysis of arterial blood pressure and cerebral blood flow velocity during supine rest and orthostasis. *J Cereb Blood Flow Metab* 19: 1136-1141, 1999.
12. **Convertino VA, Ludwig DA, and Cooke WH**. Stroke volume and sympathetic responses to lower-body negative pressure reveal new insight into circulatory shock in humans. *Auton Neurosci* 111: 127-134, 2004.
13. **Cooper VL, and Hainsworth R**. Effects of head-up tilting on baroreceptor control in subjects with different tolerances to orthostatic stress. *Clin Sci (Lond)* 103: 221-226, 2002.
14. **Dabire H, Mestivier D, Jarnet J, Safar ME, and Chau NP**. Quantification of sympathetic and parasympathetic tones by nonlinear indexes in normotensive rats. *Am J Physiol* 275: H1290-1297, 1998.
15. **Eames PJ, Potter JF, and Panerai RB**. Influence of controlled breathing patterns on cerebrovascular autoregulation and cardiac baroreceptor sensitivity. *Clin Sci (Lond)*

106: 155-162, 2004.
16. **Edwards MR, Devitt DL, and Hughson RL**. Two-breath CO(2) test detects altered dynamic cerebrovascular autoregulation and CO(2) responsiveness with changes in arterial P(CO(2)). *Am J Physiol Regul Integr Comp Physiol* 287: R627-632, 2004.
17. **Edwards MR, Shoemaker JK, and Hughson RL**. Dynamic modulation of cerebrovascular resistance as an index of autoregulation under tilt and controlled PET(CO(2)). *Am J Physiol Regul Integr Comp Physiol* 283: R653-662, 2002.
18. **Epstein SE, Stampfer M, and Beiser GD**. Role of the capacitance and resistance vessels in vasovagal syncope. *Circulation* 37: 524-533, 1968.
19. **Fitzpatrick A, Theodorakis G, Vardas P, Kenny RA, Travill CM, Ingram A, and Sutton R**. The incidence of malignant vasovagal syndrome in patients with recurrent syncope. *Eur Heart J* 12: 389-394, 1991.
20. **Fritsch-Yelle JM, Whitson PA, Bondar RL, and Brown TE**. Subnormal norepinephrine release relates to presyncope in astronauts after spaceflight. *J Appl Physiol* 81: 2134-2141, 1996.
21. **Gebber GL, Zhong S, and Paitel Y**. Bispectral analysis of complex patterns of sympathetic nerve discharge. *Am J Physiol* 271: R1173-1185, 1996.
22. **Gonzalez JJ, Cordero JJ, Feria M, and Pereda E**. Detection and sources of nonlinearity in the variability of cardiac R-R intervals and blood pressure in rats. *Am J Physiol Heart Circ Physiol* 279: H3040-3046, 2000.
23. **Hagihira S, Takashina M, Mori T, Mashimo T, and Yoshiya I**. Practical issues in bispectral analysis of electroencephalographic signals. *Anesth Analg* 93: 966-970, 2001.
24. Heart rate variability: standards of measurement, physiological interpretation and clinical use. Task Force of the European Society of Cardiology and the North American Society of Pacing and Electrophysiology. *Circulation* 93: 1043-1065, 1996.
25. **Hoyer D, Pompe B, Herzel H, and Zwiener U**. Nonlinear coordination of cardiovascular autonomic control. *IEEE Eng Med Biol Mag* 17: 17-21, 1998.
26. **Iellamo F, Legramante JM, Massaro M, Galante A, Pigozzi F, Nardozi C, and Santilli V**. Spontaneous baroreflex modulation of heart rate and heart rate variability during orthostatic stress in tetraplegics and healthy subjects. *J Hypertens* 19: 2231-2240, 2001.
27. **Jordan J, Shannon JR, Diedrich A, Black B, Costa F, Robertson D, and Biaggioni I**. Interaction of carbon dioxide and sympathetic nervous system activity in the regulation of cerebral perfusion in humans. *Hypertension* 36: 383-388, 2000.
28. **Kanters JK, Hojgaard MV, Agner E, and Holstein-Rathlou NH**. Influence of forced respiration on nonlinear dynamics in heart rate variability. *Am J Physiol* 272: R1149-1154, 1997.
29. **Kanters JK, Hojgaard MV, Agner E, and Holstein-Rathlou NH**. Short- and long-term variations in non-linear dynamics of heart rate variability. *Cardiovasc Res* 31: 400-409, 1996.
30. **Karnik R, Valentin A, Winkler WB, Khaffaf N, Donath P, and Slany J**.

Sex-related differences in acetazolamide-induced cerebral vasomotor reactivity. *Stroke* 27: 56-58, 1996.
31. **Kastrup A, Happe V, Hartmann C, and Schabet M**. Gender-related effects of indomethacin on cerebrovascular CO2 reactivity. *J Neurol Sci* 162: 127-132, 1999.
32. **Kastrup A, Thomas C, Hartmann C, and Schabet M**. Sex dependency of cerebrovascular CO2 reactivity in normal subjects. *Stroke* 28: 2353-2356, 1997.
33. **Krishnamurthy S, Wang X, Bhakta D, Bruce E, Evans J, Justice T, and Patwardhan A**. Dynamic cardiorespiratory interaction during head-up tilt-mediated presyncope. *Am J Physiol Heart Circ Physiol* 287: H2510-2517, 2004.
34. **Kubota N, Iwasaki K, Ishikawa H, Shiozawa T, Kato J, and Ogawa S**. Autoregulation of dynamic cerebral blood flow during hypotensive anesthesia with prostaglandin E1 or nitroglycerin. *Masui* 53: 376-384, 2004.
35. **Kuipers NT, Sauder CL, and Ray CA**. Aging attenuates the vestibulorespiratory reflex in humans. *J Physiol* 548: 955-961, 2003.
36. **Lagi A, Cencetti S, Corsoni V, Georgiadis D, and Bacalli S**. Cerebral vasoconstriction in vasovagal syncope: any link with symptoms? A transcranial Doppler study. *Circulation* 104: 2694-2698, 2001.
37. **Lai J, and Bruce EN**. Ventilatory stability to transient CO2 disturbances in hyperoxia and normoxia in awake humans. *J Appl Physiol* 83: 466-476, 1997.
38. **Laitinen T, Niskanen L, Geelen G, Lansimies E, and Hartikainen J**. Age dependency of cardiovascular autonomic responses to head-up tilt in healthy subjects. *J Appl Physiol* 96: 2333-2340, 2004.
39. **Lipsitz LA, Hayano J, Sakata S, Okada A, and Morin RJ**. Complex demodulation of cardiorespiratory dynamics preceding vasovagal syncope. *Circulation* 98: 977-983, 1998.
40. **Lipton JM, Dabke KP, Alison JF, Cheng H, Yates L, and Brown TI**. Use of the bispectrum to analyse properties of the human electrocardiograph. *Australas Phys Eng Sci Med* 21: 1-10, 1998.
41. **Ljung L**. *System Identification*. Englewood Cliffs, NJ: Prentice Hall, 1987.
42. **Longobardo G, Evangelisti CJ, and Cherniack NS**. Effects of neural drives on breathing in the awake state in humans. *Respir Physiol* 129: 317-333, 2002.
43. **Macdonald R, Jenkins J, and Arzbaecher R**. A software trigger for intracardiac waveform detection with automatic threshold adjustment. *IEEE Computers in cardiology proceedings* 167-170, 1990.
44. **Mansier P, Clairambault J, Charlotte N, Medigue C, Vermeiren C, LePape G, Carre F, Gounaropoulou A, and Swynghedauw B**. Linear and non-linear analyses of heart rate variability: a minireview. *Cardiovasc Res* 31: 371-379, 1996.
45. **Marinoni M, Ginanneschi A, Inzitari D, Mugnai S, and Amaducci L**. Sex-related differences in human cerebral hemodynamics. *Acta Neurol Scand* 97: 324-327, 1998.
46. **McCulloch TJ, Boesel TW, and Lam AM**. The effect of hypocapnia on the autoregulation of cerebral blood flow during administration of isoflurane. *Anesth Analg*

100: 1463-1467, table of contents, 2005.
47. **Meyer JS, and Rauch GM**. Gender differences in cerebral perfusion. *J Neurol Sci* 162: 113, 1999.
48. **Mosqueda-Garcia R, Furlan R, Fernandez-Violante R, Desai T, Snell M, Jarai Z, Ananthram V, Robertson RM, and Robertson D**. Sympathetic and baroreceptor reflex function in neurally mediated syncope evoked by tilt. *J Clin Invest* 99: 2736-2744, 1997.
49. **Mosqueda-Garcia R, Furlan R, Tank J, and Fernandez-Violante R**. The elusive pathophysiology of neurally mediated syncope. *Circulation* 102: 2898-2906, 2000.
50. **Muthuswamy J, Sherman DL, and Thakor NV**. Higher-order spectral analysis of burst patterns in EEG. *IEEE Trans Biomed Eng* 46: 92-99, 1999.
51. **Ning TK, and Bronzino JD**. Bispectral analysis of the rat EEG during various vigilance states. *IEEE Trans Biomed Eng* 36: 497-499, 1989.
52. **Novak V, Spies JM, Novak P, McPhee BR, Rummans TA, and Low PA**. Hypocapnia and cerebral hypoperfusion in orthostatic intolerance. *Stroke* 29: 1876-1881, 1998.
53. **Pagani M, Lombardi F, Guzzetti S, Rimoldi O, Furlan R, Pizzinelli P, Sandrone G, Malfatto G, Dell'Orto S, Piccaluga E, and et al.** Power spectral analysis of heart rate and arterial pressure variabilities as a marker of sympatho-vagal interaction in man and conscious dog. *Circ Res* 59: 178-193, 1986.
54. **Patwardhan A, Evans J, Bruce E, and Knapp C**. Heart rate variability during sympatho-excitatory challenges: comparison between spontaneous and metronomic breathing. *Integr Physiol Behav Sci* 36: 109-120, 2001.
55. **Patwardhan A, Vallurupalli S, Evans J, Knapp C, and Bruce E**. Use of amplitude-modulated breathing for assessment of cardiorespiratory frequency response within subrespiratory frequencies. *IEEE Trans Biomed Eng* 45: 268-273, 1998.
56. **Patwardhan A, Wang K, Moghe S, and Leonelli F**. Bispectral energies within electrocardiograms during ventricular fibrillation are correlated with defibrillation shock outcome. *Ann Biomed Eng* 27: 171-179, 1999.
57. **Patwardhan AR, Evans JM, Bruce EN, Eckberg DL, and Knapp CF**. Voluntary control of breathing does not alter vagal modulation of heart rate. *J Appl Physiol* 78: 2087-2094, 1995.
58. **Richardson L, Topor Z, Bhakta D, McCaffrey F, Bruce E, and Patwardhan A**. Assessment of ventilatory sensitivity to carbon dioxide changes during orthostasis. *Biomed Sci Instrum* 38: 301-305, 2002.
59. **Schondorf R, Benoit J, and Stein R**. Cerebral autoregulation in orthostatic intolerance. *Ann N Y Acad Sci* 940: 514-526, 2001.
60. **Serrador JM, Bondar RL, and Hughson RL**. Ventilatory response to passive head up tilt. *Adv Exp Med Biol* 450: 133-139, 1998.
61. **Serrador JM, Sorond FA, Vyas M, Gagnon M, Iloputaife ID, and Lipsitz LA**. Cerebral pressure-flow relations in hypertensive elderly humans: transfer gain in different frequency domains. *J Appl Physiol* 98: 151-159, 2005.

62. **Sharpey-Schafer EP**. Emergencies in general practice: syncope. *BMJ* 1: 506-509, 1956.
63. **Sigl JC, and Chamoun NG**. An introduction to bispectral analysis for the electroencephalogram. *J Clin Monit* 10: 392-404, 1994.
64. **Signorini MG, Cerutti S, Guzzetti S, and Parola R**. Non-linear dynamics of cardiovascular variability signals. *Methods Inf Med* 33: 81-84, 1994.
65. **Trzebski A, and Smietanowski M**. Non-linear dynamics of cardiovascular system in humans exposed to repetitive apneas modeling obstructive sleep apnea: aggregated time series data analysis. *Auton Neurosci* 90: 106-115, 2001.
66. **Van De Borne P, Mezzetti S, Montano N, Narkiewicz K, Degaute JP, and Somers VK**. Hyperventilation alters arterial baroreflex control of heart rate and muscle sympathetic nerve activity. *Am J Physiol Heart Circ Physiol* 279: H536-541, 2000.
67. **Wang X, Krishnamurthy S, Evans J, Bhakta D, Justice L, Bruce E, and Patwardhan A**. Transfer function analysis of gender-related differences in cerebral autoregulation. *Biomed Sci Instrum* 41: 48-53, 2005.
68. **Wang X, Richardson L, Krishnamurthy S, Pennington K, Evans J, Bruce E, Abraham W, Bhakta D, and Patwardhan A**. Orthostatic modification of ventilatory dynamic response to carbon dioxide perturbations. *Auton Neurosci* 116: 76-83, 2004.
69. **Witte H, Putsche P, Eiselt M, Arnold M, Schmidt K, and Schack B**. Technique for the quantification of transient quadratic phase couplings between heart rate components. *Biomed Tech (Berl)* 46: 42-49, 2001.
70. **Yambe T, Nitta S, Sonobe T, Naganuma S, Kobayashi S, Haga Y, Tanaka M, Fukuju T, Miura M, Sato N, and et al.** Identification of the deterministic chaos in cardiovascular dynamics by the use of the non-linear mathematics. *Sci Rep Res Inst Tohoku Univ [Med]* 39: 1-5, 1993.
71. **Yoshizaki H, Yoshida A, Hayashi F, and Fukuda Y**. Effect of posture change on control of ventilation. *Jpn J Physiol* 48: 267-273, 1998.
72. **Zhang R, Zuckerman JH, Giller CA, and Levine BD**. Transfer function analysis of dynamic cerebral autoregulation in humans. *Am J Physiol* 274: H233-241, 1998.
73. **Zhang R, Zuckerman JH, and Levine BD**. Deterioration of cerebral autoregulation during orthostatic stress: insights from the frequency domain. *J Appl Physiol* 85: 1113-1122, 1998.
74. **Zhong S, Zhou SY, Gebber GL, and Barman SM**. Coupled oscillators account for the slow rhythms in sympathetic nerve discharge and phrenic nerve activity. *Am J Physiol* 272: R1314-1324, 1997.
75. **Zwienenberg M, and Muizelaar JP**. Cerebral perfusion and blood flow in neurotrauma. *Neurol Res* 23: 167-174, 2001.

Vita

Xue Wang

Date of Birth: July 5th, 1979
in
Neimenggu, China

Degree awarded
Bachelor of Engineering in Information Engineering
Beijing Institute of Technology
Beijing, China July 2001